TECHNISCHE UNIVERSITÄT WIEN
Vienna University of Technology

DISSERTATION

Extending the range of feedstock of the dual fluidized bed gasification process towards residues and waste

ausgeführt zum Zwecke der Erlangung des akademischen Grades
eines Doktors der technischen Wissenschaften unter der Leitung von

Univ.-Prof. Dipl.-Ing. Dr. techn. Hermann Hofbauer
Institut für Verfahrenstechnik, Umwelttechnik
und Technische Biowissenschaften

eingereicht an der Technischen Universität Wien

Fakultät für Maschinenwesen und Betriebswissenschaften

von

Dipl.-Ing. Veronika Wilk
0425450
Josefstädterstraße 29/64
1080 Wien

Wien, im Juli 2013 .....

Doctoral committee

Supervisor:	Univ.-Prof. Dipl.-Ing. Dr. Hermann Hofbauer
External reviewer:	Prof. Umberto Arena
Chairman:	Univ.-Prof. Dipl.-Ing. Dr. Anton Friedl
Date of oral defense:	02.07.2013

Hiermit versichere ich, dass ich die vorliegende Arbeit selbstständig verfasst und keine anderen als die angegebenen Quellen und Hilfsmittel benutzt habe, dass alle Stellen der Arbeit, die wörtlich oder sinngemäß aus anderen Quellen übernommen wurden, als solche kenntlich gemacht sind und dass die Arbeit in gleicher oder ähnlicher Form noch keiner Prüfungsbehörde vorgelegt wurde.

Veronika Wilk

Abstract

The dual fluidized bed (DFB) gasifier is a proven technology for the steam gasification of woody biomass. In this process, high quality product gas is generated that is rich in H_2, CO and other combustible gases. In DFB gasification plants at industrial scale, the product gas is used for efficient heat and power production and it is also suitable for chemical synthesis processes. This thesis aims for extending the range of feedstock for the DFB gasification process towards residues and waste. Gasification of residues and waste offers several advantages, because of their availability and price. In addition to that, DFB gasification is conceivable as chemical recycling of these materials.

A 100 kW DFB gasification pilot plant is operated at Vienna University of Technology for scientific purposes. Extensive measuring equipment is available for data recording and process evaluation. As the process conditions in the pilot plant are in good agreement to industrial DFB gasifiers, the results are suitable for making statements on larger scale applications. Different kinds of waste wood, sawdust, SLF-plastics and plastics from municipal solid waste, polymer production residues as well as PE regrind were tested. Operation of the pilot plant showed that the selected residues and waste can be gasified without problems and thus, DFB gasification of these materials is technological feasible.

A special focus is placed on the influence of specific waste fuel properties on the gasification process, because residues and waste are mostly inhomogeneous, of varying quality and are most commonly challenging fuels for gasification plants. Three aspects are thoroughly discussed: i) fuels with high concentrations of nitrogen, sulfur and chlorine, ii) fuels with an increased concentration of fine particles, and iii) fuels with an extremely high concentration of volatiles. In addition, the influence of the fuel feeding position is also evaluated.

The product gas is found to be clearly influenced by the specific fuel properties. Nitrogen, sulfur and chlorine from the fuel were predominantly found in the product gas, either in the form of gases (nitrogen as NH_3, sulfur as H_2S) or bound to ash (chlorine, sulfur). Fuels with an increased concentration of fine particles or volatiles yielded higher tar loads in the product gas. The results emphasize that devolatilization is a crucial step in the gasification process. During devolatilization, volatile matter is released, also in addition to nitrogen, sulfur and chlorine. Volatile matter contains higher hydrocarbons, the primary tar. In subsequent reactions with steam, char and catalytic bed material, volatile matter is converted into product gas. For these reactions, the residence time in contact with the bed material is of great importance and, therefore, the location of volatile release. In the case of small fuel particles or on-bed feeding, the volatiles are more likely to be released in the splash zone or the freeboard with limited contact with the bed material. Thus, the product gas contained more tar and the gas composition deviated more from the water-gas shift equilibrium. It was also demonstrated, that interactions and synergistic effects occurred within plastic mixtures and co-gasification of biomass and plastics. An important synergistic effect is that wood char considerably lowered the tar formation from plastic materials. The product gas composition and other process parameters cannot be accurately predicted from the gasification of single substances. This also highlights the relevance of pilot plant experiments.

When residues and waste are used as feedstock, product gas cleaning is a crucial part of the DFB gasification process. For nitrogen and sulfur rich fuels, product gas scrubbers or other suitable cleaning devices are required according to the emission legislation. For fuels with an increased tendency towards tar formation, several measures are conceivable. In order to increase the gas-solid contact, not only the location of the feed point should be considered, but also the design of the gasification reactor itself. For product gases with high tar load, the downstream equipment of the gasifier also has to be adapted. Careful considerations are required in the design of the heat exchanger and the tar scrubber.

In a final analysis, this thesis demonstrates, that DFB gasification is suitable for residues and waste and that it is a conceivable process for the chemical recycling of these materials.

Kurzfassung

Biomasse kann in Zweibett-Wirbelschichtvergasungsanlagen mit hohem Wirkungsgrad zu Wasserstoff, Kohlenmonoxid und anderen brennbaren Gasen umgesetzt werden. Dieses Produktgas ist nicht nur zur Strom- und Wärmeerzeugung geeignet, sondern auch für chemische Synthesen von gasförmigen und flüssigen Treibstoffen und anderen Chemikalien. In dieser Dissertation wird nun die Erweiterung der Brennstoffpalette dieses Verfahrens auf Abfall- und Reststoff untersucht. Aus einer fortschrittlichen Reststoffvergasung können erhebliche Vorteile gezogen werden, wenn diese Materialen preisgünstig und in großen Mengen verfügbar sind. Außerdem kann der Vergasungsprozess zum chemischen Recycling der Reststoffe eingesetzt werden.

An der TU Wien steht eine 100 kW Technikumsanlage für Forschungszwecke zur Verfügung, die auf dem Prinzip der Zweibett-Wirbelschichtvergasung basiert. Umfassende Messeinrichtungen dienen der Datenaufzeichnung und der Beurteilung des Prozesses. Da die Prozessbedingungen in der Technikumsanlage gut mit jenen der industriellen Zweibett-Wirbelschichtanlagen übereinstimmen, können an Hand der Versuchsergebnisse Aussagen für industrielle Anwendungen getroffen werden. In dieser Technikumsanlage wurden verschiedene Arten von Altholz, Sägespäne, Autoshredder-Kunststoffe, Produktionsrückstände aus der Kunststofferzeugung sowie Regranulat getestet. Der Versuchsbetrieb zeigt, dass diese Materialien ohne Einschränkungen und problemlos vergast werden können und daher die Vergasung dieser Stoffe in der Zweibettwirbelschicht technisch machbar ist.

In der vorliegenden Dissertation wird außerdem der Einfluss verschiedener Brennstoffeigenschaften auf die Vergasung behandelt. Abfall- und Reststoffe sind zumeist inhomogen und von stark unterschiedlicher Qualität und stellen daher Herausforderungen für den Betrieb der Vergasungsanlage dar. Drei unterschiedliche Eigenschaften werden ausführlich beschrieben: i) Brennstoffe mit hohem Stickstoff-, Schwefel- und Chlorgehalt, ii) Brennstoff mit einem hohen Feinanteil und iii) Brennstoffe mit sehr hohem Flüchtigengehalt. Des Weiteren wird der Einfluss des Brennstoffeintrags in die Wirbelschicht untersucht.

Das Produktgas wird deutlich durch die vorhin genannten Brennstoffeigenschaften beeinflusst. Stickstoff, Schwefel und Chlor aus dem Brennstoff werden bei der Vergasung zu größten Teilen in das Produktgas übergeführt, entweder in Form von Gasen (Stickstoff als NH_3, Schwefel als H_2S) oder in Form von Asche (Schwefel und Chlor). Brennstoffe, die hohe Konzentrationen an kleinen Partikeln oder an Flüchtigen aufweisen, führen zu einer höheren Teerbildung. Die Versuchsergebnisse unterstreichen die besondere Bedeutung der pyrolytischen Zersetzung bei der Vergasung. Während der pyrolytischen Zersetzung werden die Flüchtigen Bestandteile des Brennstoffes freigesetzt, dabei auch Stickstoff, Schwefel und Chlor. In den Flüchtigen sind auch langkettige Kohlenwasserstoffverbindungen, die primären Teere, enthalten. Durch die Reaktionen mit Dampf, Koks und katalytischem Bettmaterial reagieren die Flüchtigen weiter zum Produktgas. Für den möglichst vollständigen Ablauf dieser Reaktionen ist der ausreichende Kontakt zum katalytischen Bettmaterial und damit die Verweilzeit in der Wirbelschicht von großer Bedeutung. Die Verweilzeit der Flüchtigen in der Wirbelschicht wird maßgeblich durch den Ort der pyrolytischen Zersetzung des Brennstoffpartikels bestimmt. Enthält der Brennstoff viele kleine Partikel oder wird der Brennstoff oberhalb des Wirbelbettes

eingebracht, werden die Flüchtigen sehr wahrscheinlich in der Splashzone oder im Freeboard freigesetzt, wo sie nur kurz mit dem Bettmaterial in Kontakt kommen. Daher enthält das Produktgas mehr Teer und die Gaszusammensetzung weicht stärker von den Gleichgewichtskonzentrationen der Wasser-Gas-Shift-Reaktion ab. Die Versuche zeigten außerdem, dass bei der Co-Vergasung von Biomasse und Kunststoffen synergetische Wechselwirkungen zwischen den Brennstoffen auftreten. Biomassekoks reduziert zum Beispiel den Teergehalt des Produktgases deutlich im Vergleich zur Vergasung von reinen Kunststoffen. Durch die Wechselwirkungen können die Produktgaszusammensetzung und andere Prozessgrößen nicht durch Vergasung der Einzelsubstanzen vorhergesagt werden. Das wiederum verdeutlicht die Bedeutung von Versuchsläufen in der Technikumsanlage.

Werden Abfälle und Reststoffe in Vergasungsanlagen eingesetzt, spielt die Produktgasreinigung eine große Rolle. Bei stickstoff- und schwefelreichen Brennstoffen müssen je nach gesetzlichen Emissionsgrenzwerten Wäscher oder andere, geeignete Gasreinigungsstufen vorgesehen werden. Bei Brennstoffen, die zu verstärkter Teerbildung neigen, sind verschiedene Maßnahmen denkbar. Der Kontakt von Gas und Bettmaterial wird stark durch die Art des Brennstoffeintrags beeinflusst. Außerdem kann der Kontakt durch konstruktive Veränderungen im Vergasungsreaktor selbst erhöht werden. Bei hohen Teergehalten im Produktgas ist außerdem die Ausführung der Wärmetauscher und der Teerwäscher von großer Bedeutung.

Zusammenfassend kann festgestellt werden, dass die Zweibett-Wirbelschichtvergasung für die Vergasung von Abfall- und Reststoffen geeignet ist und einen möglichen Prozess für chemisches Recycling dieser Materialen darstellt.

Danksagung

Mein besonderer Dank gilt Herrn Univ.-Prof. Dipl.-Ing. Dr. Hermann Hofbauer für die Möglichkeit, diese Dissertation verfassen zu können, die ausgezeichnete Betreuung, die interessanten Diskussionen und die zahlreichen Anregungen.

Auch möchte ich Herrn Prof. Umberto Arena von der Seconda Università di Napoli für die externe Begutachtung und die gründliche Durchsicht der Arbeit danken.

Großer Dank gebührt meinen Kollegen, insbesondere Stefan Kern, Fritz Kirnbauer, Hannes Kitzler, Stefan Koppatz, Johannes Schmid und Christoph Varga für die gute Zusammenarbeit bei den Versuchen, die hilfreichen Diskussionen und die schöne, gemeinsame Zeit.

Diese Dissertation ist im Rahmen des Forschungszentrums Bioenergy2020+ GmbH entstanden, das von der Österreichischen Forschungsförderungsgesellschaft im COMET Programm gefördert wird. Ich möchte den Firmenpartnern für ihre fachliche und finanzielle Unterstützung danken: Magna International AG, Repotec Umwelttechnik GmbH und Biomasse-Kraftwerk-Güssing GmbH. Für den praktische Teil der Arbeit waren verschiedene Brennstoffproben unerlässlich, daher möchte ich folgenden Firmen für die großzügige Überlassung der Reststoffe danken: EnergieAG Oberösterreich Kraftwerke AG, AVE Österreich GmbH, TBS Technische Behandlungssysteme GmbH, Stadtreinigung Hamburg GmbH, Mayr-Melnhof Pellets Leoben GmbH, Borealis Polyolefine GmbH Austria und Universität Ljubljana.

Ein sehr herzlicher Dank gilt meinen Eltern und meinem Freund Andreas, die alle auf ihre Weise zum Gelingen dieser Arbeit beigetragen haben.

Table of content

Figures and tables

List of publications relevant for this thesis

I	V. Wilk, H. Hofbauer. Conversion of fuel nitrogen in a dual fluidized bed steam gasifier. Fuel 106: 793-801(2013).
II	V. Wilk, C. Aichernig, H. Hofbauer. Waste wood gasification: Distribution of nitrogen, sulphur and chlorine in a dual fluidised bed steam gasifier. In Pugsley, T. et al, editors, Proceedings oft he International Conference on Circulating Fluidized Bed Technology (CFB10), Sunriver, Oregon, USA, May 1-5, 2011, pp. 209-216.
III	V. Wilk, H. Hofbauer. Influence of fuel particle size on gasification in a dual fluidized bed steam gasifier. Fuel Processing Technology 115: 139-151 (2013).
IV	V. Wilk, H. Hofbauer. Conversion of mixed plastic wastes in a dual fluidized bed steam gasifier. Fuel 107: 787-799 (2013).
V	V. Wilk, H. Hofbauer: Co-gasification of biomass and plastics in a dual fluidized bed steam gasifier. Energy & Fuels 27(6): 3261-3273 (2013).
VI	V. Wilk, J.C. Schmid, H. Hofbauer. Influence of fuel feeding positions on gasification in dual fluidized bed gasifiers. Biomass and Bioenergy 54: 46-58 (2013).

Contributions by the author:

I, II, III, IV, V	Responsible for experimental work, data evaluation and writing
VI	Responsible for data evaluation, partially responsible for experimental work and writing

Other publications

Several other papers have been published in the course of this work. They are not considered in the thesis, as either their content is not closely related to the core topic or they overlap with publications included in the thesis.

Journal publications

V. Wilk, H. Kitzler, S. Koppatz, C. Pfeifer, H. Hofbauer. Gasification of waste wood and bark in a dual fluidized bed steam gasifier. Biomass Conversion and Biorefinery 1(2): 91-97 (2011).

F. Kirnbauer, V. Wilk, H. Hofbauer. Performance improvement of dual fluidized bed gasifiers by temperature reduction: The behavior of tar species in the product gas. Fuel 108: 534-542 (2013).

F. Kirnbauer, V. Wilk, H. Hofbauer. The positive effects of bed material coating on tar reduction in a dual fluidized bed gasifier. Fuel 95: 553-562 (2012).

Peer-reviewed conferences

V. Wilk, H. Hofbauer. Influence of physical properties of the feedstock on gasification in a dual fluidized bed steam gasifier. In Proceedings of the 21FBC, Naples, Italy (2012).

V. Wilk, S. Kern, H. Kitzler, S. Koppatz, J.C. Schmid, H. Hofbauer. Gasification of plastic residues in a dual fluidized bed gasifier – Characteristics and performance compared to biomass. In Proceedings of the International Conference on Polygeneration Strategies (ICPS11), Vienna, Austria (2011).

Abstract reviewed conferences

V. Wilk, H. Hofbauer. Steam gasification of challenging fuels in the dual fluidized bed gasifier. In Proceedings of the 21h European Biomass Conference and Exhibition, Copenhagen, Denmark (2013).

V. Wilk, H. Hofbauer. Investigation of the thermal conversion behavior of polyethylene mixtures in a dual fluidized bed gasifier. 3rd International Symposium on Gasification and its Applications, Vancouver, Canada (2012).

V. Wilk, H. Hofbauer. Gasification: an innovative approach for the thermal treatment of plastic residues. In Proceedings of the 6th International Symposium on Feedstock Recycling of Polymeric Materials (ISFR), Toledo, Spain (2011).

V. Wilk, H. Hofbauer. Waste wood: from gasification tests in the pilot plant to simulation of industrial applications. In Proceedings of the 19th European Biomass Conference and Exhibition, Berlin, Germany (2011).

V. Wilk, H. Kitzler, S. Koppatz, C. Pfeifer, H. Hofbauer. Gasification of residues and waste wood in a dual fluidized bed steam gasifier. In Proceedings of the International Conference on Polygeneration Strategies (ICPS10), Leipzig, Germany (2010).

V. Wilk, H. Hofbauer. Efficient ulitisation of industrial residues and waste with high biomass content using gasification technology. In Proceedings of the 18th European Biomass Conference and Exhibition, Lyon, France (2010).

1 Background and motivation

The world has to face crucial challenges in the coming years. According to an OECD study [1], the size of the world economy is expected to double and the global population to grow by one-third by 2030. Rising incomes and standard of living drive the global consumption of fossil fuels, minerals, metals, timber and food crops. Intensified land-use and resource depletion generate pressure on the environment. Krausmann et al. published a comprehensive review [2] in 2009 on global material use and showed that raw material consumption has almost doubled since 1975 (Figure 1.1). A total of 60 billion tons of raw materials were used world-wide in 2005. It can be assumed that material use continued to increase thereafter.

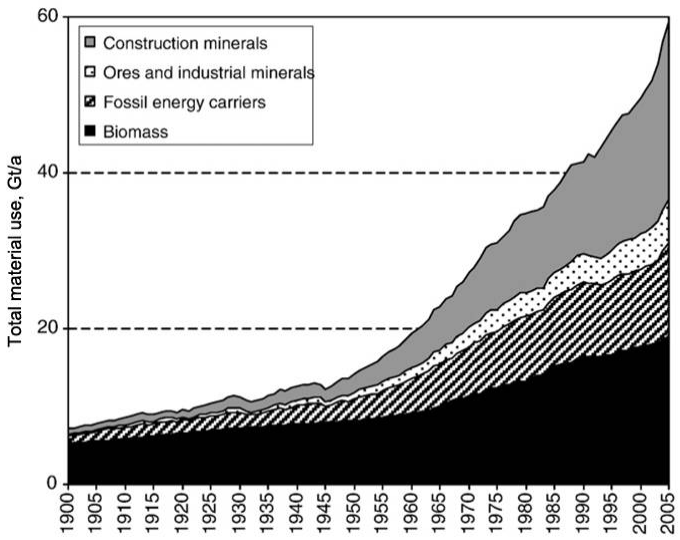

Figure 1.1: Global material use in gigatons per year, [2]

A report of the United Nations Environment Program (UNEP) lists the global change trends: urbanization, resource scarcity and increasing uncertainty because of economic, financial, environmental, and climate change. Urbanization is predominately increasing in Africa and Asia, which is considered the second wave of urbanization. It is projected that roughly 80% of the global population will live in urban areas by 2050 [3]. Concerning energy consumption, the International Energy Agency (IEA) subsumed the challenges as to satisfying the continuously growing global energy demand; providing access to energy for everybody and counteracting climate change and global warming. Figure 1.2 depicts the global primary energy demand of the last 20 years and forecasts for different environmental and energy policy scenarios. The greatest increase in primary energy demand occurs in the “Current Policies Scenario”. It assumes that the environmental and energy policies of 2012 are maintained without any changes. The “New Policies Scenario” considers plans that already have been announced by countries to reduce greenhouse gas emissions or substitute fossil fuels, even though the measures for how to achieve the proposals, are not yet identified. The smallest increase in primary energy demand is projected for the “450 Scenario”, which limits the CO_2 concentration in the atmosphere to 450 ppm so that the global increase in temperature will not exceed 2°C. Nevertheless, the global energy demand rises in all scenarios. [4]

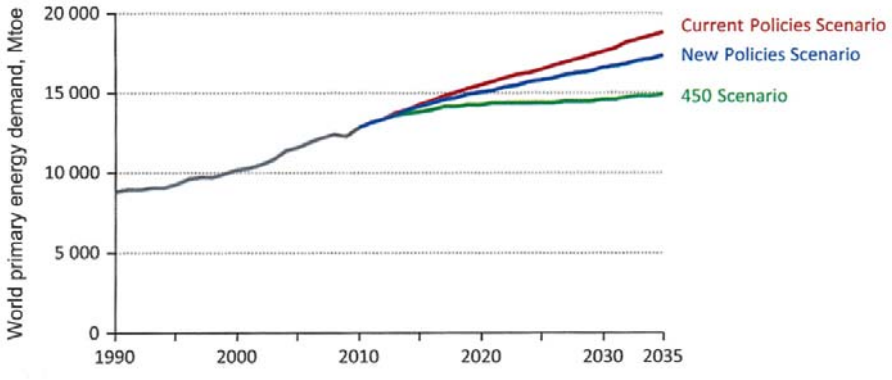

Figure 1.2: World primary energy demand projected for environmental policy scenarios, [4]

All these challenges are known and have been discussed since the 1970s, but have become more and more severe now. The ecological demand of humanity has increased steadily over time, which is illustrated in Figure 1.3. Here, the productivity of the biosphere and the consumption are compared based on the surface area of the earth. From the 1980s onwards, the annual demand for natural capital has exceeded the regenerative capacity of the earth. [5]

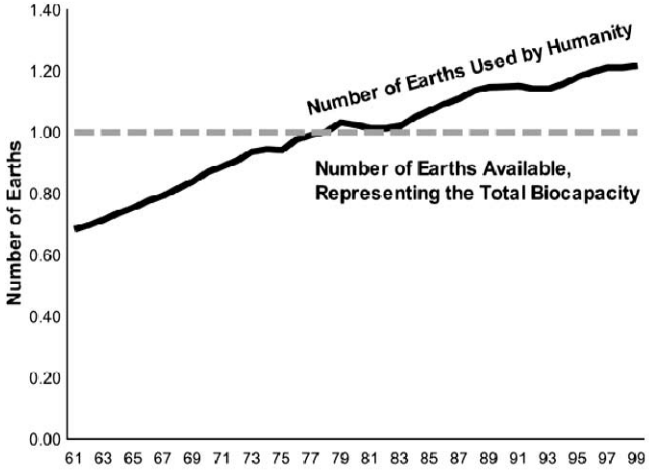

Figure 1.3: Time trend of humanity's ecological demand, [5]

Among the earliest publications addressing the finitude of natural resources was the "Limits of Growth" report commissioned by the Club of Rome in 1972. A group of scientists studied the interaction of population growth and natural resource use and pronounced for the first time that there are limits to industrial growth. [6] Sustainable development had already been identified as being suitable to address all these challenges by 1987. The United Nation World Commission on Environment and Development, also known as the Brundtland Commission [7], defined sustainable development as "[…] development that meets the needs of the present without compromising the ability of future generations to meet their own needs. It contains within it two key concepts: the concept of needs, in particular the essential needs of the world's poor, to which overriding priority should be given; and the idea of limitations imposed by the state of technology and social organization on the environment's ability to meet present and future

needs." In this sense, the sustainable use of resources requires the decoupling of material consumption from economic growth.

For several decades, there are have been international efforts to promote sustainability in the framework of national and international initiatives with the United Nations Commission of Sustainable Development leading the way. Numerous initiatives focus on resource efficiency; in the following some examples are given. UNEP started an initiative for sustainable and resource efficient cities, that are significantly decoupled from resource exploitation and environmental impacts [8]. Also the OECD has been working on policies and recommendations for sustainable materials management [9]. The European Union launched a flagship initiative under the Europe 2020 Strategy for resource efficiency. It provides a long-term action plan that aims toward a resource-efficient, low-carbon economy in order to achieve sustainable growth. Among the first member states of the EU, Austria adopted the Austrian Resource Efficiency Action Plan (REAP) in 2012. The G8 states also emphasize on efficient use of resources and materials and promote the "3Rs" (reduce, reuse and recycle). Based on the "3Rs", Japan created its waste management initiative, "A sound material cycle society". [10] In addition to the common aim of sustainable materials use, all these initiatives also want to bring about a reduction in resource imports, a more secure resource supply, cost reductions and enhanced innovation and new technologies.

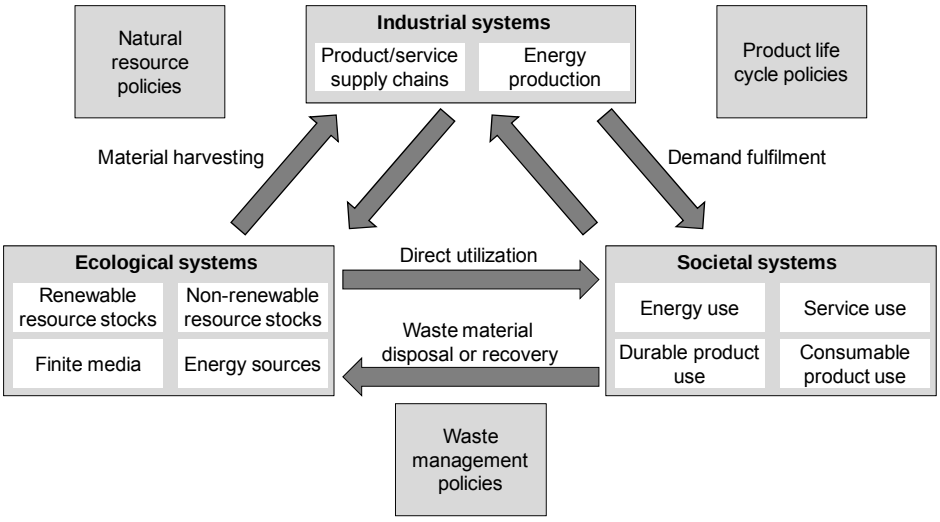

Figure 1.4: Sustainable material management, adapted from [11]

The interaction of natural resource use and the natural environment is illustrated in Figure 1.4. The material flow cycles of the earth are schematically broken down into three interconnected systems: ecological, industrial and societal. The ecological systems describe the biosphere and comprise renewable and non-renewable resource stocks, such as forests or fossil fuels, finite media and sources of energy. Finite media are air, land or water, which cannot be depleted, but can be polluted. Sources of energy contain solar, wind or tidal energy. The industrial systems consist of product or service supply and energy production, which consume natural resources and provide products and energy. The societal systems use products, energy and services provided by the industrial systems and generate waste, which is returned to the environment. [11]

Especially waste streams are of interest to increase resource efficiency, as they are considered as potential resources for new products. All initiatives mentioned focus amongst other measures on the reuse of waste materials. Thus, virgin material extraction, waste disposal and their related negative effects on the environment can be reduced.

1.1 Overview on waste generation

All kinds of human activity generate waste, hence the sources and types of waste are numerous and diverse. According to the European Waste Framework Directive [12], waste is any substance or object the holder discards, intends to discard or is required to discard. Most commonly, the different types of waste are distinguished based on their origin, such as waste from households, industrial waste, commercial waste, waste from agriculture, waste from mining and quarrying, etc.

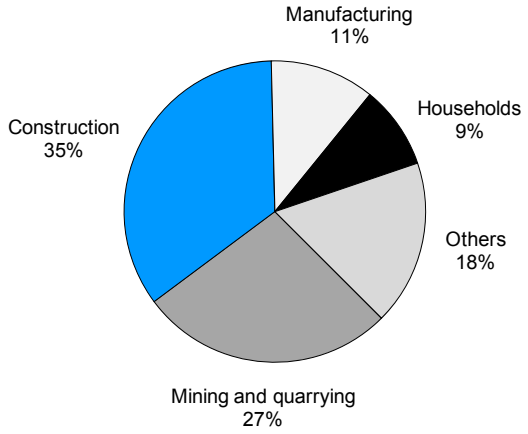

Figure 1.5: Waste generation by economic sector in the EU27 countries in 2010, [13]

Figure 1.5 presents the share of the different types of waste in the European Union in 2010 based on economic sectors [13]. The largest proportions of waste stem from construction (35%) and from mining and quarrying activities (27%). Waste from construction is generated by the erection and demolition of buildings or civil infrastructure. Mining and quarrying comprises all activities related to the extraction and processing of mineral resources. Both types of waste mainly consist of minerals and are non-combustible. Another 11% of waste accumulates in the manufacturing sector, an important part of the European industry. Manufacturing comprises all sorts of mechanical, physical or chemical processes used to transform materials into new products, such as food, paper, chemicals, electronic products, medicines, and much more. Therefore, the composition of manufacturing waste covers a wide range. In 2010, a total of 9% of waste was generated by households. This type of waste is collected by municipal authorities. It is mainly non-mineral and comprises recyclable materials, such as paper, plastics, metals, but also other mixed solid wastes. There are also other sources of waste that are summarized in Figure 1.5 as “Others”, for example waste from services, from the electricity supply (combustion residues of power plants), waste collection and treatment, or water treatment (sewage system).

Waste from households is an important waste stream because its amount increases all over the world as a consequence of urbanization, increasing consumption and the standard of living. According to UNEP, urban areas consume 75% of the natural resources and produce 50% of

the total amount of waste in the world. [3] Especially in densely populated urban areas, waste collection and treatment is of high importance. The amount and composition of solid waste from households is closely related to the standard of living. Figure 1.6 shows, how much waste is generated by urban areas all over the world and illustrates the projected increase by 2025. The countries are grouped according to their income level. It is evident, that high income countries produce the highest amount of waste per capita, the amount decreases with a decrease in income. Figure 1.7 illustrates the differences in urban waste composition per income level. In high income countries solid waste contains a high share of packaging materials and disposable products. By contrast, organic content is the highest in low income countries.

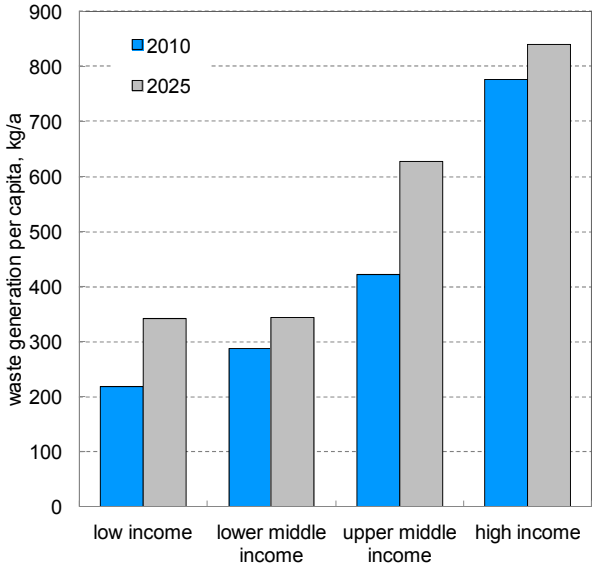

Figure 1.6: Waste generation per capita and income throughout the world, [14]

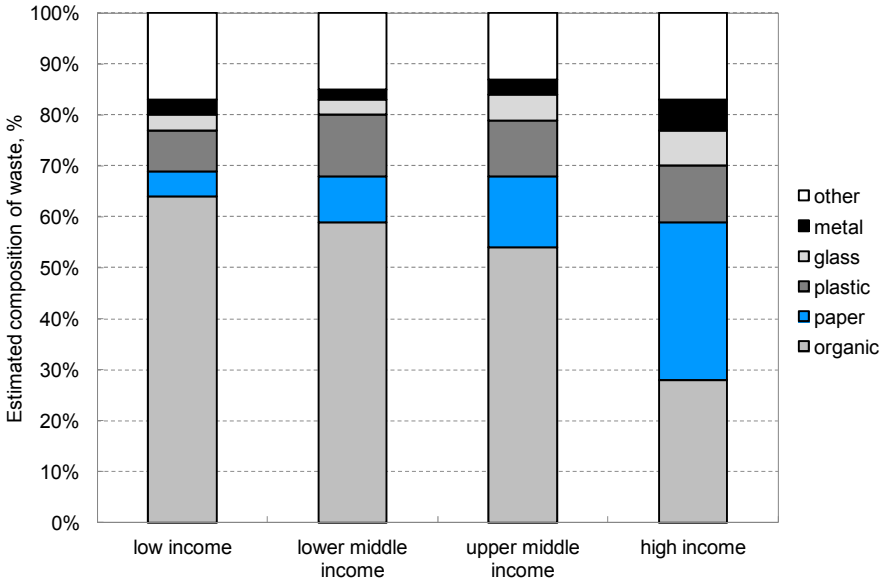

Figure 1.7: Solid waste composition by income, [14]

1.2 Waste management in the world

As it is apparent from Figure 1.7, solid waste contains a significant amount of recyclable materials, such as paper, glass, metals or plastics. Whether recycling or other ways of recovery or disposal are applied, depends on the waste management system in the respective country. The data for Figure 1.8 is retrieved from a World Bank report. Although quantitative data on waste disposal is the most difficult to obtain, it is shown that most low and lower middle income countries dispose of their waste in open dumps. In high income countries, recycling, incineration and composting are also applied, which reduces the share of landfilling. [14]

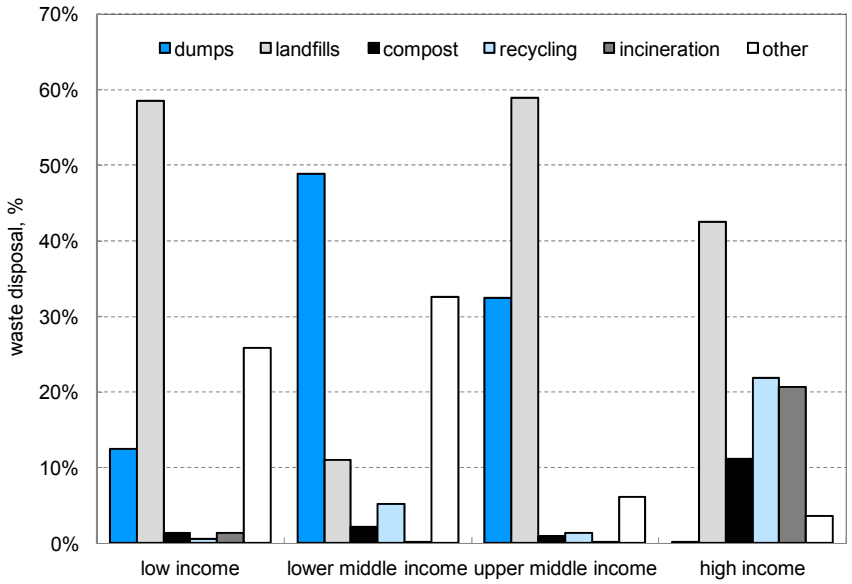

Figure 1.8: Waste disposal by income, [14]

1.3 Waste management in the European Union

In the EU, the Waste Framework Directive [12] defines some basic principles of waste management and emphasizes the reuse and recycling of waste. For that purpose, a five stage waste hierarchy has been established. It provides an order of preference for waste operations that appears in Figure 1.9.

1) Prevention
2) Preparing for re-use
3) Recycling
4) Recovery (e.g. energy recovery)
5) Disposal

Waste prevention is given the highest priority and summarizes all measures that reduce the quantity of waste, the concentration of harmful substances in waste and the negative impacts on environment and health. Measures for waste prevention aim for example at improved manufacturing methods, reduced use of substances, enhanced repair and reuse, as well as increased consumer awareness. As waste prevention addresses the manufacturing process and the use of the product, an extended producer responsibility is also part of the Waste Framework Directive. It implies that the producer also has to take responsibility for the after-life

of the product. [12] Four different options are distinguished for waste materials. Preparing for re-use is for example cleaning or repair of used products, so that they can be re-used. All other recovery operations, that reprocess waste into products are considered as recycling. Recycling is crucial for resource efficiency, as it provides secondary raw materials from waste. It can be distinguished between pre- and post-consumer recycling, the former taking place during production, when production residues are recycled during the process and the latter, when valuable materials are reclaimed from post-consumer waste streams. Recycling focuses on the use of the material itself and does not include energy recovery or the production of fuels, which are considered as recovery operations. Recovery of waste takes place, when a waste material serves as a useful purpose and replaces other materials, for example energy supply and fuel production. The least favorable option is disposal, which is most commonly landfill. [12]

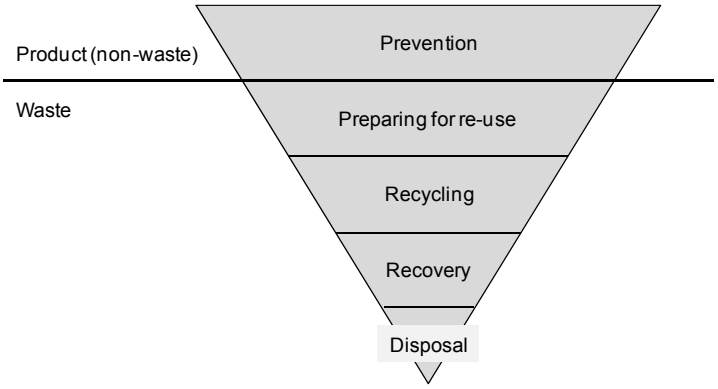

Figure 1.9: Waste hierarchy

For the successful implementation of the waste hierarchy, it is critical to clearly distinguish between products, residues, by-products and waste. Figure 1.10 illustrates the distinction of products, residues, by-products and waste for a production process based on EU legislation [15]. Products are deliberately produced and they are the purpose of the process. Production residues also occur, which are not the products of the process and which may or may not be waste. These residues are considered as by-products if there is a certain use for them, if they do not require further processing prior to use, and if they are produced as an integral part of the production process. For by-products, all three conditions have to be fulfilled. Production residues are classified as waste, if their use is uncertain, if they require further processing prior to use, if there is no market for the material or if it requires an indefinite amount of time to store it prior to a potential, but uncertain use.

Waste should be recycling and recovered according to the waste hierarchy. Due to waste treatment, waste ceases to be waste when it becomes a new product or secondary raw material. Therefore end-of-waste criteria are also defined in the Waste Framework Directive. Waste is no longer waste if the processed material is commonly used for specific purposes and if there is an existing or potential market for it. It is also crucial, that its use of the material is lawful and the use will not lead to overall adverse environmental or human health impacts. [12] An end-of-waste methodology has been developed for priority waste streams, such as iron, steel and aluminum scrap, and is in preparation for paper, glass, plastics and others.

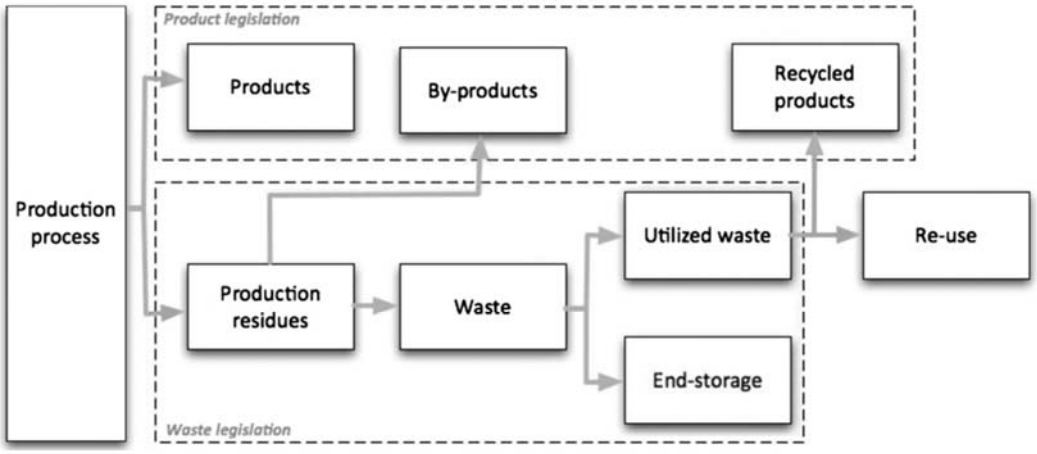

Figure 1.10: Distinction of products, residues, by-products and waste, [16]

When producing secondary raw materials, recycling is very important to achieve resource efficiency. Increased recycling rates will reduce the demand for primary raw materials and reduce energy consumption and greenhouse gas emissions from extraction and processing. [17] The EU targets at a recycling rate of 50% for glass, paper, plastics and metals and a recycling rate of 70% for construction and demolition waste by 2020. [12]

Therefore, viable and efficient recycling technologies are necessary and are now the scope of applied research. In this respect, gasification is a promising technology not only for future energy supply, but also for chemical recycling. By means of gasification, solid materials that contain carbon, such as biomass, coal, residues and waste are converted into product gas. The gas mainly consists of H_2, CO, CO_2 and CH_4 and can be further used for heat and power generation, and also for chemical synthesis processes. In this sense, gasification offers a novel approach for chemical recycling.

2 Steam gasification

Gasification is the conversion of carbonaceous solids into combustible gases by reaction with gasification agents. Oxygen, steam, carbon dioxide and hydrogen can be used as gasification agents. In practical applications only air, steam or steam-oxygen mixtures are used as gasification agents. Conventional air gasification yields a product gas which is highly diluted with nitrogen and as a consequence has a lower calorific value (LCV) of 4-6 MJ/m³. In contrast, steam gasification allows the generation of a nitrogen free product gas without the use of pure oxygen as a gasification agent. The LCV is in the range of 12-14 MJ/m³. Due to absence of nitrogen, product gas from steam gasification is suitable for chemical synthesis processes. This chapter presents fundamentals of steam gasification.

2.1 Sub-processes, reactions and product gas properties

Gasification of solid materials consists of three sub-processes: drying, devolatilization and gasification. When feedstock is heated, it is first dried at 100-150°C and water is released. With a further increase in temperature, devolatilization occurs. It is a heat-induced decomposition mechanism, where macromolecules in the feedstock are destroyed. They are released as gases and vapors, generally referred to as volatile matter and char is formed. Devolatilization is not influenced by the gasification agent, because the escaping gases prevent the contact of the particle and the gasification agent. When devolatilization is finished, residual char reacts with steam and is thereby converted into combustible carbonaceous gases. Secondary reactions, which are mostly gas-gas reactions, occur and determine the final composition of the product gas. Gasification requires temperatures above approximately 700°C and the overall energy balance of the gasification reactions is endothermic. Heat can either be supplied by partial combustion of the fuel (autothermal process) or can be transferred by heat exchanger or bed material from another reactor, where heat is generated by combustion (allothermal process).

During the gasification process, numerous reactions take place simultaneously, which are compiled in Table 2.1. Their reaction enthalpies were calculated using the NASA polynomials [18]. Heterogeneous reactions of solid carbon with gases comprise oxidation and reduction reactions. Both the partial and complete oxidation of carbon provide heat (Eqs. 2.1 and 2.2) if oxygen is available e.g in autothermal air gasification processes. The major part of combustible gases is formed by reduction reactions, which are endothermic, such as the water gas reaction (Eq. 2.3) and the Boudouard reaction (Eq. 2.4). Solid carbon can also be gasified by reaction with H_2 (Eq. 2.5). The gases yielded from drying, devolatilization and char gasification continue to react in homogeneous reactions (Eqs. 2.6-2.11). In steam gasification processes, the water-gas shift reaction and steam reforming of methane (Eq. 2.6 and 2.7) are especially important.

The main product gas compounds are CO, H_2, CH_4, H_2O, and CO_2. Also contaminants are present, such as particles and tar. Inorganic ash and unreacted char can be entrained from the gasification reactor by the gas flow in the form of particles. Tar consists of condensable hydrocarbons that are formed during devolatilization. The concentration of tar depends on the residence time of the product gas at high temperatures and on the contact with the gasification agent. With sufficient contact, reforming of hydrocarbons occurs (Eq. 2.11) and reduces the tar

content. Tar is thermally destroyed completely above 1200°C. Tar has to be removed from the product gas, because they form depositions, when the gas is cooled. In addition, disposal of tar constitutes an environmental problem. Thus, the formation of tar should be minimized. [19]

Table 2.1: Gasification reactions

$C + O_2 \rightarrow CO_2$	$\Delta H_{R,298}$ = -393.4 kJ/mol	(2.1)
$C + ½\ O_2 \rightarrow CO$	$\Delta H_{R,298}$ = -110.5 kJ/mol	(2.2)
$C + H_2O \rightarrow CO + H_2$	$\Delta H_{R,298}$ = +131.3 kJ/mol	(2.3)
$C + CO_2 \rightarrow 2CO$	$\Delta H_{R,298}$ = +172.4 kJ/mol	(2.4)
$C + 2H_2 \rightarrow CH_4$	$\Delta H_{R,298}$ = -74.9 kJ/mol	(2.5)
$CO + H_2O \leftrightarrow CO_2 + H_2$	$\Delta H_{R,298}$ = -41.2 kJ/mol	(2.6)
$CH_4 + H_2O \leftrightarrow CO + 3H_2$	$\Delta H_{R,298}$ = +206.2 kJ/mol	(2.7)
$CO + ½\ O_2 \rightarrow CO_2$	$\Delta H_{R,298}$ = -282.9 kJ/mol	(2.8)
$H_2 + ½\ O_2 \rightarrow ½\ H_2O$	$\Delta H_{R,298}$ = -241.8 kJ/mol	(2.9)
$CH_4 + CO_2 \leftrightarrow 2CO + 2H_2$	$\Delta H_{R,298}$ = -247.3 kJ/mol	(2.10)
$C_mH_n + mH_2O \rightarrow mCO + (m+ ½n)\ H_2$		(2.11)

2.2 Dual fluidized bed gasification

For gasification processes fluidized bed reactors are applied by preference. The good mixing conditions of fuel particles, bed material, and gas phase and an excellent heat transfer promote the conversion of the feedstock. Dual fluidized bed (DFB) gasification technology was developed at the Vienna University of Technology in the 1990s in order to establish an efficient conversion technology to produce electricity, heat, and fuels from solid biomass [20, 21]. The basic principle of the DFB reactor is illustrated in Figure 2.1. It is a steam gasification process, which is carried out in two reactors: an allothermal gasification reactor fluidized with steam and a combustion reactor fluidized with air that provides heat for gasification. The reactors are thermally connected by a circulating bed material. In the gasification reactor, biomass is devolatilized and the products of devolatilization react with steam to form the product gas[1]. Some ungasified char is transported with the bed material to the combustion reactor, where the char is combusted with air. The bed material is heated, separated from the flue gas, and returned to the gasification reactor. In most cases, fuel fed to the combustion reactor[2] is necessary to fulfill the energy demands of the gasification reactions and to obtain the desired temperature in the gasification reactor (e.g. 850°C). In the DFB gasifier, two separate gas

[1] also referred to as producer gas or syngas in the literature
[2] also referred to as auxiliary fuel in the literature

streams are yielded: product gas and conventional flue gas. Due to steam gasification, the product gas has a moderate LCV of 12–14 MJ/Nm³ and is rich in hydrogen (> 40%).

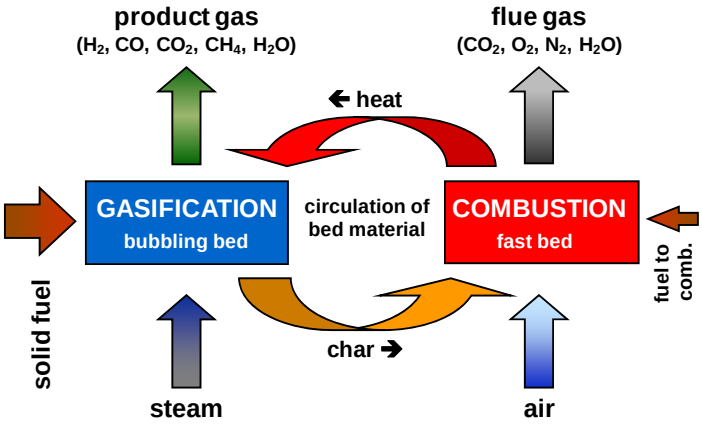

Figure 2.1: Principle of the DFB gasification process

The DFB gasification process has been successfully demonstrated in Güssing (Austria), where a DFB steam gasifier has been in operation at the scale of an 8 MW_{th} demonstration plant since late 2001. The gasifier is coupled to an internal combustion engine to produce 2 MW of electricity from the product gas. Process heat is fed into the local district heating system. This demonstration plant has now been in operation for more than 70,000 h; further information can be found in [22] and [23]. Today this technology is commercially available and several other industrial gasifiers based on DFB technology are in operation or currently under construction. The gasification plant in Oberwart (Austria) was commissioned in 2008; its average fuel input is 8.3 MW_{th}. The product gas is converted into electricity using two gas engines and an organic Rankine cycle (ORC) allowing valorization of low temperature heat. [24] In Villach (Austria) a 15 MW_{th} gasifier has been constructed. Gas engines are installed for power generation and heat is fed to the local district heating system. In summer time, heat from the gasification process is used to superheat steam from a nearby combustion plant. Thus, the low demand of district heat during summer time can be balanced. [25] More recently, a 15 MW_{th} gasifier has been built in Senden (Germany). Similar to the DFB gasifier in Oberwart, it is also equipped with gas engines and an ORC process to maximize the electricity output. [26]

Due to steam gasification the product gas is also well-suited for the synthesis of gaseous and liquid fuels such as synthetic natural gas, hydrogen, Fischer–Tropsch diesel and mixed alcohols. At the gasification plants in Güssing and Oberwart, synthesis processes are under investigation using the product gas from the DFB gasifiers [27-29]. The first industrial DFB plant producing synthetic natural gas will be realized in Gothenburg (Sweden) in the GoBiGas project [30]. There, the largest dual fluidized bed gasifier is about to be erected with a fuel input of 32 MW_{th}. The gasifier will be coupled to a methanation plant, where product gas is converted into synthetic natural gas, which will be fed into the local gas grid. It is planned to achieve a methane yield of 20 MW. [31]

2.3 Objective and relevance of this thesis

Commercially available, the DFB gasifier is a proven technology for the gasification of woody biomass. The existing industrial DFB gasifiers run on wood chips mainly from forestry. This steam gasification process could also be suitable for chemical recycling of carbonaceous materials that are present in residues and waste streams.

Therefore, one of the main objectives of this thesis is to extend the range of feedstock for the DFB gasification process towards residues and waste. However, these materials are mostly inhomogeneous, are of varying quality and are most commonly challenging fuels for gasification plants. For further investigation, several residues and waste materials have been selected: different kinds of waste wood, sawdust, various plastic residues and virgin polymers. In order to assess their suitability for the DFB process, these materials are analyzed in detail and gasified in a 100 kW pilot plant. This pilot plant is operated at the Vienna University of Technology for scientific purposes and is similar in design to the industrial DFB gasifiers.

Another objective of this work is to determine the influence of specific fuel properties. On the basis of the pilot plant experiments and the calculation of mass and energy balances, the influence of different fuels properties on the gasification performance is evaluated. In this respect, three aspects are investigated:

- fuels with high concentrations of nitrogen and sulfur (Paper I and II)
- fuels with increased concentrations of fine particles (Paper III)
- fuels with extremely high concentrations of volatiles (Paper IV and V)

These three properties can be found in nearly all residues and waste in varying extents. Due to the different nature of the selected materials, the different aspects can be varied one by one in the experiments. Their influence on gasification contributes to explaining the gasification process itself in more detail. In addition, the influence of the fuel feeding location is also analyzed, as fuel feeding is a crucial aspect, when residues and waste are employed (Paper VI).

3 Methodology

In this section methods and equipment applied in this thesis are described. For the experimental work a 100 kW gasification pilot plant was used. Extensive measurement equipment is installed at the pilot plant in order to assess the various process variables and concentrations of species. A process simulation tool was used to calculate mass and energy balances that provide all properties of the in and outgoing streams of the process. This approach yields all necessary data for a detailed assessment of the gasification process.

3.1 DFB pilot plant

At the Vienna University of Technology, a 100 kW pilot plant is available. Similar in design to industrial DFB gasifiers, the pilot plant is an essential tool for the evaluation of new feedstock, catalytic bed materials, and the further development of the DFB gasifier. A schematic illustration of the pilot plant is shown in Figure 3.1.

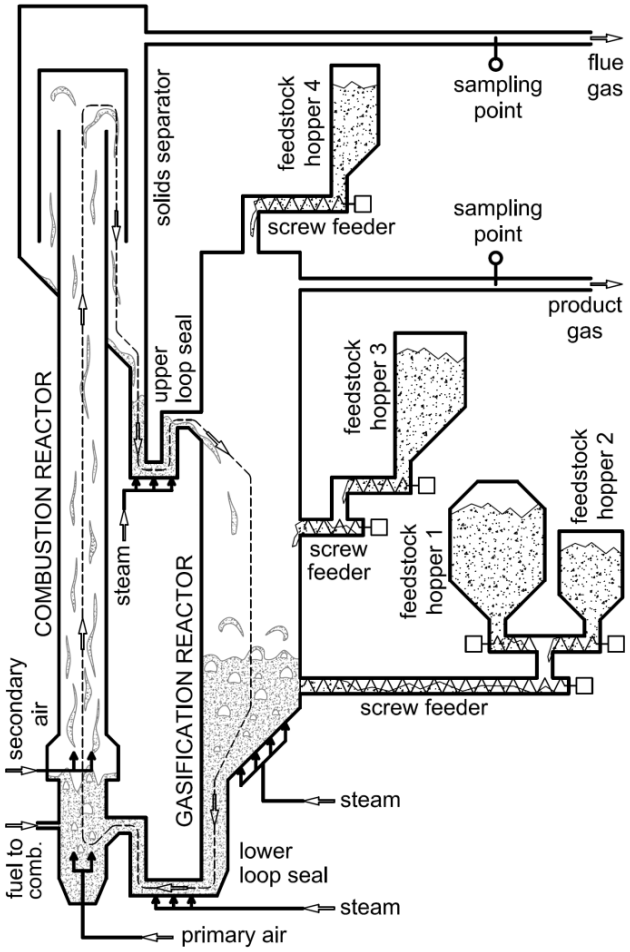

Figure 3.1: Schematic diagram of the 100 kW gasification pilot plant

The pilot plant provides flexibility for feedstock testing due to several gas-tight hoppers and screw feeders of different sizes. It is thus possible to feed material with a broad range of particle sizes and energy densities, to blend different materials for co-gasification, as well as to use different feed points located along the height of the reactor. Usually, the material is inserted directly into the fluidized bed by the screw conveyor of hoppers 1 and 2. Hopper 1 is designed for woody biomass, hopper 2 for coal. The screw feeder of hopper 3 is located above the fluidized bed and it is used for on-bed feeding of woody biomass. At the top of the gasification reactor, hopper 4 is installed, and is suitable for plastics or other material with high energy density. From this hopper, the material is also thrown onto the surface of the fluidized bed. For safety reasons, the hoppers are flushed with a constant stream of nitrogen.

Olivine is the preferred bed material for DFB gasification because it exhibits moderate tar cracking activity and offers good mechanical stability [32, 33]. Table 3.1 lists some properties of olivine as provided by an Austrian manufacturer, Magnolithe GmbH. A total of 100 kg of olivine is inserted in the gasification plant as bed material prior to the experiment. As different fuels are investigated in the pilot plant, the bed material is disposed of after each test run and fresh material is used, thus ensuring that all feedstock is tested in the same environment with regard to the bed material.

Table 3.1: Properties of olivine used in the pilot plant

Mean particle diameter d_{sv}	µm	566
Particle size range d_{p10}-d_{p90}	µm	400 – 660
Particle density	kg/m³	2850

In the gasification reactor a bubbling fluidized bed is created by superheated steam. The characteristic temperature of gasification is measured at the height, at which the screw feeder of hoppers 1 and 2 discharges the fuel into the bed. It is typically around 850°C. Loop seals are installed to connect the gasification and combustion reactor; these seals are fluidized with steam in order to efficiently prevent gas leakage between the two reactors and to promote the transport of solids.

In the combustion reactor, air is injected at two heights: primary air at the bottom of the reactor, where a dense fluidized bed is formed, and secondary air at a higher level in order to transport particles to the top of the reactor in a fast fluidized bed. In this reactor heat is generated via combustion, which determines the temperature in the gasification reactor. The gasification temperature is moderated according to the energy demand of the gasification reactions and the amount of ungasified char available for combustion. In addition to char from the feedstock, some fuel for combustion is inserted for temperature control. In industrial gasifiers, ungasified char that is transported with the bed material, as well as tar and char separated from the product gas are fed to the combustion reactor as fuel for combustion. As a matter of simplicity, light fuel oil is used in the pilot plant for this purpose. The temperature difference between the combustion and the gasification reactor amounts to 40-80°C on average. Bed material is precipitated from the flue gas stream of the combustion reactor and returned to the gasification reactor, where it supplies heat for endothermic gasification reactions. Table 3.2 lists some of the characteristics of the pilot plant.

Downstream equipment is not included in Figure 3.1. A heat exchanger is positioned after the gasification reactor, where the product gas is cooled to about 250°C before being sampled for analysis. Both product gas and flue gas are then mixed and combusted in a post-combustion chamber with air. A cyclone removes particles before the gas reaches the stack.

Table 3.2: Characteristics of the pilot plant

		Gasification reactor	Combustion reactor
Fluidization agent		steam	air
Fluidization regime		bubbling	fast fluidized
Reactor height	m	2.3	3.9
Reactor inner diameter	mm	304[a)]	98
Fluidization ratio U/U_{mf} [b)]		3-4	80-85
Fluidization ratio U/U_t [b)]		0.09-0.11	2.0-2.2

[a)] rectangular shape, diameter of a circle equivalent in area

[b)] calculated with complete product or flue gas formation

3.2 Typical pilot plant operation

Table 3.3 provides an overview of the key parameters for operation of the DFB pilot plant. The fuel input of the pilot plant was in the range of 90-100 kW. The target temperature in the gasification reactor is 850°C. This temperature was measured at the position of the in-bed feed point. The gasification reactor was fluidized by 14-16 kg/h of steam in order to form a bubbling fluidized bed. The combustion reactor is fluidized by 54-56 Nm³/h of air, whereas primary air amounts to approximately 8-10% of the total air supply. The steam input was adjusted according to the fuel water content, so that the steam-to-carbon ratio was kept at 1.8 kg/kg. The steam-to-carbon ratio relates the mass flows of the fluidization steam and the fuel water to the mass flow of carbon of the fuel, Eq. 3.1.

$$\frac{S}{C} = \frac{\dot{m}_{H_2O,\,fluidization} + \dot{m}_{H_2O,\,feedstock}}{\dot{m}_{carbon,\,feedstock}} \tag{3.1}$$

Table 3.4 shows the average product gas composition when wood pellets are gasified in the pilot plant. Wood pellets are the standard fuel of the pilot plant and will be further described in chapter 4.3. Roughly speaking, 1 Nm³ of dry gas is generated from 1 kg of wood. The water content of the product gas amounts to 45 vol.-%.

Table 3.3: Typical operation parameters for the 100 kW pilot plant

Fuel input	kW	90 – 100
Gasification temperature	°C	850
Fluidization steam	kg/h	14 – 16
Combustion air	Nm³/h	54 – 56
Steam-to-carbon ratio	kg/kg	1.8

Table 3.4: Product gas from wood pellets

H_2	vol.-%, dry	40 – 43
CO	vol.-%, dry	26 – 28
CO_2	vol.-%, dry	19 – 21
CH_4	vol.-%, dry	8.5 – 10
C_2H_4	vol.-%, dry	1.5 – 2.5
C_2H_6	vol.-%, dry	0.2 – 0.4
C_3H_8	vol.-%, dry	0.1 – 0.2

3.3 Measuring equipment

Feedstock analysis is carried out according to international standards by the Test Laboratory for Combustion Systems at the Vienna University of Technology. The analysis usually comprises elemental composition and volatiles, water, and ash contents of the feedstock, as well as the ash melting behavior.

A wide array of measuring and automatic data recording equipment was used at the pilot plant for data acquisition and process control. Temperatures of up to 1000°C were measured with high temperature thermocouples, while high quality flow meters (Krohne) were employed for the adjustment of process media inputs such as the fluidization agents, steam and air. Pressures were measured along the height of the reactors using pressure sensors relative to ambient pressure. Temperature and pressure measurements are the basis of an effective process control, which guarantees smooth operation of the pilot plant.

The main product gas components - H_2, CO, CO_2, CH_4, and O_2 - were measured online with a Rosemount NGA2000 device. C_2H_4, C_2H_6, N_2, and the sum of gaseous C_3- and C_4-hydrocarbons were analyzed with a Syntech Spectras GC 955 gas chromatograph, with a sample taken every 20 min. Over the course of this work, this gas chromatograph was replaced by a Perkin Elmar Arnel RGA1015, sampling every 15 min and analyzing N_2, C_2H_4, C_2H_6, and C_3H_8.

Tar measurement was based on an impinger bottle method developed at the Vienna University of Technology. Similar to the conventional tar protocol, this method was adapted for the analysis of product gas from steam gasification using toluene as the absorbent. Dust, entrained char, water, and tar contents can be analyzed using the same sample. A slip stream of product

gas was taken out after the heat exchanger by a heated probe. Solids in the gas (dust and char) were collected by a cyclone and a filter cartridge, which were heated to prevent condensation of tar and water. Tar was then dissolved in impinger bottles, which were filled with toluene and arranged in a cooling bath at -10 to -5 °C. Tar was also extracted from the solids in the cyclone and the filter cartridge and then the dust (inorganic) and char (organic) content were determined. Water in the product gas was condensed in the impinger bottles. As toluene is non-miscible with water, the water phase can be separated and determined volumetrically. Two different tar analyses were employed: gravimetric tars and GCMS tars. For the assessment of gravimetric tar, the solvent was evaporated and the residues were weighed. For GCMS tar, a GCMS device (gas chromatography with mass spectrometer) was used to measure the content of 50 different tar species of medium molecular weight in the product gas. For easier comparison, they were grouped according to their chemical functionality based on [34]. Table 3.5 lists the substance groups and their constituents. The sum of these tar species was referred to as GCMS tar. As the measuring range of both analyses overlaps, both values are given. Figure 3.2 shows the gas sampling setup.

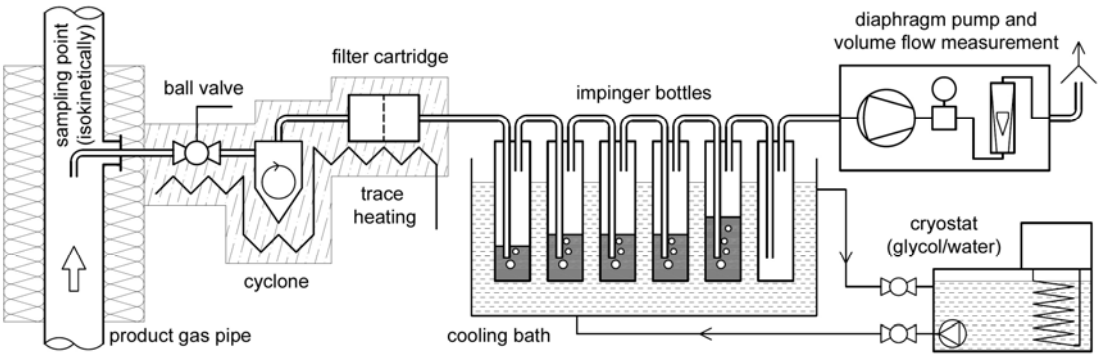

Figure 3.2: Gas sampling setup for tar measurement

An absorption method was also used for NH_3, HCN, H_2S and HCl sampling in the product gas. The sampling setup was similar to that used for tar measurement, whereas different solvents were applied. For NH_3 measurement the impinger bottles were partly filled with 0.05 M H_2SO_4, which solved NH_3 in the form of NH_4^+ ions. For HCl 0.3% H_2O_2 was used, so that Cl^- ions were formed. NH_4^+ and Cl^- ions were detected by ion chromatography (Dionex ICS 5000). H_2S and HCN were absorbed in impinger bottles filled with 35% KOH and were detected by potentiometric titration using $AgNO_3$ as the titrant and a silver electrode (Titrino 794 Basic).

In the flue gas of the combustion reactor, CO, CO_2, O_2, NO and SO_2 were measured by another Rosemount NGA2000 MLT4. For SO_2 a Binos 1004 was also used. The HCl concentration in the flue gas stream was analyzed with impinger bottles in the same way as in the product gas.

Table 3.5: GCMS tar substance groups

Group	Substance
Phenols	phenol, 2-methylphenol, 4-methylphenol, 2,6-methylphenol, 2,4-methylphenol, 2,5-methylphenol, 3,5-dimethylphenol, 2,3-dimethylphenol, 3,4-dimethylphenol, 2-methoxy-4-methylphenol, catechol
Furans	benzofuran, 2-methylbenzofuran, dibenzofuran
Aromatics	phenylacetylene, styrene, mesitylene, 1-H indene, 1-indanone
Naphthalenes	naphthalene, 2-methylnaphthalene, 1-methylnaphthalene
PAH	biphenyl, acenaphthylene, acenaphthene, flourene, anthracene, phenanthrene, 4,5-methylphenanthrene, 9-methylanthracene, flouranthene, pyrene, benz[a]anthracene, chrysene, benz[b]flouranthene, benz[k]flouranthene, benz[a]pyrene, benz[g,h,i]perylene, indeno[1,2,3-cd]pyrene, dibenz[a,h]anthracene

3.4 Process simulation with IPSEpro

For more detailed process description, the simulation software IPSEpro was applied. IPSEpro (Integrated Process Simulation Environment) is frequently used for process simulation of power plants in industry. It uses an equation-oriented solver for the calculation of mass and energy balances of stationary processes. The process, which should be analyzed in IPSEpro, is described as a flow diagram, which corresponds to the actual process setup. The flow diagram of the pilot plant appears in Figure 3.3. The units of the process (reactors, etc) are connected by streams transferring mass and energy. At Vienna University of Technology a comprehensive model library for gasification plants has been developed. This set of models comprises all necessary process units of a gasification plant, such as gasification and combustion reactor, filter, scrubber, heat exchanger, etc. The process units are balanced according to the conservation of mass and energy and can also contain related functional equations, such as kinetic properties or geometric correlations. Mass and energy balances are strictly fulfilled for all process units. Detailed information on the model library is available in [35]. Due to the model library for gasification plants, IPSEpro is a useful tool for process evaluation and for plant design of industrial gasifiers.

Mass and energy balances of gasification tests were also calculated with IPSEpro, because IPSEpro allows the use of measurement data containing uncertainty. For this purpose, measurement data of stationary operation of the pilot plant was used as input data for the flow diagram. An over-determinated equation system was formed, which contained the measurement data and a range of tolerance (e.g. the standard deviation of the measured value). The equation system was solved by the Method of Least Squares. More information on this procedure is provided in [36]. The reconciled solution best describes the actual operation of the pilot plant within the limits of the model.

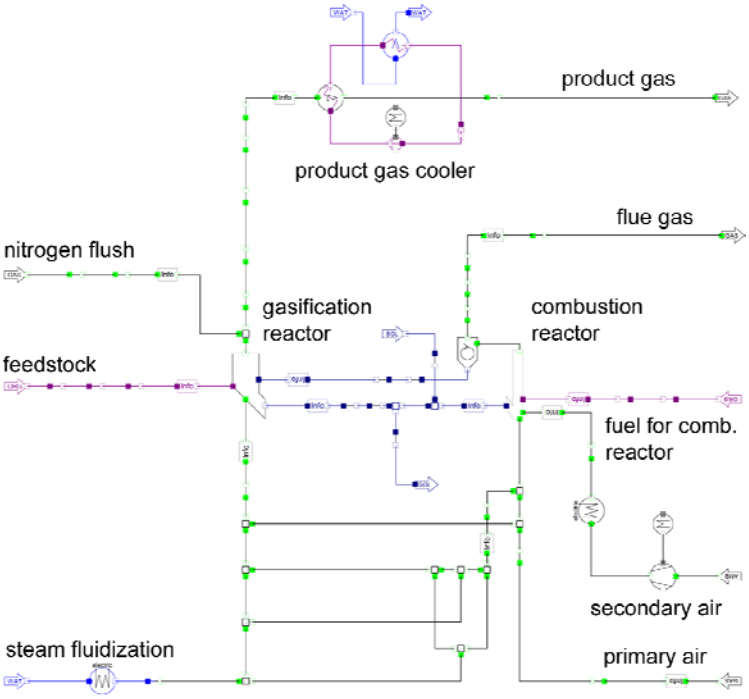

Figure 3.3: Flow diagram of the 100 kW pilot plant in IPSEpro

4 Selected residues and waste

Several materials have been selected for detailed investigation in this thesis: different kinds of waste wood and plastic residues from various origins. For comparison clean materials, such as wood pellets, sawdust, and virgin polymers were also considered. In the following, information on the origin of the residues, the current use and importance of the materials, as well as their physical and chemical properties are compiled.

4.1 Waste wood

In the European Union (EU27) 57 million tons of wood wastes were generated in 2010, which corresponds to 2.5% of the total amount of waste [37]. In Austria, a total of 8.3% of waste consists of wood wastes in 2009. The share of waste wood is continually high in Austria. It is projected that the amount of waste wood will increase by 13% compared to 2009 to 5 million tons in 2016. [38] In the “Resource efficiency action plan” for Austria, waste wood is considered as an important waste stream, aimed at material use at a high quality level. Therefore, the selective collection and labeling of waste wood with different degrees of contamination is important. [39]

In Figure 4.1 the life cycle of wood is illustrated. Wood is processed into products that become waste, when they are no longer used. The material can either be used again or is discarded and becomes waste. Waste wood is also generated in forestry, such as wood from thinning and logging debris or in the wood processing industry in the form of slabs, small logs, saw dust, etc. Depending on the degree of pollution, there are three ways to further use waste wood. Clean waste wood can be recycled in a material-sensitive way, for example as raw material in the pulp and paper industry or for the production of fiber boards, chipboards or wood-polymer-composites (WPC). Clean waste wood can also be composted to be biologically degraded, e.g. saw byproducts as structural material in composts. [38]

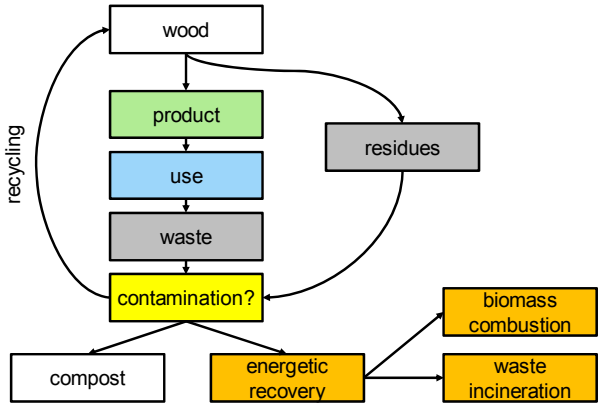

Figure 4.1: Life cycle of wood

Contaminated waste wood is most commonly recovered thermally. According to national legislation, it is either suitable for biomass combustion plants or it has to be treated in waste incineration plants. Slightly contaminated wood, such as slabs, logs or chippings, bark, fiberboards and surface-treated wood are suitable for conventional biomass combustion plants.

Those plants use biomass from forestry as standard fuel. In Austria there are several power plants, where waste wood is combusted, among them biomass plants in Timelkam and St. Veit an der Glan. The boilers are bubbling fluidized beds [40, 41]. However, heavily contaminated wood, such as coal tar oil treated wood or wood-polymer-composites containing halogens, is not suitable for those plants and has to be treated in waste incineration plants [42].

Waste wood is already used in gasification processes at industrial scale. In the autothermal gasifier in Lahti (Finland) waste wood was part of the feedstock mix [43]. In the Amer power plant in the Netherlands 150.000 t/a of demolition wood are gasified [44]. In both plants product gas is combusted in a coal fired power station. The gasifiers are circulating fluidized beds with air as the gasification agent.

In this work, waste wood from three different sources was used. Waste wood A consisted of residues from the wood-processing industry and contained pieces of coated chipboard, fiberboard, surface treated wood and cardboard. Waste wood B mainly consisted of shredded furniture. Waste woods A and B were provided by EnergieAG Oberösterreich Kraftwerke AG and are usually used as fuel for the biomass combustion plant in Timelkam. Waste wood C contained shredded bulky waste made from wood and was provided by Stadtreinigung Hamburg GmbH. All types of waste wood were in the form of chips and fibers with varying contents of fine particles.

4.2 Plastic residues

Modern societies consume more and more plastic materials every year. According to PlasticsEurope, an association representing Europe's plastic producers, 47 million tons of plastic materials were produced or converted in Europe in 2011. The largest segment of end-use applications of plastics is packaging that amounts to 40%. A total of 21% is used in construction, 8% in automotive applications and 5% for the production of electrical and electronic equipment, as shown in Figure 4.2. [45]

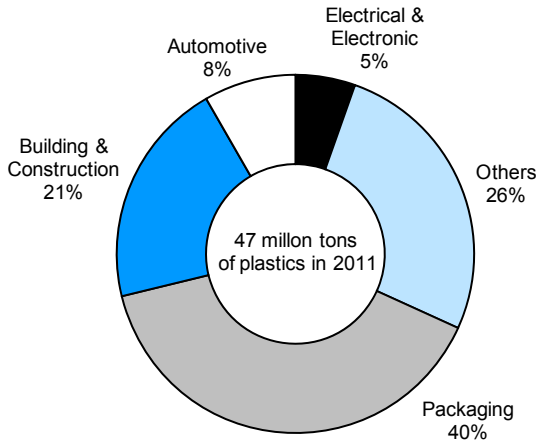

Figure 4.2: European plastics demand by segment 2011 in the EU27, Norway and Switzerland, [45]

Since plastic materials are processed into a multitude of products, such as foils, foams, fibers or resins, a huge variety of plastic wastes occurs at the end of the product lifetimes. Plastics currently represent 11% of municipal solid waste in OECD countries [14], mainly originating from the packaging of consumer goods and commodity products. The European Union considers plastic materials as a valuable waste stream. High recycling rates of plastics are imposed by several directives on packaging waste, end-of-life vehicles or waste electrical and electronic equipment (WEEE).

Several methods of treating plastic residues are possible, depending on the origin of the materials. Material-sensitive recycling is often possible for pre-consumer wastes that are generated during the production process. Thermoplastic materials such as polyethylene (PE) or polypropylene (PP) can be recycled during production without loss in quality as long as they are homogenous and not mixed with other polymers. The presence of fillers, coatings or blends deteriorates the properties of the recycled materials, also called downcycling. The production of regrinds from post-consumer waste is also material-sensitive recycling. The materials are sorted, crushed, washed, dried, melted and regrinded, so that they can be reused. Owing to initiatives for selective collection, a total of 33% of plastic packaging was already recycled in a material-sensitive way in the EU27 countries in 2010 [46]. Plastic recycling is also important for end-of-life vehicles, because a car contains 8-18% of plastics [38]. It can be recovered in the form of shredder light fraction (SLF) produced from shredded and graded end-of-life vehicles. Chemical or feedstock recycling describes the re-use on a molecular level. An example is PET (polyethylene terephthalate), which can be hydrolyzed to yield the educts, terephthalic acid and ethylene glycol [47].

Thermal treatment of plastic materials allows the recovery of the energy content. Most commonly, plastic residues are disposed of with the mass of municipal solid waste in waste incineration plants. An interesting application of plastic wastes is their use as a reducing agent in blast furnaces for steel production [48], where plastic wastes replace heavy fuel oil. There are also several industrial gasifiers, where plastic residues are used as feedstock. Mixtures of plastic residues and other fuels are gasified in air blown large scale circulating fluidized bed gasifiers in Lahti [43] and Rüdersdorf [49]. The new gasification plant in Lahti recently started operation on refuse-derived fuels, which mainly consist of plastics and paper [50]. In another case, automotive shredder residues and other plastic waste are used as feedstock for a pyrolysis plant coupled to the boiler of a hard coal power plant [51].

In this thesis, several types of plastic, which are available in large amounts in waste streams, were investigated: SLF-plastics, pellets made of selected plastic waste (MSW), PE regrind, mixtures of PE + polystyrene (PS), mixtures of PE+PET and mixtures of PE+PP.

SLF-plastics employed in the experiments was produced by TBS Technische Behandlungssysteme GmbH in a mechanical sorting plant where different plastic residues (SLF, plastics and films from commercial and electrical equipment waste) are processed. Plastic pellets are produced by AVE Österreich GmbH from a mixture of classified municipal solid waste (MSW), plastics derived from the bio-mechanical treatment of waste, and selectively collected plastic packaging. SLF- and MSW-plastics contain a variety of different polymers, but can no longer be used in a material-sensitive manner. PE regrind is a recycled product usually made of used foils derived from packaging waste, trashed plastic bags and waste bottles and

has been provided by the University of Ljubljana. Three different mixtures of PE and other polymers were gasified, that are typically used for the production of foils and other types of packaging for consumer goods. Table 4.1 provides the composition of the PE mixtures.

Table 4.1: Composition of PE mixtures

		PE+PET	PE+PS	PE+PP
Share of PE	wt.-%	20	40	50
Share of other polymer	wt.-%	80	60	50

4.3 Clean materials

For comparison and for systematic evaluation of specific fuel properties, not only waste materials were investigated, but also “clean” materials, such as soft wood pellets, sawdust, virgin PE and PP.

Soft wood pellets are the reference fuel for the 100 kW pilot plant. The pellets are standardized according to the European Standard EN14961 [52], and thus their LCV, water and ash content remain constant over many years. Due to their size (6 mm diameter, 3.15-40 mm length) they are well-suited for the screw feeding system utilized at the pilot plant. Furthermore, it has been proven that gasification of soft wood pellets in the pilot plant is in good agreement with gasification of wood chips in industrial gasifiers, which is another reason for using wood pellets as the standard feedstock in the 100 kW pilot plant [53].

Sawdust was provided by Mayr-Melnhof Pellets Leoben GmbH, an Austrian manufacturer of pellets. In a strict sense, sawdust is also a residual material from forestry and wood processing. It is the raw material for pellets production and was selected for this work because of its particle size distribution to investigate the influence of fine fuel particles.

PE and PP were also used as pure substances in the form of unused, virgin granulates. These polymers were provided by Borealis Polyolefine GmbH Austria and are used e.g. for the production of foils, plastic bags, food packages and other disposable products [54]. Gasification of PE and PP provides information on the behavior of materials with very high volatile matter content.

4.4 Physical properties

In this chapter the most important physical properties for gasification are discussed. The particle size of the feedstock and its distribution, as well as the particle density influence the behavior of the particles in fluidized bed processes.

Table 4.2 provides a visual impression of the materials. All types of waste wood were available as chips and fibers with varying content of fine particles. SLF-plastics was a granular material with an average particle size of 5 mm. MSW-plastics had cylindrical shape with a diameter of 6 mm and length of about 10 mm. PE regrind consisted of 5 mm colored chips. The mixture of PE+PP and the mixture of PE+PET were mixed using granulates of the pure substances. Virgin PE and virgin PP were also available as granulates. Granulates were all almost spherical with

an average diameter of 3 mm. The mixture of PE+PS had the form of thin flakes and was waste material from a foil production process. The surface of the flakes had an average diameter of 7 mm.

Table 4.2: Photographs of the materials used in the gasification tests


Waste wood A


Waste wood B


Waste wood C


Soft wood pellets


PE, PP, PET


SLF-plastics


MSW-plastics


Saw dust


PE+PS flakes


PE regrind

Average values for particle densities are listed in Table 4.3. Waste woods from different sources were used in this work. Owing to the inhomogeneity of the samples, it was assumed that waste wood consisted of 70% soft wood and 30% hard wood on average. The mean particle density was calculated based on the density of spruce (soft wood) and oak (hard wood) and the water content of the waste wood sample [19]. Similar to the waste wood samples, the mean particle density of saw dust was calculated from spruce and the water content of the saw dust sample. The density of SLF-plastics was also estimated, as the sample consisted of particles made from different materials. As the majority of particles did not float in water, an average particle density of 1100 kg/m³ was estimated. The particle densities of soft wood pellets and PET were taken from literature, [47, 55]. PE and PP data was provided by the manufacturer. PE regrind is produced from PE waste, therefore a similar density can be assumed. Due to the regular forms of MSW-plastics and PE+PS flakes, the densities were assessed by measuring the volume and the mass of the samples. Generally speaking, the density of non-compacted wood, such as saw dust or waste wood averages 500 kg/m³. As a result of pelletization, the particle density of soft wood pellets has more than doubled. Particle densities of PE, PE regrind, PP, PS+PE, and MSW-plastics are in the range of 900 kg/m³. PET and SLF-plastics have higher densities.

Table 4.3: Particle density of the materials used in gasification tests

	Density, kg/m³
Waste wood A	520
Waste wood B	540
Waste wood C	540
Saw dust	470
Soft wood pellets	1150
PE granulate	920
PP granulate	910
PET granulate	1400
PE regrind	920
PE+PS flakes	950
SLF-plastics	1100
MSW-plastics	900

4.5 Chemical properties

The proximate and ultimate analyses of the investigated materials are compiled in Table 4.5, Table 4.6 and Table 4.7 and highlight that the elemental compositions of wood and plastics differ markedly. Generally, wood consists of three biopolymers - lignin, cellulose and hemicellulose - that are mainly composed of carbon, oxygen and hydrogen. Cellulose is an unbranched long-chain polysaccharide. Lignin and hemicellulose are more complex biopolymers, whereas hemicellulose is composed of branched polysaccharides of different types and lignin consists of various three dimensionally cross-linked aromatic compounds. [19] Owing to the complexity of lignin and hemicellulose, only the constitutional repeating unit of cellulose is shown in Table 4.4. Woody biomass typically consists of 50% carbon, 43% oxygen, and 6% hydrogen.

Unlike woody biomass, polymers are synthesized materials with a specific molecular structure formed by repeating constitutional units. As shown in Table 4.4, PE and PP are long alkane molecules. PS comprises an aromatic ring as a substituent. PE, PP and PS consist of approximately 86% carbon and 14% hydrogen. Since PET is formed by the polycondensation of ethylene glycol and terephthalic acid, it also contains a significant amount of oxygen. PE, PP and PET were used in the form of virgin granulates, PE+PS was a production residue and PE regrind was intended for the use as a raw material in the polymer processing industry. In contrast to these rather “clean” polymers, SLF- and MSW-plastics are waste plastics which contain a variety of different polymers that are not further specified.

Table 4.4: Molecular structure of cellulose and selected polymers

Cellulose, [19]	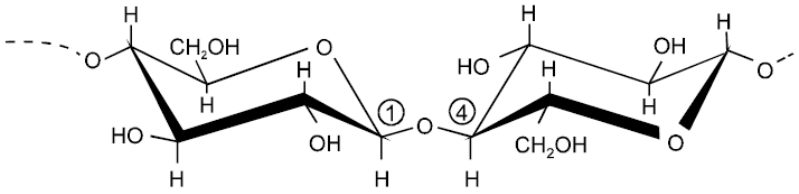
Polyethylene	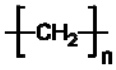
Polypropylene	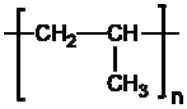
Polystyrene	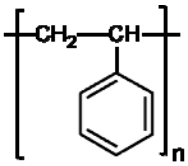
PET	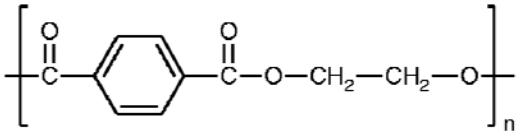

The LCV of the different wet materials covered a broad range from 16 MJ/kg for woody biomass to 43 MJ/kg for polymers, such as PE or PP. The LCV describes the energy available from complete oxidation of the fuel and is determined by the elemental composition as the oxidation of carbon, hydrogen, nitrogen, sulfur and chlorine provides energy. Oxygen containing compounds reduce the LCV, because they can only be further oxidized to a limited extend. Therefore, woody biomass has a lower LCV than plastic materials. The LCV is also strongly influenced by the water and ash content of the fuel.

The water content is particularly important for woody biomass with high contents resulting in a lower LCV due the high enthalpy of evaporation of water. The water content is determined by the pretreatment of wood and the storage conditions. For plastic materials, however, it is only of minor importance, as they do not absorb water to such a high extent and contain virtually no water. The highest water content of all samples was measured in the sawdust. Fresh sawdust contained 45% water on average; it was dried to about 17% prior to the experiments. The water content of waste woods was also in a similar range (7-15%).

The ash content remains after gasification or combustion and is composed of inorganic compounds present in the fuel. Ash originates from inorganic nutrients in the biomass, fillers of plastic materials, or from contaminants introduced during production and manipulation, such as sand. The highest ash contents were measured in SLF-, MSW-plastics and waste wood B, which is typical for waste fuels. PE+PS, which was waste material from a production process contained more ash than granulated materials, such as PE, PP or PET. The clean materials used for comparison were almost ash free.

In particular, the concentrations of compounds that form undesired pollutants during gasification are of interest. Nitrogen, sulfur and chlorine are trace compounds in untreated wood, but were present in waste wood and plastic residues. Waste wood C contained 2.7% of nitrogen, which is part of adhesives and coatings of chipboards, fiberboards or furniture. The nitrogen content of waste woods A and C were in a comparable range. The chlorine and sulfur contents were also higher in waste wood samples than in untreated wood. In SLF- and MSW-plastics, the nitrogen content amounted to approximately 1%. The chlorine and sulfur contents in SLF-plastics were higher than in all other samples. Nitrogen, sulfur and chlorine can be present in polymers as heteroatoms, such as nitrogen in polyamides, sulfur in vulcanized rubber or chlorine in PVC.

Determination of volatile content enables a first assessment of fuel devolatilization and gasification behavior. Therefore, feedstock was heated to 900°C in a nitrogen atmosphere, where volatile matter was released and char and ash remained. In order to eliminate the influence of the ash content, these volatile data are given on a water and ash free basis (waf). The volatile content of woody biomass amounted to 86% on average, more volatile matter and less char were found in plastics, ranging from 90% in SLF- and MSW-plastics to more than 99% in PE, PP and PS.

Table 4.5: Feedstock analysis of waste woods

		Waste wood A	Waste wood B	Waste wood C
LCV (wet)	MJ/kg	17016	14596	16230
Water	wt.-%	6.73	15.49	14.56
Ash	wt.-%, dry	1.67	7.90	3.03
C	wt.-%, dry	48.31	48.71	50.67
H	wt.-%, dry	5.51	4.78	5.61
O[a)]	wt.-%, dry	41.97	36.41	37.84
N	wt.-%, dry	2.49	1.99	2.70
S	wt.-%, dry	0.03	0.08	0.10
Cl	wt.-%, dry	0.02	0.13	0.05
Volatiles	wt.-%, waf[b)]	84.7	88.2	83.7

[a)] calculated as sum to 100%, [b)] water and ash free

Table 4.6: Feedstock analysis of plastic residues

		SLF-plastics	MSW-plastics	PE regrind	PE+PET	PE+PS
LCV (wet)	MJ/kg	31946	24092	43270	26337	39787
Water	wt.-%	0.87	2.81	<0.10	<0.10	<0.10
Ash	wt.-%, dry	10.67	12.47	0.36	<0.10	1.46
C	wt.-%, dry	65.00	54.16	87.09	66.89	87.18
H	wt.-%, dry	7.95	7.32	12.42	6.06	11.12
O[a)]	wt.-%, dry	13.47	24.08	<0.01	26.67	0.08
N	wt.-%, dry	0.93	0.94	<0.05	0.08	0.16
S	wt.-%, dry	0.31	0.21	0.01	<0.005	<0.005
Cl	wt.-%, dry	1.67	0.82	0.07	<0.005	<0.005
Volatiles	wt.-%, waf[b)]	89.2	90.2	99.5	95.6	>99

[a)] calculated as sum to 100%, [b)] water and ash free

Table 4.7: Feedstock analysis of clean materials

		Wood pellets	Sawdust	Sawdust pellets	PE	PP
LCV (wet)	MJ/kg	17458	15485	17572	43379	43419
Water	wt.-%	6.11	16.78	6.74	<0.10	<0.10
Ash	wt.-%, dry	0.29	0.47	0.32	<0.10	<0.10
C	wt.-%, dry	50.23	51.38	51.07	85.84	85.86
H	wt.-%, dry	6.04	5.76	5.79	14.07	13.91
O[a)]	wt.-%, dry	43.38	42.18	42.68	<0.01	0.13
N	wt.-%, dry	0.05	0.17	0.13	0.09	0.10
S	wt.-%, dry	0.005	<0.005	0.005	<0.005	<0.005
Cl	wt.-%, dry	0.003	0.04	<0.005	<0.005	<0.005
Volatiles	wt.-%, waf[b)]	86.7	84.9	86.4	>99	>99

[a)] calculated as sum to 100%, [b)] water and ash free

4.6 Ash properties

The ash melting behavior is crucial for the operation of fluidized beds. If the ash melting temperature of a feedstock is too low, liquid ash is formed at operation temperatures of the gasification process, which renders fluidization impossible. Deformation and flow temperature were analyzed by a heating microscope (Hesse Instruments). Table 4.8 gives an overview on the ash melting temperatures of the materials used in this work. As PE, PP, PE+PS, PE+PET and PE regrind contained virtually no ash, the ash melting behavior was not analyzed. The gasification temperature in the fluidized bed amounted to 850°C and in the combustion reactor the temperature was about 920°C. As it can be seen from Table 4.8, the deformation temperatures of all samples were much higher than the maximum temperatures reached in the process. From this point of view, all feedstock are suitable for the use in fluidized beds.

Table 4.8. Ash deformation temperature (DT) and flow temperature (FT)

		Wood pellets	Saw dust	Waste wood A	Waste wood B	Waste wood C	SLF-plastics	MSW-plastics
DT	°C	1240	1230	1140	1210	1180	1200	1170
FT	°C	1470	1500	1210	1310	1240	1320	1230

5 Fuels with high concentrations of nitrogen, sulfur and chlorine

During gasification, fuel-bound nitrogen, sulfur and chlorine are converted into gaseous compounds, such as NH_3, H_2S, HCl and the like. When product gas is combusted, these compounds are oxidized to NO, NO_2, SO_2, SO_3, HCl, etc. Since they are toxic and form acid rain, smog, and other environmentally damaging products, there are severe emission limits for flue gases from combustion processes. In contrast to combustion, gasification processes provide the possibility of product gas cleaning prior to its application (combustion, synthesis) and thus, precursors of harmful emissions can be removed. This chapter describes the conversion of fuel nitrogen, sulfur and chlorine in the DFB gasifier. The DFB gasifier consists of two coupled reactors, and therefore the compounds can be distributed in the two reactors which makes the situation more complex. In Paper I the conversion of fuel nitrogen is investigated in detail, whereas in Paper II the distribution of sulfur and chlorine is discussed based on two waste wood samples. Balances of nitrogen, sulfur and chlorine in the DFB gasifier are established in order to trace the pathway of conversion in both reactors of the DFB gasification plant, which determines the requirements for gas cleaning.

5.1 Nitrogen

In Paper I, biogenous materials as well as plastic waste were compared: wood pellets, bark, waste woods A, B and C, SLF- and MSW-plastics. Wood pellets contain 0.05 wt.-% of nitrogen. Nitrogen in wood mainly occurs in proteins and amines, which are typical in living organic tissues [56]. The concentration of nitrogen in waste wood ranges from 2–3 wt.-%. The concentration is significantly higher compared with wood from forestry, because nitrogenous adhesives are used e.g. for the production of chipboard. Examples are urea resin chipboards or melamine resin adhesives [57]. In the gasification experiments SLF-plastics and MSW-plastics are gasified in a mixture with wood pellets. A total of 50% of the fuel input in terms of energy content is plastics and 50% is wood. Thus, the mixtures contain lower amounts of nitrogen (0.4 wt.-%). Nitrogen is found in several polymers such as polyamides, polyacrylonitriles or copolymers with acrylonitrile, and also in polyurethanes and in melamine resins.

In addition to the materials presented in Table 4.5, Table 4.6 and Table 4.7, bark was included for comparison. It is a side-product of the wood-processing industry, which is most commonly used for the production of bark-chip mulch or as fuel in combustion plants. For the test runs, bark has been dried and pelletized to be suitable for the screw conveying system of the pilot plant. The pellets are 8 mm in diameter and 5–20 mm in length. The nitrogen content of bark amounts to about 0.6 wt.-% in dry fuel.

5.1.1 Conversion products of fuel nitrogen during steam gasification

Fuel-bound nitrogen is released in several sub-processes during steam gasification, which are compiled in Figure 5.1. When feedstock is inserted into the gasifier, it is dried and volatile matter is released. The release of fuel-bound nitrogen also starts during devolatilization at 300–400°C [56, 58]. The products of devolatilization are gases, primary tar and char. Devolatilization is not

influenced by the gasification agent, because during devolatilization, the gasification agent does not come into contact with the fuel particle due to the escaping volatiles [59].

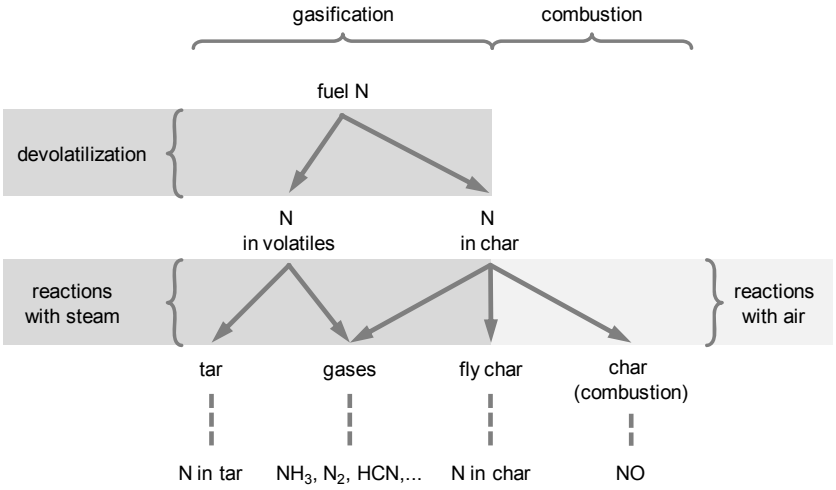

Figure 5.1: Pathway of nitrogen in the DFB gasifier

When devolatilization is complete, reactions with steam occur. Nitrogenous gases, such as NH_3, N_2 and HCN, are formed. The most important nitrogenous gas is NH_3. Three pathways of NH_3 formation are distinguished by Tian et al. [58]: (i) hydrolysis of N-containing structures in the solid phase during primary pyrolysis, (ii) thermal cracking and gasification of solid nascent char and (iii) thermal cracking and reforming of nitrogen in volatile matter. During steam gasification NH_3 is mainly formed by reaction with H radicals, which are available from the interaction of char and steam. Generally, the concentration of HCN is much lower compared to NH_3, which is reported by Leppälahti and Koljonen [56] for various gasification systems. In their experiments, Tian et al. [58] show that the HCN concentration in the initial volatile matter from pyrolysis is higher than during steam gasification. They concluded that HCN is mainly formed by reactions of the volatiles, whereas steam gasification of char mainly yields NH_3. Molecular nitrogen is also a conversion product of fuel nitrogen. Zhou et al. [60] assessed the formation of molecular nitrogen in a fluidized bed reactor, which is fluidized with oxygen only. They found opposite trends for NH_3 and N_2 formation and concluded that N_2 is primarily produced by the thermo-chemical conversion of NH_3. They also reported on the formation of NO during oxygen gasification. However, the formation of NO during steam gasification is very unlikely because of the strongly reducing atmosphere. Nitrogen is not only present in gases, which are formed from volatile matter and char gasification; minor concentrations of nitrogen are also found in tar and fly char which is entrained by the product gas. Unlike in single fluidized bed reactors, nitrogen can also be present in the combustion reactor of the DFB gasifier, if char, which remains after gasification, contains nitrogen. It is transported to the combustion reactor together with the circulating bed material and is converted into NO during combustion.

Figure 5.2 shows a correlation of fuel nitrogen and NH_3 formation in the DFB gasifier product gas as obtained in the gasification tests. Data points in the diagram represent different materials. A linear relationship with very high accuracy was found for the correlation of fuel nitrogen and NH_3 formation. The coefficient of determination of the linear regression R^2 was 0.93.

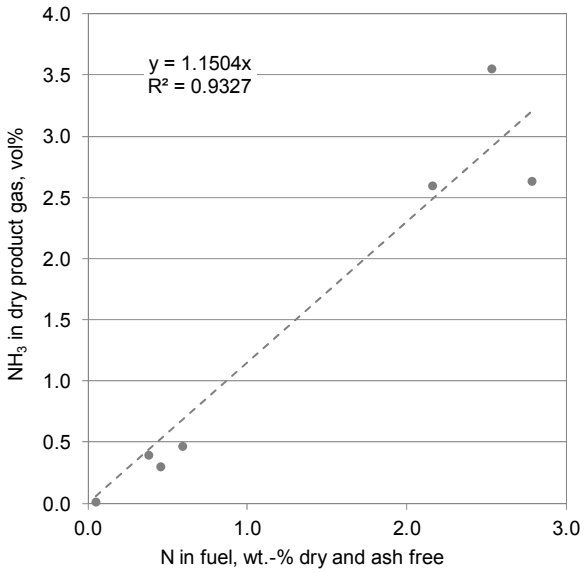

Figure 5.2: Correlation of fuel nitrogen and ammonia yield

This is in accordance with other studies. Van der Meijden et al. gasified waste wood (1.0 wt.-% N in dry and ash free fuel) with steam in the Milena gasifier and measured comparably high levels of NH_3 of 1.9 vol.-% in the product gas. [61] This value is within the scattering of the measured values in Figure 5.2 and is therefore in agreement with the three types of waste wood tested here, although a different reactor system was used. Similar findings are available for air gasification: Turn et al. gasified several fuels with varying concentrations of nitrogen. They used a bench scale fluidized bed reactor with air fluidization and reported a linear relationship of fuel nitrogen and NH_3 in the product gas with high accuracy. [62] Van der Drift et al. studied the conversion of ten residual biomasses in a 500 kWth air-blown circulating fluidized bed gasifier and confirmed that the NH_3 formation depends on the fuel nitrogen content. [63] Goldschmidt et al. showed that this dependency is also valid for pressurized air gasification at industrial scale in the Värnamo IGCC power plant. There different types of biomass and RDF were gasified. [64] Zhou et al. continued the work of Turn et al., but used oxygen as the gasification agent. They tested four types of biomass in the same reactor and found that NH_3 formation is also proportional to fuel nitrogen. [60]

Remaining fuel nitrogen is converted to N_2 and HCN. In the pilot plant at Vienna University of Technology, a small stream of N_2 from gas bottles was constantly injected into the hoppers in order to prevent product gas accumulation there. This N_2 flush was calculated out of the following considerations and only N_2 generated by fuel nitrogen was taken into account. During the experiments the N_2 concentration from fuel nitrogen in the product gas was in the range of 0.2 vol.-%. In contrast to NH_3 concentration, no clear relationship of N_2 and fuel nitrogen was found (Figure 7 in Paper I). HCN measurement was only carried out during gasification of waste wood C. It was found the HCN content amounted to roughly 10% of the NH_3 concentration. A similar ratio is given by van der Meijden et al. for gasification of wood pellets in the Milena gasifier. [65] It is likely that HCN formation increases with the increase in fuel nitrogen in analogy to NH_3.

Minor amounts of nitrogen are present in the form of NO in the flue gas. Ungasified char is transported to the combustion reactor and is combusted in an atmosphere of excess oxygen. If significant amounts of nitrogen were found in the char, NO was measured in the flue gas. In general, three different types of NO are distinguished in combustion: prompt, thermal and fuel NO. In this case, only fuel NO is likely because the temperature in the combustion reactor was in the range of 900°C. The formation of thermal NO from nitrogen in the combustion air and prompt nitrogen from radicals only occurs at significantly higher temperatures [66]. The combustion air supply and the primary-to-secondary air ratio only varied on a small scale during the test runs, therefore formation of NO can be mainly attributed to the nitrogen content of the char. Similarly to NH_3, the relationship was also linear, but the accuracy was lower (Figure 8 in Paper I). The concentration of NO was very low during all test runs. Approximately 1-2% of the fuel nitrogen was converted into NO in the flue gas. This led to an NO emission of about 100 ppm for the waste woods (referred to 6% O_2 in dry flue gas).

Nitrogen was also in found in the tar. Among 50 species identified in the GCMS tar, four tar species containing nitrogen were detected: isoquinoline, indole, carbazole and quinoline. In general the GCMS tar content in the product gas is in the range of 6 g/Nm³ when soft wood pellets are gasified in the DFB pilot plant. Nitrogenous tar species were not detectable during gasification of wood pellets and bark. For the other materials, about 0.5% of the GCMS tar consisted of nitrogenous tar species, the most frequently formed of which was indole. No tar measurement was available for waste wood B, since it was not possible to take a representative tar sample because of the high dust load of the product gas. On average only 0.1–0.2% of fuel nitrogen was converted into nitrogenous tar species.

In the product gas, there was also entrained char in the range of 20–40 g/Nm³. It was calculated that the char contained roughly 0.1 wt.-% of nitrogen, which corresponds to the small amount of 0.1–0.3% of the fuel nitrogen.

5.1.2 Conversion of fuel nitrogen to NH_3

The conversion of fuel nitrogen to NH_3 is defined as the ratio of the mass flow of nitrogen in NH_3 in the product gas to the mass flow of fuel nitrogen according to Eq. 5.1.

$$X_{N\,to\,NH_3} = \frac{\dot{m}_{N\ in\ NH_3}}{\dot{m}_{N\ in\ feedstock}} \tag{5.1}$$

The degree of conversion to NH_3 differs in the experiments. Waste wood A and waste wood B show very high conversions of around 85%. Medium conversion of 70% is achieved for SLF-plastics and waste wood C. Lower conversion occurred during gasification of bark and MSW-plastics (50%). Apparently the degree of conversion to NH_3 does not only depend on the nitrogen content of fuel, but is also influenced by other parameters.

Some data are available for the conversion of fuel nitrogen to NH_3 in steam gasifiers in literature. Pröll et al. mentioned a conversion of 70% in the DFB gasifier in Güssing, where wood chips from forestry are gasified [67]. A total of 50% of conversion to NH_3 is reported in [68] for steam gasification of waste wood in the Milena gasifier. For air gasification of ten residual

biomasses Van der Drift et al. found a wide range of conversions to NH_3 from 27-83% with no clear dependency on the nitrogen content of the fuel [63].

According to literature there are several parameters which influence the NH_3 conversion. The most important factors for steam gasification seem to be the amount of fluidization steam, the residence time of the product gas, the location of fuel feeding, and the different nitrogen functionality in the fuels. The most important influence in the gasification test considered here was the gas residence time, which is discussed briefly in the following. The other influences were difficult to identify, further details on that are available in Paper I. The gas residence time was likely to influence the NH_3 conversion because NH_3 can react further to other products, Eq. 5.2, depending on the prevailing temperature.

$$2\ NH_3 \leftrightarrow N_2 + 3H_2 \tag{5.2}$$

At 850°C, NH_3 should be reduced to N_2 and, thus mainly N_2 and H_2 should be present in the reducing atmosphere of the gasification reactor. The measured concentration of NH_3 was much higher than the equilibrium concentration, which indicated kinetic constraints for significant NH_3 reduction. However, longer gas residence times in the hot reducing atmosphere could be related to lower concentrations of NH_3 and, consequently, to lower conversion to NH_3. The design of the gasifier and the feedstock properties influence the residence time of the gas in the gasification reactor. All types of waste wood used in the experiments had a wide particle size distribution and contained significant amounts of fine particles. Fine particles were easily carried out of the bubbling fluidized bed and, thus, may devolatilize in colder parts of the reactor. Fuel nitrogen, which was released there in the form of NH_3, could be reduced to N_2 at the prevailing temperatures. This could explain the high NH_3 conversion of waste wood A and B and the lower conversion in case of bark pellets that contained much less fine particles. Although waste wood C contained comparable amounts of fine particles, it showed lower NH_3 conversion.

5.1.3 Nitrogen distribution in the DFB gasifier

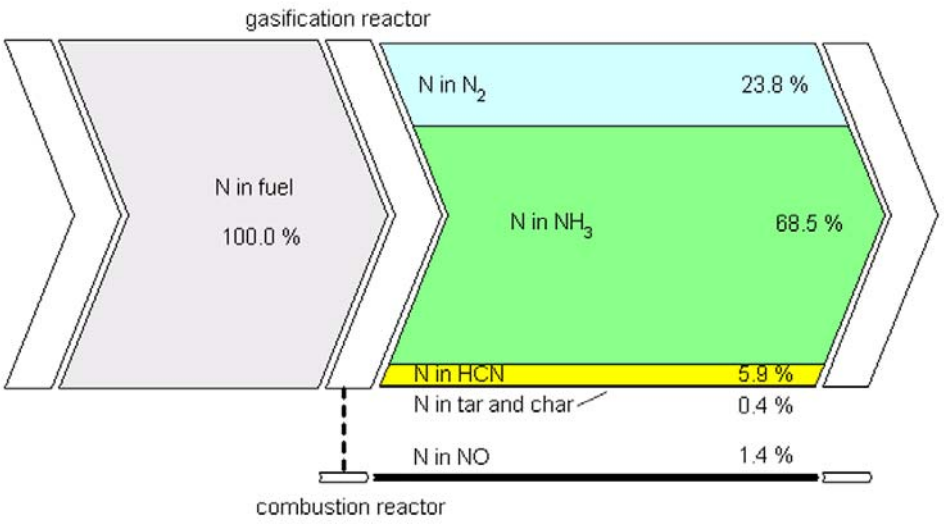

Figure 5.3: Nitrogen distribution in the DFB gasifier

Experimental data of all fuels was averaged to establish a diagram of the nitrogen distribution in the DFB gasification system which is shown in Figure 5.3. Nitrogen conversion mainly took place in the gasification reactor. The majority of fuel nitrogen was converted to NH_3. N_2 was also present in the product gas. NH_3 and N_2 were the most important conversion products of fuel nitrogen with a share of more than 90%. In the product gas, HCN was also found as well as nitrogenous tar and traces of nitrogen in entrained char. Only 1.4% of fuel nitrogen was liberated as NO in the flue gas of the combustion reactor.

5.2 Sulfur

The distribution of sulfur in the DFB gasifier was investigated based on waste woods A and B in Paper II. The sulfur content amounted to 0.03 wt.-% in waste wood A and to 0.08% wt.-% in waste wood B. These were still small amounts, but exceeded the sulfur concentration in wood pellets by a factor of 10 to 20. In woody biomass, sulfur is absorbed by the roots and is mainly present in the form of amino acids, vitamins and enzymes, which are necessary for the formation of proteins and the chlorophyll balance of the plant. [19] The increased sulfur content of waste wood is mainly due to wood processing, as wood stains and impregnations often contain copper or chrome salts. For this purpose copper sulfate is frequently used. [69]

During thermal conversion, sulfur is converted to gases, but it is also bound in char, tar and ash. The majority of sulfur is released in the form of H_2S during devolatilization at temperatures around 450°C. [70] Lab-scale air gasification tests in a bubbling bed gasifier show that 50-90% of sulfur from non-woody biomass, such as straw or sewage sludge is present in the product gas. Sulfur compounds in product gas are mainly H_2S, but also COS and CS_2 in minor amounts. The remaining sulfur is bound to ash particles. [71] When RDF and coal mixtures are used, 40-75% of sulfur is converted to H_2S in the product gas. [72] When coal with high ash content was gasified with steam and oxygen, about 25% of sulfur is found in the product gas. [73] Comparison of raw coal and demineralized coal shows that most H_2S is released from the demineralized sample, as mineral matter act as absorbent for H_2S. [70] Calcium in the ash is found to strongly reduce H_2S concentration. [72]

The studies mentioned above show, that mostly inorganic H_2S is formed from fuel sulfur, but also organic sulfur compounds, such as COS, thiophenes and mercaptans are also observed in minor amounts. H_2S concentration in the product gas predominantly depends on the sulfur content of the fuel. It is also strongly influenced by the ash content and its composition. Alkali and earth alkaline metals are capable of reacting with H_2S formed during devolatilization and therefore reduce the H_2S concentration in the product gas.

Figure 5.4 illustrates the distribution of sulfur in the DFB gasifier. Sulfur was supplied to the gasification system with the fuel, but also with light fuel oil that is fed to the combustion reactor. It contains minor amounts of sulfur, but is calculated out of the sulfur balance. Waste wood B contained more than double the concentration of sulfur of waste wood A. More than 99% of the fuel sulfur is present as H_2S in the product gas, which corresponds to a H_2S concentration of 570 ppm in dry product gas for waste wood B. A small amount of sulfur sticks to ash. In the pilot plant, product gas and flue gas were mixed after gas analysis and combusted, then particles were separated in a cyclone. Thus, ash in product gas and flue gas were analyzed as a mixture.

Ungasified char from gasification is transported to the combustion reactor. The combustion products of sulfur are SO_2 and SO_3, whereas the majority of sulfur is present as SO_2. The SO_2 concentration in the flue gas was rather low; it was below the detection limit when waste wood A was gasified and amounted to 4 ppm of SO_2 (referred to 6 vol.-% O_2 in dry flue gas) for waste wood B. Sulfur can also be found in tar and entrained char in the product gas. In the GCMS analysis of waste wood A, the concentration of 1-benzothiophene and dibenzothiophene was below the detection limit. Similar to nitrogen in fly char, the sulfur content could be estimated based on the formation of SO_2 in the flue gas, which was below the detection limit for waste wood A. No tar and char measurements were available for waste wood B. Thus, these streams are omitted in Figure 5.4.

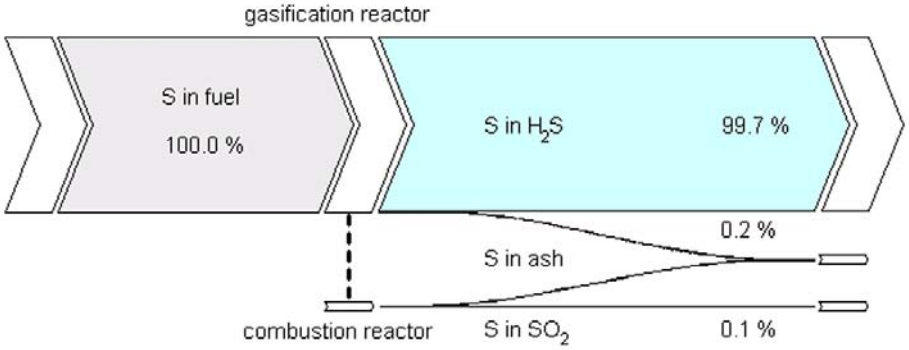

Figure 5.4: Distribution of sulfur in waste woods A and B

5.3 Chlorine

The distribution of chlorine in the DFB gasifier was also investigated based on waste woods A and B in Paper II. An additive in fertilizers based on potassium, chlorine is predominantly found in crops and other fertilized plants, but it is only a trace substance in wood (0.003 wt.-% in wood pellets). Chlorine is absorbed by the roots; that is why the chlorine concentration is higher in roadside plantings or plants growing close to the sea. It is also considered as an indicator for biomass treatment. [19] In waste wood higher concentrations of chlorine were found because of the use of PVC in cabinetry. [74] Wood preservatives and coatings also can contain chlorine or other halogens. Waste wood treated with halogen containing preservatives has to be disposed in waste incineration plants. [42]. The chlorine content of waste wood A amounted to 0.02 wt.-% and of waste wood B to 0.13 wt.-%.

Chlorine is converted to HCl during thermal conversion, but also bound to ash in a large amount. Then alkali salts are formed, such as KCl and NaCl which are gaseous at temperatures exceeding 700°C. [72] Chlorine can also react further to organic species, such as chlorobenzenes and dioxins. Björkman and Strömberg systematically investigated the release of chlorine from different types of biomass (straw, switchgrass, lucerne and sugarcane trash). A total of 20-50% of the chlorine is already released during pyrolysis at 300-400°C, and at 900°C 30-60% of the chlorine is still left in the char. Different gasification atmospheres and increases in pressure do not significantly change the chlorine release, nor is a difference in organic and inorganic bound chlorine. [75] When non-biomass is gasified with air in bubbling bed gasifier, the HCl formation correlates with the chlorine content of the fuel. A total of 50-90% of chlorine

remains in the ash. The concentration of chlorine in the ash depends on the ash composition and the temperature of ash removal. [71]

The chlorine balances of the DFB gasifier appear in Figure 5.5. Fuel is the only source of chlorine in the pilot plant. Minor contents of HCl were measured in dry product gas, 35 ppm for waste wood A and 70 ppm for waste wood B. The majority of chlorine, about 94%, is bound to ash particles. HCl in the flue gas was below the detection limit in all experiments. Other chlorine compounds that might occur have not been determined.

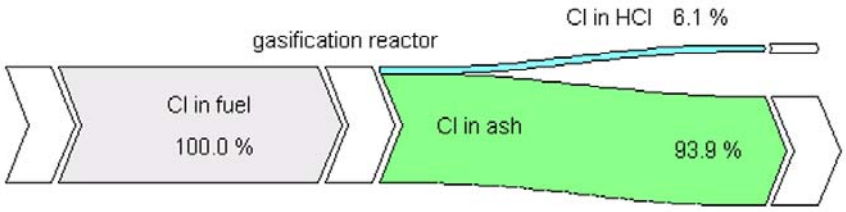

Figure 5.5: Distribution of chlorine of waste woods A and B

5.4 Conclusion

Nitrogen, sulfur and chlorine are released during devolatilization of the fuel at temperatures of 300–400°C. The balance of inorganic species showed that nitrogen, sulfur and chlorine conversion occurred almost exclusively in the gasification reactor. The vast majority of nitrogen and sulfur was present in the form of NH_3 and H_2S in the product gas respectively. Chlorine was mainly found in the ash.

The distribution of inorganic species in the DFB gasifier has important consequences for the gas cleaning equipment of gasification plants. In the industrial DFB gasifiers which are currently in operation, two-stage product gas cleaning equipment is implemented. The product gas filter precipitates entrained particles and part of the tar. They are returned to the combustion reactor, so that fly char and tar can be used for heat production. The remaining tar is removed by a scrubber using rapeseed methyl ester (biodiesel) as an organic solvent. Saturated solvent is combusted in the combustion reactor. The flue gas cleaning equipment consists only of a bag-house filter for particle removal. This gas cleaning equipment has proven to be suitable for the requirements of a gas engine, when wood from forestry is gasified [22, 76].

When fuels with high concentrations of nitrogen, sulfur and chlorine are to be gasified, NH_3 and H_2S have to be removed from the product gas e.g. by scrubbers to fulfill the environmental requirements. Only traces of pollutants were present in the flue gas in the pilot plant. As a preliminary assessment, no adaption of the flue gas cleaning equipment (consisting solely of a bag house filter) is necessary. A chlorine balance of the demonstration plant in Güssing has shown that more than 95% of chlorine, which is present in product gas as HCl, is captured in the product gas filter by the fly char and finally ends up in the ash. [77] Therefore, no additional measure or separator is necessary for HCl removal.

6 Fuels with high contents of fine particles

This chapter focuses on the influence of fuel particle size and distribution on the DFB gasification process. Woody residues, such as bark, waste wood, and sawdust are interesting feedstock due to their availability and price. However, they are mostly inhomogeneous and have varying quality. Depending on the origin of the residues, the particle size of the materials covers a wide range, from fine particles such as sawdust to large pieces of chipped wood, shredded furniture or bulky waste.

The influence of fuel particle size was systematically studied in pilot plant gasification experiments using sawdust and pellets made from the same raw material. In particular, the behavior of small particles is of interest. Waste woods A, B and C were also considered for comparison because of their different particle size distributions.

6.1 Theoretical background

The particle size of the biomass has an important influence on its thermal conversion and this has been studied by several research groups. It is commonly agreed on that the particle size determines the mass and heat transfer into and from the particle. Four different regimes of heat transfer are distinguished related to particle size: In the kinetic regime, particles are considered to be isothermal and to heat up instantly. In the thermally thin regime, external heat transfer occurs between the particle and the surroundings, but the intra-particle temperature gradient is found to be negligible. In the thermally thick regime, the reactions of the particles are controlled by external and internal heat transfer [78]. A thermal wave regime is established, when the internal heat transfer rates are much slower than the external heat transfer rate [79]. As the heat conductivity of biomass is low, large temperature gradients can be established in the thermally thick regime and in the thermal wave regime [80]. The particle size and the temperature of the radiant heat source determine the regime of heat transfer and the devolatilization time, which increases with an increase in particle size.

The product distribution is also influenced by the thermal regime and therefore by the particle size. Pyrolysis models by Bryden and Hagge [81] and Di Blasi [78] show that for smaller particles the gas production decreases and tar formation increases. The influence of particle size on pyrolysis has also been studied experimentally in different types of reactors, such as entrained flow combustors [82], drop tube reactors [83], and fluidized bed reactors [84, 85]. All experimental studies show that the devolatilization time is proportional to the particle size. With decreasing particle size, more gas and less char and tar are measured, which is in contrast to the results of the pyrolysis models [78, 81]. The influence of fuel particle size on gasification in bubbling fluidized bed reactors has also been studied using different size fractions of pine wood [86], wood spheres [84, 85] or almond shells [87]. All gasification studies report more gas production and lower char and tar formation for smaller particles. The product gas composition is strongly influenced by the type of gasification agent and the catalytic activity of the bed material. However, the studies agree on an increase in CO and CH_4 when smaller particles were used. In Paper III, two figures graphically compare the literature findings for pyrolysis and gasification.

The particle size distribution of the biomass also has an influence on the residence time of the fuel particles in a fluidized bed reactor. This is of importance when catalytic bed materials are used in order to reduce the extent of tar formation. Small particles can be entrained very easily by the product gas stream if their terminal velocity is sufficiently low. They are very likely to react in the freeboard without contact with the bed material. Larger particles can segregate on the surface of the bubbling fluidized bed. In that way, volatiles are released to the freeboard having only limited contact with the bed material in the splash zone [85]. If good inter-mixture of fuel particles and bed material is provided, larger particles remain within the fluidized bed as long as the particle size is large enough. During thermal conversion, the particle size of all fuel particles decreases due to weight loss and chemical reactions. Gasification assisted attrition occurs, which further reduces the particle size. Due to carbon consumption, the structure of the fuel weakens by pore enlargement, leading to secondary fragmentation [88]. Small char and ash particles are entrained by the product gas. In addition to these factors, the residence time of the fuel particles is also influenced by the design and operation of the fluidized bed: the bed and the freeboard height, the type and size of the bed material, the fluidization velocity, etc. Therefore, experimental studies can often only be compared to a limited extend.

6.2 Particle size distribution

Unprocessed sawdust and pelletized sawdust were used in the experiments. Because of the limitations of the feeding system, pure sawdust could not be gasified and thus it was mixed with pellets. The mixture consisted of 69 wt.-% of sawdust, which corresponds to 66% of fuel input in terms of energy due to the different water content of sawdust and pellets.

As sawdust was the raw material for the pellet production, both materials were considered to be chemically identical. However, as can be seen from Table 4.7, there were some unexpected differences, mainly in the ash, nitrogen, and chlorine contents. The reason for these differences will be most probably natural deviations of different samples, which were taken from a huge pile of sawdust. It can be assumed that these small differences in elemental composition will not interfere too much with the behavior of different particle sizes and the size distributions, which was the main target of this study. The water content of fresh sawdust amounted to 45% on average; it was dried to about 17% prior to the experiments. The water content of pellets was already 6% when delivered.

In order to characterize the differences in particle size distribution, a sieving analysis was performed based on the standard DIN 66165 [89]. For the pellets, the three different waste wood samples, and the mixture of sawdust and pellets a sieving analysis was carried out. However, a sieving analysis is not suitable for particles, which are extremely different from spherical particles, such as present in the waste wood samples. The sieving analysis only employs one dimension to describe the particle size. Most of the particles in the waste wood samples can be described either as needle-shaped particles or as disk-shaped particles. In case of needle-shaped particles, the diameter and the length are equally important. Thus, all sieve fractions larger than 1 mm were sorted into different shape groups. The shape groups comprise various types of needles with different lengths and diameters, as well as numerous disks with different cross sections and thicknesses. All dimensions of a shape group were measured and the shape group was weighed. For each shape group, an equivalent diameter,

d_{sv}, was calculated. It is the diameter of a sphere with the same ratio of surface area to volume as the particle, which is given in Eq. 6.1. Thus, the particle size distribution was described by the equivalent diameter d_{sv} and the mass fraction of the shape group. For particles smaller than 1 mm, a mostly spherical shape with an equivalent diameter equal to the sieving diameter was assumed.

$$d_{sv} = \frac{6 \cdot V_{particle}}{S_{particle}} \tag{6.1}$$

In the next step, the ash content was subtracted from the mass fractions. Untreated wood typically contains approximately 0.5 wt.-% ash (referred to as dry fuel). Ash from untreated wood mainly consists of nutrients, such as calcium and potassium, which are integrated into the structure of the wood. Waste fuels contain very frequently sand particles originating from the collection of the waste. Waste wood also comprises coated wood, which contributes to the ash content, e.g. TiO_2 in white coatings. That was most likely the case for waste wood B (7.90% ash, dry basis). It can be anticipated that sand in the fuel has a small particle size. When waste wood is shredded, also small pieces of coating dismantle. Thus, the ash content of the sieve fraction < 1 mm was determined by ashing at 550°C. In case of the mixture of sawdust and pellets and waste wood A, the ash was distributed fairly evenly in all particles independently of their size. In case of waste woods B and C, however, small particles contained significantly more ash than larger ones. Based on that, the ash-free particle size distribution for all fuels was calculated, so that only the organic part of the fuel was considered.

Figure 6.1 illustrates the ash-free particle size distribution of all materials used in the gasification experiments for this chapter. The mixture of pellets and sawdust has a bimodal particle size distribution representing the two compounds of the mixture. The first maximum at about 0.5 mm of equivalent diameter d_{sv} is attributed to the sawdust. The second maximum at d_{sv} around 6 mm was caused by the pellets. The pellets were cylindrical in shape with a diameter of 6 mm and lengths ranging from 5–40 mm. In the sieving analysis, 100% of pellets were found on the 4 mm mesh. The particle size distributions of the waste wood samples were much broader, including dusty material and large pieces. Waste wood B contained a higher concentration of small particles and a maximum at 0.5 mm of equivalent diameter. In this sample, larger particles were mostly present in the form of needles, which result in smaller equivalent diameters. There were no particles larger than 10 mm equivalent diameter. In waste wood A, the particle size maximum occurs at d_{sv} = 1.5 mm. This sample mostly consisted of disk shaped particles: the particle size distribution has a large shoulder ranging from 3 to 12 mm equivalent diameter. In waste wood C the highest concentration of large particles was found. The maximum occurs at 3 mm and the concentration of particles below 3 mm was considerable lower than in all other samples. This sample comprised both disk-shaped and needle-shaped particles. In the literature cited above, either small particles that have diameters of 1 mm or below were used or wooden spheres having diameters exceeding 5 mm. The materials used here cover the whole range from below 1 mm up to 12 mm of particle diameter.

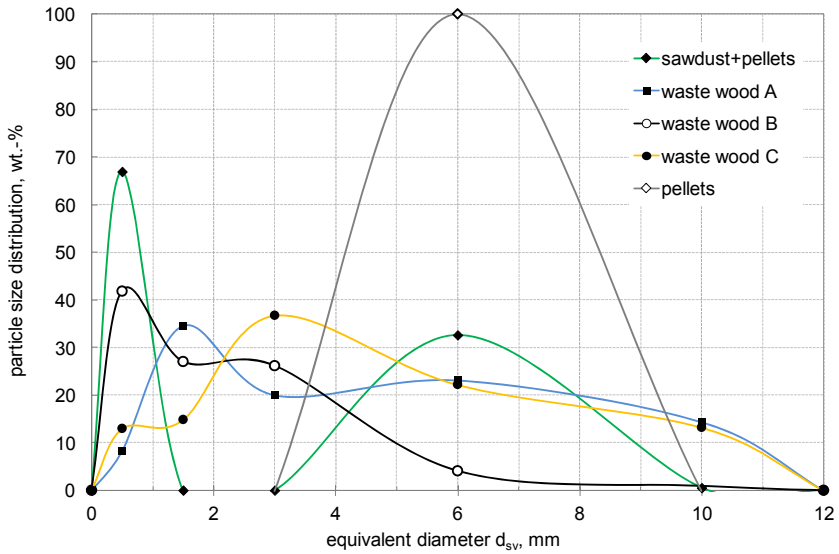

Figure 6.1: Particle size distribution (ash-free) in terms of equivalent diameter d_{sv}

As the basis for the discussion of the experimental results, the concentration of particles smaller than 1 mm best reflects the differences in the particle size distributions. The values in Table 6.1 were obtained from the cumulative mass distribution based on Figure 6.1.

Table 6.1: Concentration of particles smaller than 1 mm

		Sawdust+ pellets	Wood pellets	Waste wood A	Waste wood B	Waste wood C
Particles < 1 mm	wt.-%, ash-free	67	0	28	58	20

6.3 Influence on gasification behavior

Pellets and the mixture of pellets and sawdust were very similar in terms of chemical composition of the fuels as they were produced from the same raw material. However, the product gas composition differed markedly due to the increased proportion of fine particles in one of the feedstock. The composition of the product gas is greatly influenced by the water–gas shift reaction ($CO + H_2O \leftrightarrow CO_2 + H_2$, Eq. 2.6). Although several other gas–gas reactions also occur that counteract it, the water–gas shift reaction is the most dominant reaction in the freeboard of the gasification reactor. The water–gas shift equilibrium gas composition was calculated for each experiment using IPSEpro. It is the gas composition that would have been reached if the water–gas shift reaction had been in equilibrium. The calculation was based on the gasification temperature and other measured properties. The deviation of the measured gas composition from water–gas shift equilibrium is described by δ_{WGS} using Eq. 6.2.

$$\delta_{WGS} = \log_{10}\left(\frac{K_{real}}{K_{eq}}\right) = \log_{10}\left(\frac{p_{CO_2,real}\, p_{H_2,real}}{p_{CO,real}\, p_{H_2O,real}} \cdot \frac{p_{CO,eq}\, p_{H_2O,eq}}{p_{CO_2,eq}\, p_{H_2,eq}}\right) \quad (6.2)$$

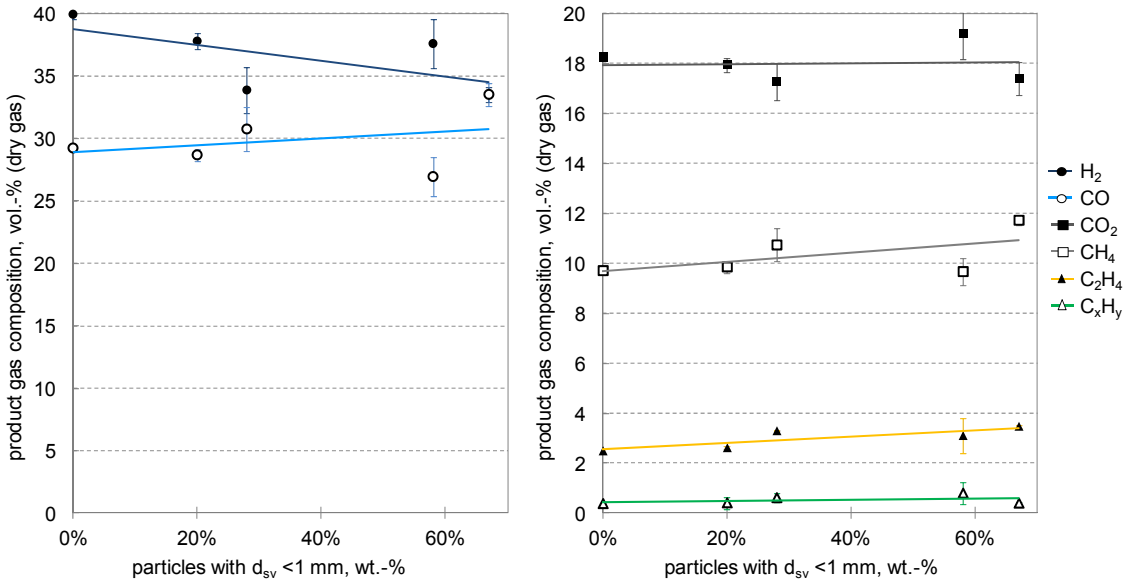

Figure 6.2: Product gas composition as a function of particles < 1 mm

If δ_{WGS} is negative, the concentrations of CO_2 and H_2 were lower than they would have been in the equilibrium state. If the reaction continues, the concentrations of CO_2 and H_2 will increase. Positive values of δ_{WGS} indicate that more reagents, CO and H_2O, will be present. If δ_{WGS} reaches zero, equilibrium is reached and the concentration of all gas species involved in the water–gas shift reaction will remain constant. The values of δ_{WGS} are compiled in Table 6.2 for sawdust, pellets and waste wood gasification and show that the product gas composition was closer to the water–gas shift equilibrium when the amount of fines was smaller.

Table 6.2: Logarithmic deviation from water-gas shift equilibrium

	Wood pellets	Waste wood C	Waste wood A	Sawdust+ pellets
δ_{WGS}	-0.51	-0.51	-0.64	-0.73

The concentrations of tar and char in the product gas are presented in Figure 6.3 in the left diagram. All values are referred to a fuel input of 100 kW in order to eliminate other parameters. Detailed information on the process parameters of the experiments are available in Paper III. Compared to wood pellets, the tar concentration increased drastically when the mixture of sawdust and pellets was gasified. GCMS tar amounted to 30 g/Nm³ and gravimetric tar to 13 g/Nm³. This was twice as much as the tar content in product gas from pellets alone. During gasification of waste woods A and C, the measured concentration of gravimetric tar fits a linear trend based on the content of particles < 1 mm. The concentration of GCMS tar varied more, but in general also increased with increasing fine material. Char is a combustible material, which is entrained from the gasification reactor by the product gas stream. There was no clear trend for the char content and the concentration of fine particles in the biomass.

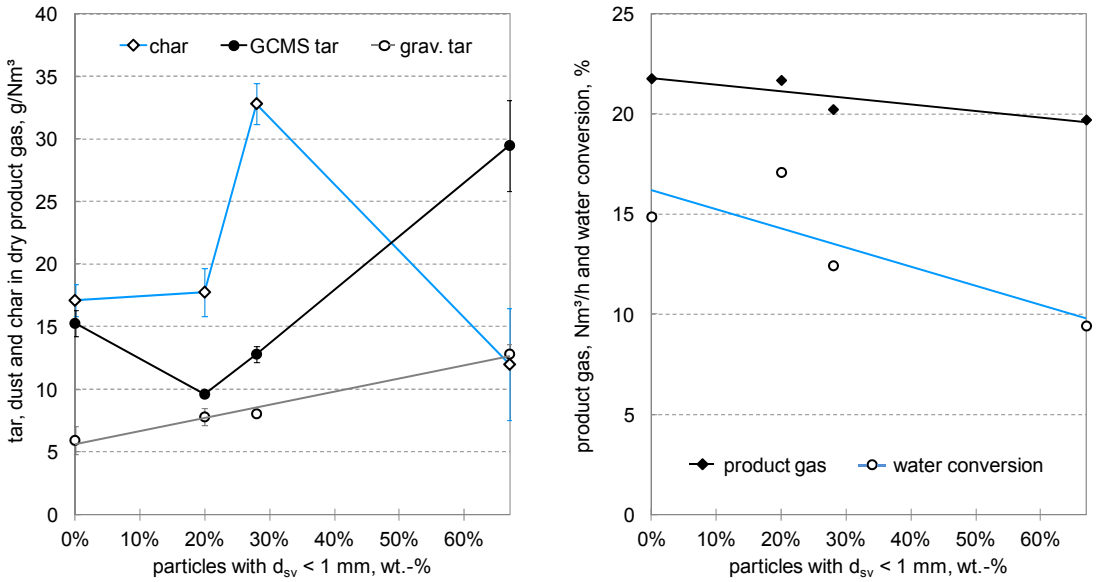

Figure 6.3: Influence of particle size on tar and char formation (left) and on product gas volume flow and water conversion (right)

Mass and energy balances were calculated for each test run using IPSEpro in order to compare several reaction parameters of the DFB gasifier, such as the gas production and the water conversion. For comparison, all values are referred to a fuel input of 100 kW. Figure 6.3 presents the influence of particle size on the product gas volume flow and the water conversion in the right-hand diagram. Gasification of the mixture of sawdust and pellets resulted in a lower product gas volume flow than gasification of pellets alone. Waste woods A and C followed the same trend of lower gas production with an increase in fine particles.

$$X_{H_2O} = \frac{\dot{m}_{H_2O,consumed}}{\dot{m}_{H_2O,fluidization} + \dot{m}_{H_2O,feedstock}} \cdot 100\% \qquad (6.3)$$

The water conversion X_{H2O} describes how much steam reacts with the fuel to form product gas. It is defined as the ratio of water consumed by the gasification reactions to the water supplied to the gasification reactor in the form of steam and fuel water according to Eq 6.3. It summarizes the effect of several gasification reactions, including steam gasification of solid carbon (Eq. 2.3), water-gas shift reaction (Eq. 2.6), and steam reforming reactions of hydrocarbons (Eq. 2.11). In general, the water conversion correlates with the dry product gas flow, since at high levels of water conversion more water is converted into combustible product gas compounds. The water conversion was 40% higher during the gasification of pellets compared to saw dust and pellets, which accords with the equilibrium considerations of the water–gas shift reaction mentioned previously. The higher the water conversion, the closer the gas composition was to the composition of the water–gas shift equilibrium. This is mainly because of the lower contact of fine particles and their volatiles with the bed material that is catalytically active for reforming reactions.

6.4 Particle entrainment

The experiments in the DFB gasification pilot plant showed that the particle size of the biomass influences the gasification behavior. With increasing proportion of particles < 1 mm, the product gas contained less H_2 and more CO and CH_4. Similar changes in the product gas composition are presented by Jand and Foscolo [84] using wooden spheres in a bubbling fluidized bed gasifier. The product gas composition deviated more from the water–gas shift equilibrium gas composition when more particles < 1 mm were present in the fuel. The water conversion decreased likewise and more specific power for combustion was required, as less char could be transferred from the gasification reaction to the combustion reactor. Less product gas was generated and the concentration of tar increased. This is not in agreement with the gasification studies cited before, where more gas is produced from smaller particles and the tar formation is lowered [84-87].

Entrainment of fine fuel particles has an important influence on the formation of gas and tar. Fuel particles that are carried out immediately after feeding because of their small size, have limited contact with the catalytic bed material. Volatiles are mostly released in the freeboard of the gasifier and are less likely to be reformed, and therefore tar formation is enhanced. In the gasification studies [84] and [85] wooden spheres are used as feedstock ranging from 5 mm to 25 mm diameter. Thus, no fine particles are fed to the gasifier that are carried out immediately. In [86] and [87] fractions of sawdust with different mean particle sizes are gasified, which also contain elutriable fine fuel particles. The fluidization velocity was chosen fairly low to prevent entrainment.

In this study, the minimum fluidization velocity and the terminal velocity were calculated for the bed material particles, which consisted of olivine with particle sizes in the range of 400-660 µm and a particle density of 2850 kg/m³. The velocities were in the typical range for bubbling beds [90]. The superficial gas velocity in the freeboard of the gasification reactor was approximately equal during all gasification experiments (0.62 m/s for pellets, sawdust and waste wood C and 0.58 m/s for waste woods A and B).

spheres:
$$C_d = \frac{24}{Re} + \frac{4}{\sqrt{Re}} + 0.4 \tag{6.4}$$

irregular shapes:
$$\frac{C_d}{K_2} = \frac{24}{Re\,K_1 K_2}(1 + 0.1118(Re\,K_1 K_2)^{0.6567}) + \frac{0.4305}{1 + \frac{3305}{Re K_1 K_2}}$$

$$K_1 = \left(\frac{1}{3}\frac{d_n}{d_v} + \frac{2}{3}\phi^{-0.5}\right)^{-1} - 2.25\frac{d_v}{D} \tag{6.5}$$

$$K_2 = 10^{1.8148(-\log\phi)^{0.5743}}$$

$$\phi = \left(\frac{d_v}{d_s}\right)^2$$

In order to estimate the extent of fuel particle entrainment, the terminal velocity for biomass particles of different sizes was calculated. As the waste wood samples mostly contained non-spherical particles such as needles and disks, the drag coefficient C_d was not only calculated for

spheres using Eq. 6.4, but also for irregular shapes using the correlation of Ganser, Eq. 6.5 [91]. This correlation is also mentioned in a review by Cui and Grace [92] because of its good overall agreement for complex shapes. Two different shapes of particles were considered that can be found typically in waste wood samples: needles and disks. For simplification fixed relations were assumed for these types of particles: disks with a ratio of diameter : thickness of 1 : 0.13 and needles with the dimension ratios of length : width 1 : width 2 of 1 : 0.15 : 0.05.

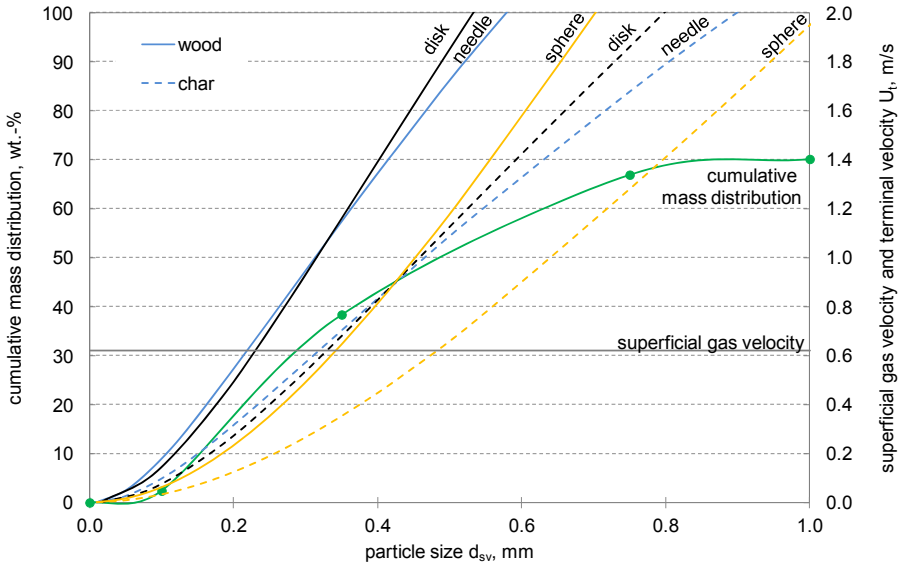

Figure 6.4: Terminal velocity as a function of particle size, shape, and density, and the cumulative mass distribution for sawdust and pellets

Figure 6.4 shows the terminal velocity as a function of particle size, shape, and density, for particles smaller than 1 mm. It demonstrates that the assumption of spheres for fuel particles underestimates the terminal velocity. The terminal velocity does not differ much for disks and needles with fixed dimensions as mentioned above. During thermal conversion also the density of the fuel particles also decreases. Therefore, two different stages of thermal conversion are considered: i) fresh wood particles (e.g. spruce with a water content of 17%) with a particle density of 480 kg/m³ (solid lines) and ii) wood char with a particle density of 250 kg/m³ (dashed lines). Based on the superficial gas velocity in the freeboard of the gasification reactor, a limiting diameter for entrainment can be found. Particles smaller than this diameter are carried out of the fluidized bed with the product gas stream. The limiting diameter for the operation conditions in the pilot plant for disks and needles was about 0.22 mm, and about 0.34 mm for spheres. The cumulative mass distribution of the mixture of sawdust and pellets is also included in the chart as a solid line with dots. It can be deduced that roughly 22% of the particles in the mixture of sawdust and pellets were smaller than the limiting diameter and would be entrained by the product gas stream because of their particle size, in case of disks and needles. In case of spheres, even more particles would be entrained (38%). After devolatilization, the particle density was much smaller than the 480 kg/m^3 for the fresh spruce wood, because about 70-75% of the mass was lost during this phase. As can be seen, char particles can have even larger diameters when they are able to leave the gasification reactor.

In case of the tested materials, a considerable amount of particles was likely to be carried out of the bubbling fluidized bed of the gasification reactor immediately after feeding. Interestingly, the

limiting diameter for entrainment was in the same range as the transition from the thermal thick to the thermal thin regime according to [78, 79]. Therefore, mostly thermally thin particles were entrained. The model of Di Blasi [78] predicts higher tar yields for thermally thin particles than for thermally thick particles. In thermally thin particles, drying, devolatilization and char gasification occur sequentially. The beneficial effects of the catalytic char layer on tar reduction do not occur [79], which increases tar formation. Entrained particles mainly reacted in the freeboard and have less contact with the bed material. Therefore, enhanced reforming reactions due to close contact with the bed material do not occur either. Furthermore, the residence time of these fine particles in the gasification reactor was short. Therefore, the product gas composition deviated more from the water–gas shift equilibrium and the tar concentration was higher when more small particles were present in the fuel. In this case the water conversion was also found to be lower similarly to the deviation from the water–gas shift equilibrium. More fuel for combustion was necessary with a decrease in particle size. This can also be explained by the enhanced entrainment. As more particles were entrained, less char was available for combustion.

6.5 Conclusion

The influence of particle size distributions, as they occur in fresh and waste biomass, on steam gasification, was studied systematically in the DFB pilot plant. Sawdust and pellets made from the same raw material and three different kinds of waste wood with a broad particle size distribution were compared.

For the description of the particle size distribution, sieving analyses of the five materials were performed. As waste wood mostly comprises non-spherical particles with shapes similar to needles and disks, equivalent diameters for similarly shaped spherical particles were calculated, instead of simply using the sieving diameter as a reference length. The different fuels were compared based on their content of particles < 1 mm. The particle size distribution was found to influence the gasification behavior. With an increasing proportion of particles < 1 mm, the product gas contained less H_2 and more CO and CH_4. Thus, the product gas composition deviated more from the water–gas shift equilibrium gas composition. The water conversion decreased likewise, and more specific power for combustion was required for gasification of biomass with high share of particles < 1 mm. Less product gas was generated and the concentration of tar increased.

It was observed that the entrainment of small fuel particles plays an important role in the DFB gasifier. Based on the superficial gas velocity in the freeboard of the gasification reactor, a limiting diameter for the entrainment of needle- and disk-shaped particles was found. A total of 22% of the particles present in the mixture of sawdust and pellets were smaller than this limiting diameter for entrainment at the operation conditions in the pilot plant. These particles were carried out very rapidly after feeding, and were mainly devolatilized in the freeboard, where they had limited contact with the catalytic bed material. Therefore, the volatiles were less likely to be reformed and more tar was found in the product gas. In conclusion, the particle size determines the region in which the thermal conversion of the fuel particles mainly takes place: within the fluidized bed or in the freeboard.

7 Fuels with high amounts of volatile matter

This chapter presents extensive investigations on gasification of plastic materials which are an interesting feedstock, because they are available in large amounts from packaging materials and commodity products. For plastic materials, the reuse of carbon or of larger molecules via chemical recycling is especially promising. Paper IV provides information on gasification of different types of plastics that are typically found in waste streams: PE, PP, mixtures of PE+PS, mixtures of PE+PET and mixtures of PE+PP. The gasification characteristics of these materials were analyzed, because their molecular structure differs significantly from wood.

A DFB gasification process involving an extended range of feedstock that can use biomass as well as plastics would offer an innovative approach for the chemical recycling of plastics. Paper V focuses on co-gasification of plastics and biomass. Four different types of plastics were used in the experiments, both waste materials and virgin polymers: SLF- and MSW-plastics, PE regrind, and virgin PE. Different mixtures of plastics and soft wood pellets, as well as gasification of the pure substances were considered, since co-gasification could also bring about synergistic effects.

7.1 Mono-gasification of plastics

The thermal decomposition mechanism of polymers is mostly based on radical chain scission. The polymer chain breaks into smaller molecules, which leads to a variety of molecules that continue to react further. They vaporize if they are gaseous at the prevailing temperature. Depending on the type of material, thermal decomposition of polymers also comprises the formation of char. PE, PP, PS and PET are thermoplastics, which are charring materials similar to wood [93]. The detailed degradation mechanisms of PE, PP and PS are described by Bockhorn [94, 95] and are comprised of random chain scission and beta scission of radicals. Pyrolysis of PE yields mainly linear alkanes and alkenes, in contrast to PP, which predominantly produces alkenes [95]. When pure PS is pyrolyzed, the main product is the monomer styrene [94]. PET is decomposed by scission of the alkyl-oxygen bond into acetaldehyde, CO, CO_2 and water when heated [93].

Some studies on mono-gasification of plastic materials in bubbling fluidized bed gasifiers have been published. Mastral et al. [96] compared pyrolysis and air gasification of PE in a lab-scale gasifier. At 850°C, the main products of PE were C_2H_4 and aromatics during both pyrolysis and gasification. But CO and CO_2 were only produced during gasification via reactions with the gasification agent. Arena et al. [97] and Mastellone et al. [98] gasified recycled PE with air and Sancho et al. [99] and Xiao et al. [100] carried out gasification tests with PP waste in an air-blown gasifier. As different inert and catalytic bed materials were used, the results of these studies differ greatly, however some similarities can be stated. Air gasification is a suitable conversion technology for PE and PP to yield a product gas with a lower calorific value of approximately 6 MJ/Nm³. The product gas composition strongly depends on the bed material and the amount of fluidization air (the equivalence ratio; ER). The tar formation has been reported to be minimized by in-bed catalysts. The literature cited above primarily describes how

plastic materials are converted by air blown bubbling fluidized bed gasification. Only little information is available on steam gasification.

7.2 Co-gasification of plastics and biomass

Co-gasification of biomass and plastics has been studied in reactors of different types and scales. In order to describe the interaction of the two materials, all phases of thermal conversion have to be considered, including devolatilization, gasification of carbon, and secondary gas-gas reactions. Devolatilization without secondary reactions can be studied using thermogravimetric analysis (TGA) devices, whereas pyrolysis experiments can be employed to illustrate the combined effect of devolatilization and secondary reactions of volatile matter. Gasification tests involve analysis of both the gasification of solid carbon and the influence of the gasification agent. Therefore, a short overview on literature is given for all these important aspects of gasification.

Several TGA studies using biomass and plastics have been published. Jakab et al. [101, 102] investigated the effect of wood, cellulose, lignin and activated charcoal on the thermal decomposition of PS, PE and PP. Sharypov et al. [103] tested beech wood, pine wood, cellulose and hydrolytic lignin in mixtures with PE and PP. Dong et al. [104] used different mixtures of sawdust and PE. In all these TGA studies, the decomposition of biomass and plastics occurs sequentially and, therefore, the interaction of the materials is rather small. Although biomass decomposition is not affected by the presence of plastics, the char from biomass accelerates the decomposition of PP and hinders the decomposition of PS. The behavior of mixtures can nevertheless be approximated using linear combinations of pure substances, with good agreement.

In contrast to TGA studies, flash pyrolysis experiments involve higher heating rates being applied to samples; as a consequence, biomass and plastics decompose simultaneously and thus interactions are more probable. Co-pyrolysis of biomass and plastics has been studied in different reactors, including pyrolyzers for GCMS [101, 102], autoclaves [103, 105], fixed bed [104] and fluidized bed reactors [106]. Although different reactors, and both slow and fast pyrolysis were applied, all provide evidence of the synergistic effects of biomass and plastic materials. Non-linear phenomena are commonly observed that would be underestimated if only tests with single substances were carried out adding the contribution from each feedstock according to its weight ratio in the mixture.

During gasification, volatiles and char can interact with each other and with the gasification agent. Ahmed et al. [107] studied steam gasification of four different mixtures of PE and wood chips in a semi-batch fixed bed reactor at 900°C. An increase in the PE content in the mixture results in the production of more gas, including higher yields of H_2 and C_2H_4, as well as increased carbon conversion and energy content of the gas. These increases are all non-linear; linear interpolation underestimates gas, H_2, C_2H_4, and energy yield. Pinto et al. [108] studied systematically co-gasification of biomass and plastics in a steam-blown bubbling bed gasifier, using different mixtures of pine and PE (up to 60 wt.-% PE). With an increasing proportion of PE in the mixture, more H_2 and C_xH_y, and smaller volumes of CO and CO_2 are produced. The observed change in gas composition is non-linear for a PE content of up to 20 wt.-%. At higher

proportions of PE the gas composition remained almost unchanged. Ruoppolo et al. [109] compared gasification of pine to that of pellets made from a mixture of 20 wt.-% PE and pine, using a bubbling bed gasifier fluidized with air and steam. More CH_4 and tar are produced from the pellets made of the mixture of PE and pine. Studies on various mixtures of coal, biomass and plastics provide a broad overview as to potential feedstock mixtures for co-gasification in bubbling fluidized bed gasifiers with air or air and steam fluidization and summarize the influence of many different factors involved in the process. Mastellone et al. [110] attributed increased gas yield, increased LCV of product gas and increased tar formation to the presence of plastics in the feedstock. Pinto et al. [111] found an increase in plastics to result in greater concentrations of CH_4 and tar, and in reduced H_2 production. The cited literature provides evidence of the non-linear effects that may occur during the co-gasification of biomass and plastics. It is important to investigate feedstock mixtures as the nature of the associated synergetic effects cannot be hypothesized from gasification of the pure substances.

7.3 Product gas composition and gas production

Figure 7.1 illustrates the product gas composition yielded from the different plastic materials during gasification in the 100 kW DFB pilot plant. The standard deviation of the measured values is also shown in the diagram. The deviations were mainly based on the varying degree of filling of the screws used for fuel feeding. However, the differences in product gas composition between the experiments were significantly large, so that the deviations were still small enough to be negligible.

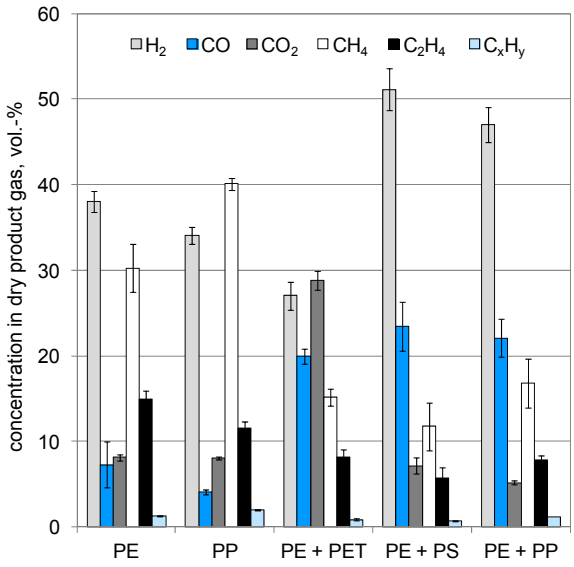

Figure 7.1: Product gas composition from pure substances and mixtures

The main gasification products of pure PE and pure PP were H_2, CH_4 and C_2H_4. Gasification of PE resulted in a high concentration of the monomer C_2H_4, while PP yielded a higher concentration of CH_4 and less C_2H_4. PP contains a methyl group in the constitutional repeating unit, which apparently favored the formation of CH_4, a stable gaseous product. The CO and CO_2 content were in the range of 5-10% during gasification of PE or PP. As neither polymer contains

oxygen, CO and CO_2 were the reaction products of carbon with steam. In contrast, the mixture of PE+PET contained about 27% oxygen and the product gas consisted of about 50% CO and CO_2. The mixtures of PE+PS and PE+PP yielded the highest concentrations of H_2 in the range of 50%. The concentrations of CO were relatively high (20%), although there was no oxygen in the mixtures of PE+PS and PE+PP. The reaction of carbon with steam forms CO and H_2 is also produced from steam. Thus, an increase in CO and H_2 occurs together and indicates more interaction with steam. This is also supported by the decrease in CH_4 and C_2H_4 compared to pure PE. C_xH_y is the sum of C_2H_6 and the gaseous C_3- and C_4-hydrocarbons, which was in the range of 1%.

Co-gasification of biomass and plastics is illustrated in Figure 7.2. Different mixing ratios of biomass and plastics influence the product gas composition. A share of 0% plastics corresponds to gasification of wood alone. Not only measured values for H_2 and CO production are given, but also a linear interpolation based on experimental data for pure materials. Here the lines do not appear as linear relationships, because the energy-based mixing ratios and not the mass-based ratios are used on the x-axis in Figure 7.2. The dashed lines present the values of the linear interpolation, where the H_2 or CO production from the mixture is calculated from the results of gasification of the pure feedstock according to their mass fraction. More H_2 was generated from mono-gasification of PE regrind and SLF-plastics than from wood pellets alone. Virgin PE yielded slightly less H_2 compared to wood. When mixtures were gasified, non-linear effects occurred, but no general trend was observed in terms of H_2 formation for the different materials. While linear interpolation overestimated H_2 yield from SLF- and MSW-plastic mixtures, more H_2 was produced from PE and PE regrind than calculated. Interestingly, PE and PE regrind behaved differently despite varying the least in elemental composition. This discrepancy was eventually traced to the presence of impurities in the employed PE regrind material.

The concentration of CO decreased strongly when only plastics or any mixture of plastics and wood were gasified compared to gasification of pure wood. Non-linear effects are also visible but not as much as for H_2. Similar to CO, the concentration of CO_2 also decreased, which is not shown here, but available in Paper V. A slight decline was apparent during co-gasification of SLF- and MSW-plastics, a steeper decline for PE and PE regrind. These decreases in CO and CO_2 are mainly related to the reduced amount of oxygen in the feedstock. None at all was present when 100% of PE and PE regrind were gasified. In this case, CO and CO_2 were only formed by reactions with steam. The results presented here are in good agreement with a similar gasification study using a steam-blown bubbling bed gasifier. Pinto et al. [108] also observed increased production of H_2 and a decline in CO and CO_2 with increasing proportions of PE in mixtures with pine. As shown previously, CH_4 and C_2H_4 are typical decomposition products of polymers produced in DFB gasifiers. For SLF-plastics, CH_4 increased almost linearly with an increasing proportion of SLF-plastics, but for PE and PE regrind this increase was non-linear. Gasification of the 75% PE regrind mixture produced significantly lower CH_4 and C_2H_4 concentrations than expected from mono-gasification. Changes in CH_4, C_2H_4 and CO_2 in co-gasification are illustrated in Paper V.

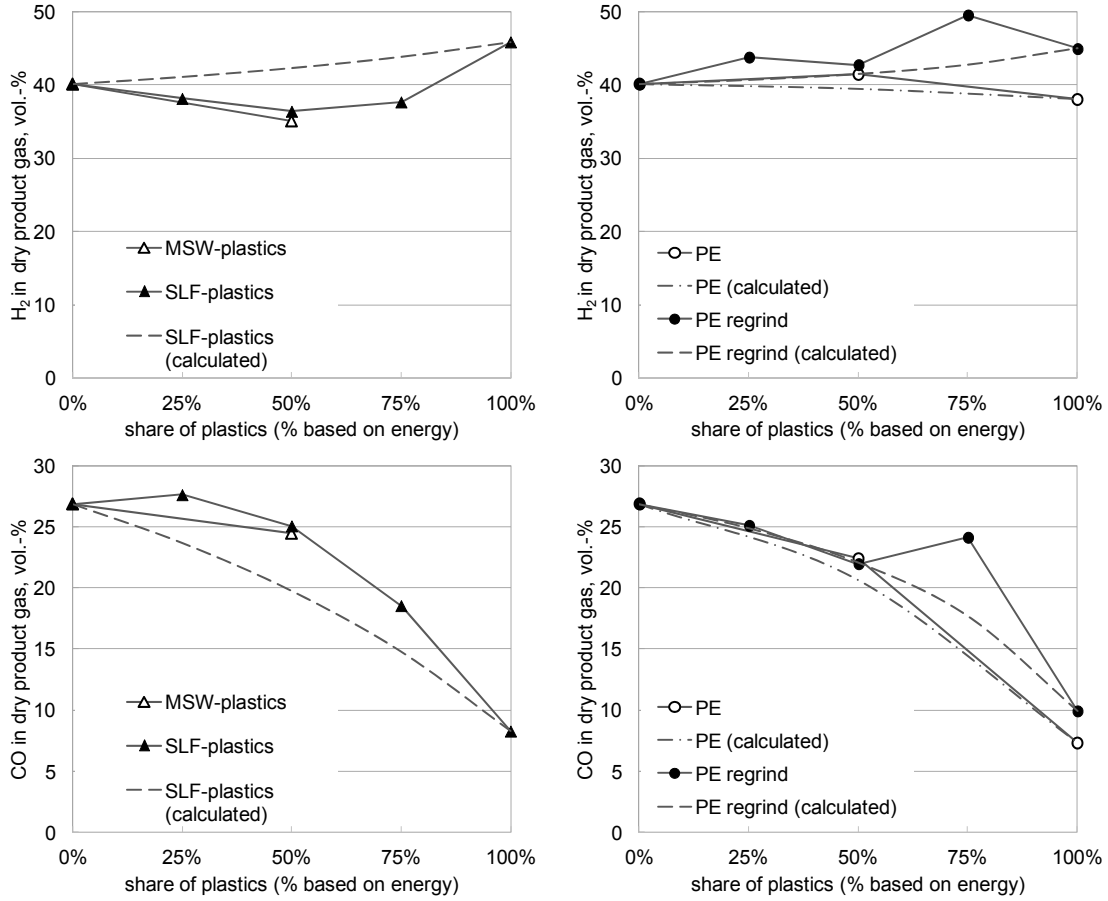

Figure 7.2: H_2 and CO in dry product gas (measured and calculated)

Biomass and polymers interact during steam gasification, resulting in non-linear changes to product gas composition. According to the pyrolysis studies carried out by Jakab and co-workers [101, 102], the presence of biomass char has a significant effect on product distribution. It influences both inter- and intramolecular H transfer during the radical decomposition mechanism of polymers. The effect of char on polymer decomposition was also found to depend on the type of polymer. Ahmed et al. [107] determined an alternate influence of wood and plastics, and postulated that wood chips absorb PE volatiles and hence promote steam reforming of the volatiles. PE radicals might act as H donors that stabilize the radicals formed by wood chips. Co-gasification in the DFB gasifier yielded lower CH_4 and C_2H_4 contents than expected, but higher concentrations of CO and H_2. The change in gas composition is indicative of enhanced steam reforming. These results could possibly be related to the presence of char from biomass.

Several key parameters characterize gas formation summarized in Table 7.1 for PE, PP and PE mixtures and in Figure 7.3 for co-gasification with biomass. For sound comparison, volume flows were converted into those for a fuel input of 100 kW. Gasification of the PE mixtures yielded higher concentrations of H_2 and CO than the gasification of PE or PP. When PE or PP was gasified as a virgin polymer, it resulted in CH_4 and C_2H_4 rich product gases. Larger gaseous molecules led to lower gas production from a fixed quantity of substance, which is

given by the specific gas production. The specific gas production of PE+PET was lower than the other PE mixtures because of the lower LCV of PET.

In Paper V, the influence of co-gasification on product gas volume flow is presented in terms of Nm³/h dry gas. It decreased when mixtures of wood pellets and plastics, and plastics only were gasified, although this decline was less intense than expected from mono-gasification. For example, a mixture of 50% PE and 50% wood produced considerably more gas than gasification of 100% PE. Mastellone et al. investigated co-gasification of coal, plastic waste and biomass in a bubbling fluidized bed gasifier and compared the relative influences of the different fuels. Plastics are found to increase the specific gas production [110]. The values in Figure 7.3 were expressed in terms of the mass of fuel input and show a similar pattern. Mixtures containing plastics yielded specifically more product gas compared to wood (0% of plastics in Figure 7.3).

Table 7.1: Key parameters for gas production

		PE	PP	PE+PET	PE+PS	PE+PP	Wood
Product gas	Nm³/h	10.0	8.1	13.8	17.1	17.5	20.8
Specific gas production	Nm³/kg	1.2	1.0	1.0	1.9	2.1	1.0
LCV	MJ/Nm³	25.8	27.2	16.4	17.0	19.4	12.9
Water conversion	%	11.4	8.0	22.7	31.1	27.4	8.4

The LCV of the product gas was also calculated. Tar and dust were not considered in the calculation. Due to higher concentrations of CH_4 and C_2H_4, the LCV of the product gas from PE or PP amounted to about 26 MJ/Nm³. The product gas from PE+PET had a lower LCV because of the formation of 28% CO_2 which dilutes the gas and does not contribute to the LCV. The product gas from PE+PS and PE+PP had a LCV in the range of 18 MJ/Nm³, because more H_2 and CO were formed compared to gasification of pure PE or PP. The concentrations of CH_4 and C_2H_4 decreased, which would have increased the LCV. In the co-gasification tests, the LCV behaved similarly to the variations in CH_4 and C_2H_4 productions. It increased with higher proportions of plastics in the mixtures.

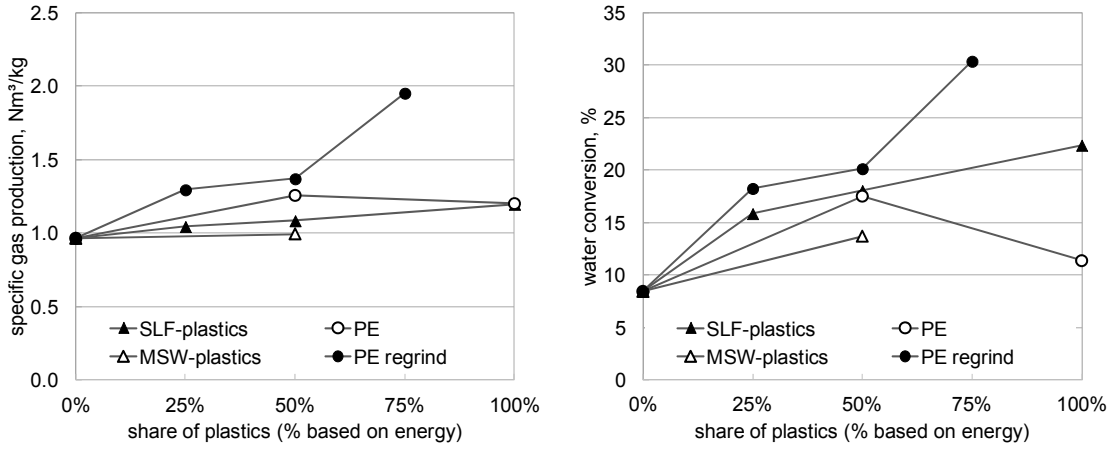

Figure 7.3: Product gas volume flow (dry) and water conversion

Water conversion, X_{H2O}, Eq. 6.3, is an indicator for the interaction with the gasification agent, similar to CO and CO_2 formation for oxygen-free polymers. Mono-gasification of plastics shows, that the water conversion was higher for the plastic mixtures compared to pure PE. It can be explained by the thermal decomposition mechanism of polymers that is mainly based on radical chain scission. The polymer chain breaks into smaller molecules, which leads to a variety of molecules that continue to react further. When mixtures of polymers were gasified, it is likely that a larger variety of radicals was available. These radicals interacted with the steam and enhanced the formation of the smaller molecules such as H_2 and CO. Thus, the water conversion was higher. Co-gasification of plastics and wood resulted in an increase in water conversion, a pattern which also correlates with the deviation from the interpolation based on pure substances. The lowest water conversion values were determined for 100% wood and 100% PE. As is apparent in Figure 7.2, larger volumes of H_2 and CO than expected were measured when PE or PE regrind were part of the mixtures. The water conversion was also higher. Apparently, the steam reforming reactions were enhanced. In contrast, mixtures containing SLF- and MSW-plastics behaved in a different manner. The water conversion continues to increase with an increasing share of SLF-plastics. Furthermore, less H_2 than expected was found in the product gas while CH_4 increased almost linearly, which differs from the other polymers. This might be explained by the radical decomposition. SLF- and MSW-plastics are comprised of a broad range of polymers; hence more radicals of different types are available to interact with steam. Similar to the PE mixtures, the water conversion during mono-gasification of SLF-plastics was greater compared to that of the mixtures with biomass. In contrast, the water conversion of 100% PE was lower compared to that observed during co-gasification. PE only consists of one type of polymer.

7.4 Tar formation and composition

In the DFB gasifier, a low concentration of tar is achieved, when woody biomass is gasified. The tar content ranges from 2-6 g/Nm³ of gravimetric tar and 5-15 g/Nm³ of GCMS tar in dry product gas. As the specific gas production varies significantly among the tested plastics, the tar concentration is referred to the fuel power input of the DFB gasifier to eliminate this influence. Concentrations <1 g/kWh wood of gravimetric tar and 1-3 g/kWh wood of GCMS tar in dry product gas are produced on average. Several co-gasification studies have shown that the presence of plastics in the fuel mixture increases the tar concentration in the product gas. This increase in tar concentration is also accompanied by rising yields of CH_4 and light hydrocarbons [109-111].

Figure 7.4 illustrates the tar, dust and char contents measured during the gasification of PE, PP and PE mixtures. Figure 7.5 summarizes the tar concentrations measured during the co-gasification experiments. No tar measurement was available for the 75% SLF mixture, and the measurement failed for 100% PE regrind. Polymerization occurred in the tar sampling equipment, and thus, the particle separators and piping were rapidly clogged. Since it was not possible to dissolve all the tar, which was stuck throughout in the equipment, part of the sample had to be removed via combustion and could not be considered in the analysis. Because of this fact the tar sample of 100% PE regrind was then omitted from further consideration.

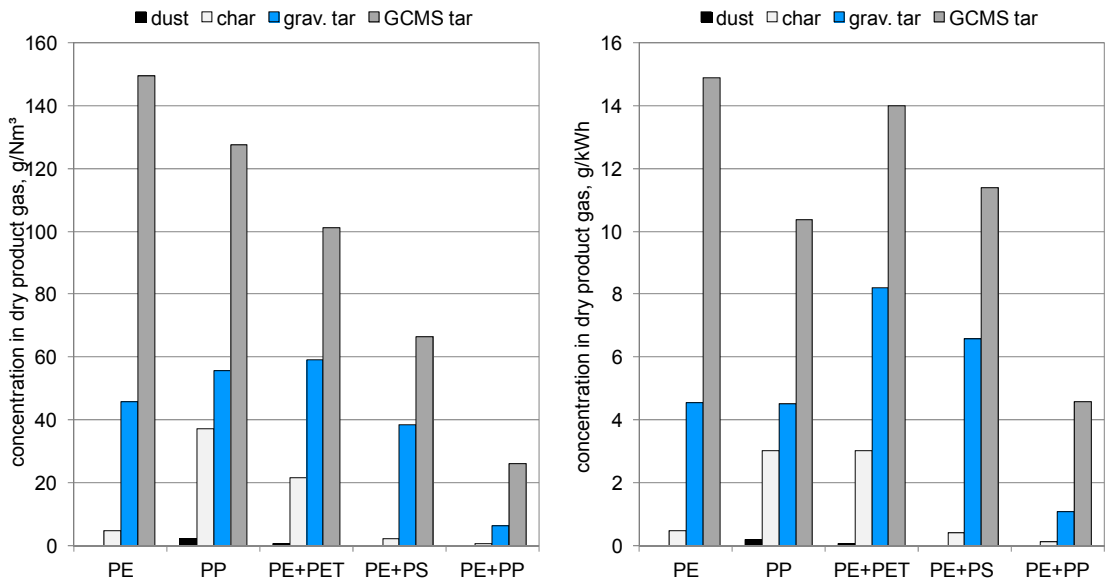

Figure 7.4: Concentration of tar, dust and char in dry product gas (left: g/Nm³, right: g/kWh_{fuel})

When PE, PP and PE mixtures were gasified, the tar content was markedly high: 4-8 g/kWh of gravimetric tar and 10-15 g/kWh of GCMS tar. The mixture of PE+PP was an exception, yielding a significantly lower tar content of 1 g/kWh of gravimetric tar and 4.5 g/kWh of GCMS tar. As described by Bockhorn in [95], PE decomposes in linear alkanes and alkenes, whereas PP predominantly produces alkenes. Apparently, the mixture of decomposition products of PE and PP interacted with each other and enhance the reforming reactions. This might result in markedly lower tar formation than during the gasification of the pure substances.

Co-gasification of biomass and plastics appears in Figure 7.5. It resulted in a non-linear increase in tar formation with increasing proportion of plastics in the fuel mixture, similar to the change in CH_4 content. The difference in tar concentration between the 50% mixture of PE and wood and 100% PE was large. The tar content yielded from 75% PE regrind was also comparably lower than tar from 100% PE and 100% SLF. The latter results could provide an estimate for tar formation from the gasification of 100% PE regrind. Similar results are also reported by Berrueco et al. [106] and Mastellone et al. [110]. These authors explained their results by the presence of wood char, as also demonstrated in the experiments of Boroson et al. [112]

The concentration of entrained solids in the product gas was rather low. There was virtually no dust in the product gas, such as ash or entrained bed material. As PE or PP contained almost no ash, the dust mainly consisted of bed material. When SLF- and MSW-plastics were gasified, the dust content increased, which is typical for waste fuels as they contain more ash. Interestingly, dust content decreased during gasification of 100% SLF, potentially indicating that the ash remained in the bed instead of being carried out. Detailed figures on dust and char content during co-gasification can be found in Paper V. In general, less char is available from highly volatile fuels. However, some char entrainment occurred during the gasification of PP and PE+PET. During co-gasification with biomass, the char content decreased with an

increasing share of PE. More char was entrained when mixtures containing SLF-, MSW-plastics, and PE regrind were gasified, which might be related to the increased gas formation.

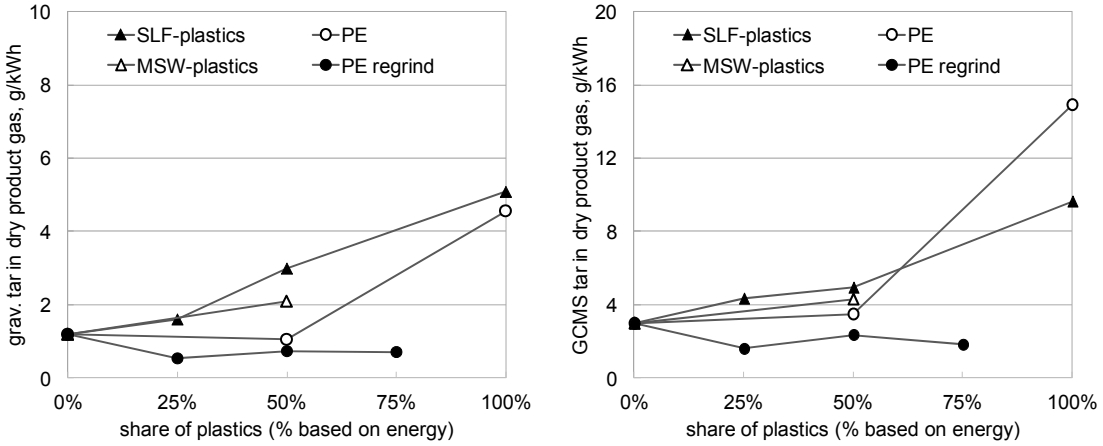

Figure 7.5: Gravimetric and GCMS tar content of dry product gas

The GCMS analysis provides information on tar composition. Tar formation is influenced by the process conditions, such as the gasification agent, temperature and bed material, but also strongly depends on the nature of the feedstock. For biomass gasification, the mechanisms of tar formation are described in detail by several authors, for example by Milne et al. [113], Elliot [114] or Devi [115]. Milne et al. distinguished four groups of tar: Primary tar is formed rapidly at low temperatures and is based on the main constituents of wood: lignin, cellulose and hemicellulose. Secondary tar consists of phenols and olefins. Tertiary tar is formed at higher temperatures from primary and secondary tar and is made of methylic or condensed aromatic ring systems. The most significant tar compound is naphthalene. [113] Although the pyrolysis products of polymers used in the experiments differ greatly from wood and comprise large linear hydrocarbons, the tar which was formed during gasification was similar to tar from wood, mainly aromatic and condensed ring systems. The tar generated during the gasification of PE, PP and PE mixtures was mainly comprised of PAH (50%) and naphthalenes (35%). Roughly 15% of tar were aromatic compounds, such as phenylacetylene, styrene or mesitylene. Virtually no phenols or furans were found in the GCMS tar. Naphthalene was the most important tar compound. About 50% of the tar from polymers were PAH, which are also called recombination or high temperature tar. They were not present in the original feedstock, but formed from devolatilization products (primary and secondary tar). PE, PP and PE+PS produced rather similar GCMS tar. Although styrene is the main pyrolysis product from pure PS, only small amounts of styrene were measured during gasification of PE+PS. It seems that styrene continues to react to larger compounds within this feedstock mixture. In general, the mixture of PE+PP yielded lighter tar compounds compared to tar from the pure substances. This strongly indicates that the mixtures behaved differently and the decomposition products alternately influenced each other.

According to the GCMS analysis, tar from co-gasification of wood and plastics contained less phenols and furans than tar from wood only. Phenols and furans contain oxygen and are typically associated with wood gasification. This decrease was once again non-linear and steeper than expected. Tar from plastic materials did not contain any oxygenated compounds.

The substance groups of naphthalenes increased with increasing proportion of plastics. In conclusion, the composition of GMCS tar is influenced by the fuels used in the gasification process. This is in agreement with the findings of Ruoppolo et al. [109]. More details on GCMS tar are available in Papers V and IV.

7.5 Carbon balance

Carbon is introduced into the gasification reactor with the feedstock and is converted into four possible products in the DFB gasifier, carbonaceous product gas compounds (CO, CO_2, and CH_4, etc), tar and char in the product gas and ungasified char, which is transported to the combustion reactor by the circulating bed material.

The carbon balance was calculated with IPSEpro using measured values from stationary operation of the pilot plant. As there was no measurement of the char composition available in the product gas or in the combustor, it was assumed that char consists of 8% hydrogen and 92% carbon similar to polyaromatic hydrocarbons. In contrast, the following values determined in earlier work were used for wood char: 3.8% hydrogen, 14% oxygen and 82.2% carbon [36]. It was also assumed, that no char was transported back from the combustion to the gasification reactor. Figure 7.6 shows the carbon balance for PE, PP, PE mixtures and wood. When wood was gasified, almost 70% of carbon was present as carbonaceous gases and 25% of carbon was used for combustion. During gasification of PE, a large quantity of carbon was bound in tar (20%), which considerably reduced the share of carbon in the product gas (58%). The lowest tar value was found during gasification of PE+PP; thus the share of carbon in the product gas amounted to 82%. Although the amount of volatiles in polymers was virtually 100%, the calculation showed that 11% of carbon was still available for combustion as char.

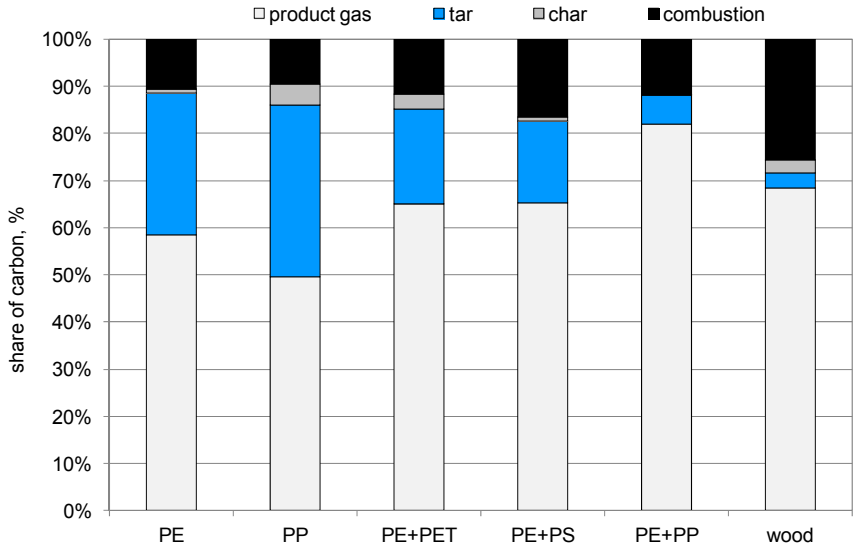

Figure 7.6: Carbon balance in the DFB pilot plant

Char formation from polymers is also described by other researchers. Mastellone and Arena gasified recycled PE in an air-blown bubbling fluidized bed gasifier with olivine [98]. They report that 65% to 85% of carbon is converted into product gas depending on the amount of air used

as gasification agent. The product gas has an average LCV of 6 MJ/Nm³, was rich in H_2, CO, and N_2 and contains low concentrations of CH_4 (5%) and C_2H_m (1%). No tar is measured in the product gas after syngas treatment. The remaining carbon from PE forms a carbonaceous layer on olivine during gasification, which is documented by X-ray spectroscopy analysis. Carbon depositions on the catalyst are also reported by other authors [116, 117].

It might be that a similar layer was formed on the olivine in the DFB gasifier. According to [93], thermoplastics, such as the polymers used in the experiments, also form char during thermal decomposition. In the DFB gasifier, bed material coated with a carbonaceous layer can be regenerated in the combustion reactor. The layer is burnt there and clean material returns to the gasification reactor. The amount of char entrained by the product gas flow was comparably low. This also indicates that char is more likely to be attached to the bed material than to be present as a char particle.

7.6 Energy balance of the DFB gasifier

Figure 7.7 illustrates the energy streams in the DFB pilot plant during gasification of PE. The ingoing streams into the gasification reactor are plastics, steam and hot bed material from the combustion reactor. Product gas, tar and char leave the gasification reactor, as well as bed material with residual char from gasification that is transported to the combustion reactor. Fuel for combustion and air are also fed into the combustion reactor. Flue gas and hot bed material leave the combustion reactor. Due to the high operating temperature of the system, the bed material is the largest energy stream in the DFB gasifier.

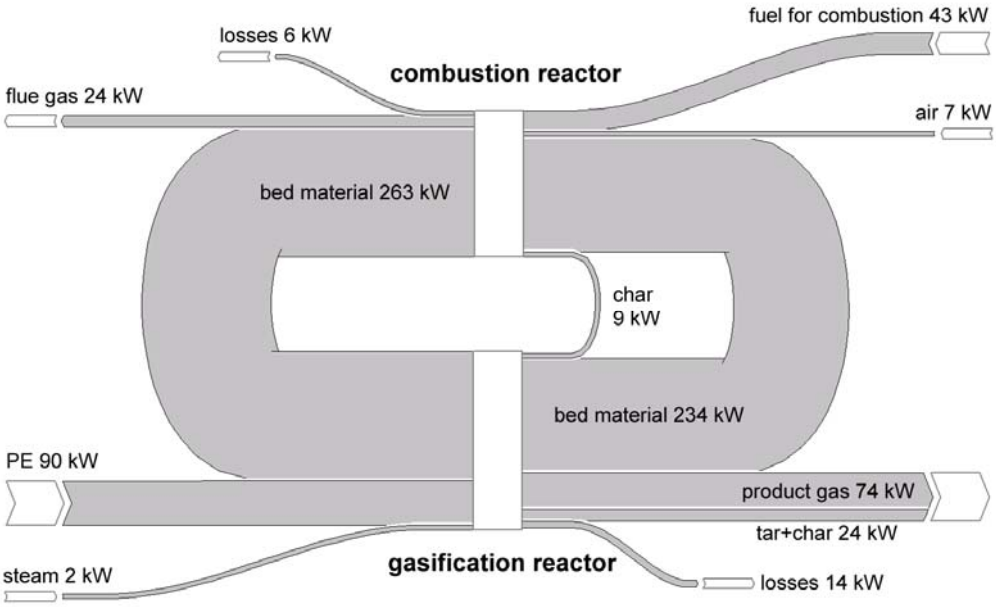

Figure 7.7: Energy streams in the DFB gasifier for gasification of PE

Combustion of residual char and fuel for combustion controls the gasification temperature. In industrial gasifiers, tar and char from the product gas and other combustible streams are recycled to the combustion reactor for this purpose. In the pilot plant, light fuel oil is used

instead of recycled streams. Thermal losses are also included in Figure 7.7. In the 100 kW pilot plant, heat losses to the environment are much higher compared to any industrial plant because of the quality of the insulation and the disadvantageous volume to surface ratio of the pilot plant. In industrial plants, heat losses are more or less negligible.

Three energy streams were selected to describe the energy distribution between the two reactors of the DFB gasifier: char for combustion, fuel fed to the combustion reactor and the in and out-going bed material. The other energy streams did not change significantly when comparing the different experiments, because the operating conditions (temperatures and mass flows of air and steam) were kept within a comparable range.

The specific power of gasification reactions, p_{react} (Eq. 7.1), describes the power consumption of the gasification reactions. The circulating bed material delivers thermal power to the gasification reactor, which is mainly determined by the temperature difference of the in and outgoing bed material. Part of the energy stream is used to cover the thermal losses of the gasification reactor, $P_{losses,gasif.}$, and to heat the fluidization steam from approximately 250°C to the gasification temperature of 850°C, $P_{heat,steam}$. The remaining power is consumed by the gasification reactions. The specific power of combustion is calculated from the fuel fed to the combustion reactor. The measured fuel demand of the combustion reactor is corrected for the heat losses of the pilot plant to obtain a rough estimation for an industrial plant, Eq. 7.2. The amount of residual char for combustion results from the mass and energy balance, which is calculated using measured data. It is referred to as the fuel power for comparison, Eq. 7.3. These values are compiled in Table 7.2 for PE, PP, PE mixtures and wood, and in Figure 7.8 for co-gasification with biomass.

Specific power of gasification reactions[3]

$$p_{react} = \frac{P_{bed,in} - P_{bed,out} - P_{losses,gasif.} - P_{heat,steam}}{P_{feedstock}} \quad (7.1)$$

Specific power of combustion[4]

$$p_{comb} = \frac{P_{fuel,combustion} - P_{losses}}{P_{feedstock}} \quad (7.2)$$

Specific power of char

$$p_{char} = \frac{P_{char}}{P_{feedstock}} \quad (7.3)$$

The specific power of combustion was considerably higher for polymers compared to biomass. This is mainly due to the high content of volatile matter in the polymers. Thus, comparably less char was available for combustion. The gasification of PE mixtures (PE+PS, PE+PP) required more specific power of combustion and also more specific power of gasification reactions compared to pure substances. Apparently, the interaction of the polymers and the water conversion enhanced endothermic reactions that consume energy. PE+PET differed from the other mixtures, because it required less power of gasification reactions and combustion. This might be attributed to the oxygen bonds in the PET polymer which are very reactive.

[3] also referred to as SPG or specific power of gasification in the papers
[4] also referred to as SPC in the papers

Table 7.2: Reaction parameters for energy streams (PE, PP and PE mixtures)

		PE	PP	PE+PET	PE+PS	PE+PP	Wood
Specific power of gasification reactions	kW/kW	0.07	0.06	0.06	0.15	0.11	0.11
Specific power of combustion	kW/kW	0.25	0.25	0.18	0.27	0.30	0.12
Specific power of char	kW/kW	0.10	0.09	0.13	0.16	0.11	0.27

During co-gasification, the amount of residual char decreased, when the proportion of plastics increased in the mixtures. The specific power of combustion rose markedly and non-linearly with increasing share of plastics. The interpolation based on pure substances underestimated the required specific power of combustion. The maximum specific power of combustion was necessary for gasification of the mixture containing 75% PE regrind during which the highest water conversion rate occurred. The specific power of gasification decreases with increasing share of plastics, which is most likely a property of the material. The waste materials, SLF- and MSW-plastics, required a lower power of combustion than PE regrind and PE. Similar to PET, waste materials contained oxygen, which is a possible explanation for the lower power of the gasification reactions.

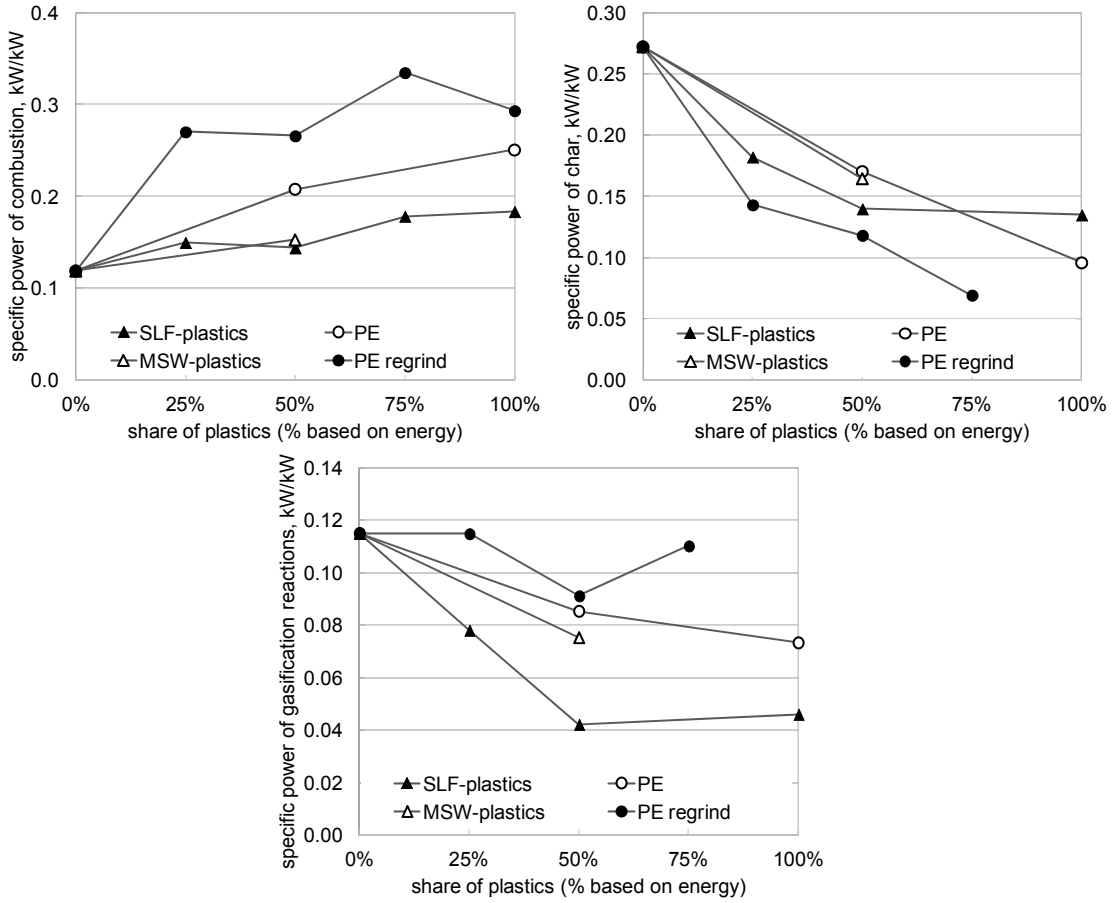

Figure 7.8: Reaction parameters for energy streams (co-gasification with biomass)

7.7 Fluid dynamic considerations

Product gas yield depends on the composition of the fuel mixture and the operating conditions. Figure 7.9 shows the fluidization number, U/U_{mf}, for each of the co-gasification experiments. In the gasification reactor, product gas velocity decreased from about 0.7 to 0.4 m/s with an increasing share of plastics, while the averages of the gas residence time varied between 2.5 and 4 s. The minimum fluidization velocity was calculated for olivine particles and amounted to 0.16 m/s for all test runs. The fluidization number declined with an increasing proportion of plastics in the fuel mixtures. This shows that the bubbling bed was less active during the gasification of these samples.

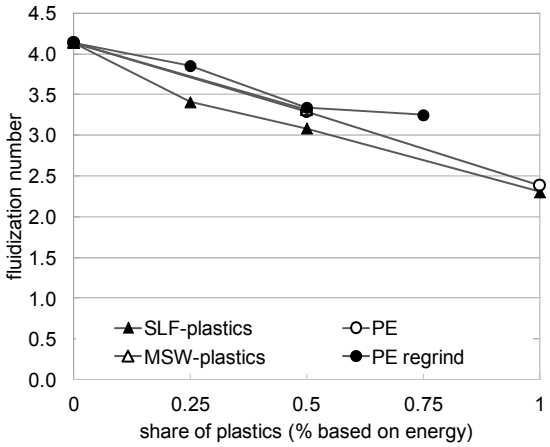

Figure 7.9: Fluidization number U/U_{mf} in the gasification reactor with complete gas formation

In the DFB pilot plant, feedstock can be inserted into the gasification reactor at different heights. During the gasification tests, polymers were mostly fed from the top of the gasifier, while wood pellets were fed directly into the fluidized bed. The feeding positions used in all test runs are given in Table 3 and 4 in Paper V. Plastic particles are discharged from the screw conveyor at the top of the gasification reactor and fall onto the fluidized bed. Terminal velocity was calculated for the smallest and lightest PE particles in order to check whether the particles really fell down in the counter-current product gas flow. According to these calculations, the terminal velocity of PE particles amounted to 14 m/s, it took the particles 0.1 s to fall through the freeboard and land in the bubbling bed. Wood pellets were fed directly into the fluidized bed, which is the part of the reactor characterized by the highest heat transfer rates. Here the pellets heat up, dry and devolatilize. The emerging volatiles form bubbles that lift the pellets up in the bubbling bed [59]. Due to devolatilization, the splash zone is more active when wood is fed into the bed. The bed material that returns from the combustion reactor is then thrown onto the surface of the fluidized bed, which enhances intermixing of fuel particles, gases and bed material. Plastic materials have a high content of volatile matter, especially PE and PE regrind. Therefore, their polymers are likely to react mainly in the freeboard and splash zone. When 100% polymer samples were gasified, the splash zone was less active compared to during gasification of mixtures, because the gas bubbles of the volatiles from wood were absent and thus less gas was produced. However, the polymers still entered the bed as they contributed to char combustion in the combustion reactor.

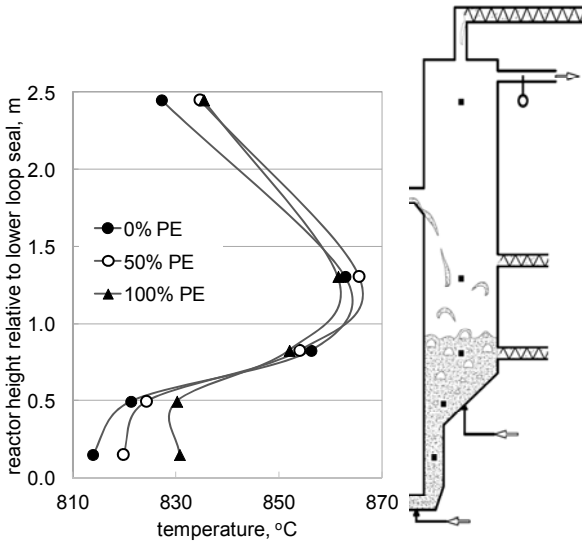

Figure 7.10: Temperature profile along the height of the gasification reactor during gasification of PE mixtures

The temperature profile of the gasification reactor appears in Figure 7.10. A total of five temperature measurement points were positioned along the height of the reactor and show hot and cold spots. The characteristic gasification temperature was measured at a height of 0.8 m. This is the height, at which the wood pellets were inserted into the bed. During gasification of wood, the temperatures deep in the bubbling bed were lower. This indicates that heat was consumed by the gasification reactions taking place there. Bed temperature increased with an increasing share of PE in the fuel mixture, therefore the gasification reactions moved upwards to higher levels of the bubbling bed. The highest temperature was achieved in the lower part of the freeboard, where the hot bed material returned from the combustion reactor. In the upper part of the freeboard, the temperature decreased with increasing height, mainly due to thermal losses from the pilot plant. Figure 7.10 shows the beneficial effects of the co-gasification of biomass and plastics. Due to the fuel mixture, gasification took place deep within the bed and inside the splash zone. The splash zone was also more active due to the bubbles generated by the volatiles from wood. Contact between gas and bed material was, therefore, enhanced, which is decisive in catalytic tar reduction. This is confirmed by the lower tar concentrations observed during co-gasification. Co-gasification also resulted in enhanced steam reforming, and therefore higher water conversion rates.

7.8 Conclusion

Steam gasification of plastic waste materials was carried out successfully in the DFB pilot plant. In order to investigate the significant reaction parameters of gasification, mono-gasification of PE, PP and PE mixtures, as well as co-gasification with biomass were carried out.

The plastic mixtures PE+PP, PE+PS and PE+PET behaved differently from the pure substances PE and PP. Significantly more H_2 and CO were generated from PE+PP and PE+PS. It was assumed that the decomposition products of the two polymers in the mixture

interacted strongly and alternately influenced the gasification process. More steam was converted to product gas, and therefore, the gas production increased. The reforming reactions were enhanced and yielded H_2 and CO at the expense of CH_4 and C_2H_4. Also more power for gasification reactions and combustion was necessary for gasification of the PE mixtures. Gasification of plastics resulted in significantly high tar loads in the product gas in the range of 100 g/Nm³ or 13 g/kWh fuel of GCMS tar. GCMS analysis of tar showed that tar from polymers mainly consisted of PAH and aromatics. Despite the originally linear structure of the polymers, the tar generated contained aromatic molecules, similar to tertiary tar from the gasification of biomass. The PE+PP mixture yielded considerably less tar, which had a different composition than the tar from the two pure substances, PE and PP. This also indicates interactions between the polymers in the mixtures.

Co-gasification of biomass and plastics was also investigated systematically. Product gas composition was considerably influenced by co-gasification. Significantly, these changes were non-linear and therefore, the gas composition could not be accurately predicted based on mono-gasification of the materials only. More CO and CO_2 were measured in the product gas from co-gasification than would have been expected from linear interpolation of the pure substances, whereas H_2 production was either under- or overestimated depending on the plastic material. Smaller amounts of CH_4 and C_2H_4 were formed than expected. The tar content in the product gas was also lower than presumed. With an increasing share of plastics in the fuel mixtures, the composition of the GCMS tar changed to less phenols and furans and more naphthalenes. Co-gasification of biomass and plastics yielded more product gas than expected, largely due to the enhanced reactions with steam and therefore increased water conversion. This was also the reason for the deviation of product gas composition from the results of linear interpolation. It also matches with the observation that apparently more endothermic reactions took place during co-gasification; as the steam reforming of hydrocarbons was enhanced. As a consequence, the fuel demand for combustion increased non-linearly, while less char from the feedstock was available for combustion. When biomass was gasified in the DFB gasifier, gasification occurred throughout the height of the fluidized bed. Mono-gasification of plastics mainly occurred in the upper part of the bubbling fluidized bed and the freeboard. Due to devolatilization of wood pellets in the fluidized bed, more bubbles were formed in the bed. Compared to mono-gasification of plastics, a more active splash zone was established during co-gasification. Thus, the contact between gas and bed material was prolonged, which is crucial for catalytic tar reduction. Co-gasification of wood and plastic materials also had other beneficial effects: more radicals of different types were available from fuel mixtures that interacted with each other and with the fluidization steam. In addition, the presence of wood char had a positive effect on polymer decomposition, steam reforming and tar reduction.

This experimental work demonstrates that the tested polymers are suitable feedstock for the DFB gasifier. In contrast to incineration, steam gasification can also be applied for chemical recycling of polymer wastes. In addition to heat and power production, the selective separation of valuable compounds, such as CH_4 and C_2H_4, could also be an interesting application for product gas from plastic gasification. Whereas the high tar formation during mono-gasification of plastics is problematic for industrial applications, co-gasification of plastics and biomass significantly reduces the tar formation due to the beneficial effect of wood char.

8 Influence of fuel feeding position

Paper VI investigates the influence of the fuel feeding position. The feeding system is a crucial part of the gasification plant and requires careful consideration. Most commonly, a screw feeding system is implemented in industrial DFB gasifiers. This is an in-bed system with a plug screw that inserts the solid fuel directly into the fluidized bed of the gasification reactor. In-bed feeding systems provide intensive mixing of the fuel and the bed material and therefore increase the conversion efficiency. As the end of the screw enters the fluidized bed, mechanical and thermal stress and abrasion are very likely and can cause damage. Normally such in-bed feeding screws are water cooled. However, on-bed feeding systems are usually applied in fluidized bed combustion plants. These systems are simpler, more reliable, and more economic compared to in-bed feeding systems. Biomass is well suited for on-bed feeding, since biomass is a very reactive fuel compared to bituminous coal or lignite. Thus, less unburned carbon is elutriated, which constitutes the majority of combustion losses. Examples of on-bed feeding systems are gravity chutes, where the biomass drops on the fluidized bed, or spreader-stoker systems, which throw the biomass onto a large bed area [118].

Whether the fuel is fed into or onto the fluidized bed influences the gasification process. Several studies have shown that fuel particles tend to float onto the surface of bubbling beds. During devolatilization endogenous bubbles are formed that are able to lift the particles to the surface of the fluidized bed. [59] The time that it takes a particle to reach the surface is called segregation time; it is shorter than the devolatilization time of the fuel. This implies that the majority of volatile matter is released on the bed surface even though the particles are inserted deep into the bubbling bed. [119] In single bubbling bed gasification reactors, it is observed that fuel particles are likely to accumulate on the surface and are not mixed with the bed again. This phenomenon is enhanced by on-bed feeding. As a consequence, on-bed feeding leads to poorer gas quality, increased tar formation, and lower conversion in bubbling bed gasifiers. [85, 120, 121] The effect is stronger for smaller fuel particles, as for them the segregation time is long enough for significant devolatilization to occur. Larger particles mostly react on the surface with less contact with the bed material. [85]

In fast fluidized beds there is no distinct surface, as the particles are spread over the height of the reactor. Due to the higher lateral mixing capacity and deeper bed, considerably fewer feed points are necessary for circulating beds compared to bubbling beds. The number of feed points depends on the properties of the fuel, such as char reactivity and volatile concentration, and is found empirically [118].

DFB reactor systems are more complex, as they are combinations of bubbling and fast fluidized beds. The results from bubbling bed experiments with single reactors cannot be transferred to DFB systems without critical review. In the DFB gasifier there is constant circulation of bed material between the bubbling bed of the gasification reactor and the fast fluidized bed of the combustion reactor. Thus, regenerated hot bed material is fed into the gasification reactor, whereas devolatilized wood char and somewhat colder bed material are transported to the combustion reactor. This circulation cannot be considered in single bed gasification systems. Another point is that most of the mentioned experiments were carried out in very small reactors that were sometimes also operated in batch mode. The position of the fuel feeding system is

closely related to segregation and mixing phenomena, which are likely to be influenced by the size of the reactor.

In Paper VI, two different bed materials and two different fuels were used for a detailed investigation into the influence of the feed point. When the feeding position is changed from in-bed to on-bed feeding, the residence time of the gas phase inside the bubbling bed is likely to be shorter. Sufficient contact of gas and bed material is necessary for catalytic tar reforming. Thus, fresh and used olivine were used as bed material to assess the impact of different catalytic activity. Fresh olivine was provided by Magnolithe GmbH that had never been used in the gasification process before. It is the standard bed material for the pilot plant and is described in Table 3.1. Used olivine was taken from the biomass DFB gasifier in Güssing. Recent research by Kirnbauer et al. [23, 53] has shown that the properties of olivine change over time when used in biomass gasifiers. Due to reactions with additives and compounds from biomass ash, an active layer is built around olivine particles. It is rich in calcium and enhances the reforming capacity. Thus, used olivine is catalytically more active than fresh olivine. More details on used olivine from the Güssing gasifier are available in [23, 53].

In the experiments two different fuels were used that have different devolatilization behavior: wood pellets and SLF-plastics. As reported in [59] and [119], volatile matter forms endogenous bubbles that lift the fuel particles to the surface of the fluidized bed and the segregation time is shorter than the devolatilization time of the fuel. Thus, not only the feeding position but also the devolatilization behavior of the fuel may influence the gasification process.

Table 8.1: Overview on experimental series

	Wood pellets	SLF-plastics
Fresh olivine	A, B (series 1)	A, C+A (series 3)
Used olivine	A, B (series 2)	

Table 8.1 shows the experimental matrix with all series of experiments. In series 1, wood pellets were fed into the bubbling bed by screw A in Figure 8.1 and onto the bubbling bed by screw B using fresh olivine as bed material. In series 2, used olivine was employed as the bed material and wood pellets were also fed by screws A and B. In series 3, SLF-plastics was gasified in a mixture with wood pellets. The mixture consisted of 50% wood pellets and 50% SLF-plastics in terms of fuel energy content. During this series, only the feeding position for SLF-plastics was varied, whereas wood pellets were constantly fed into the bed by screw A. For in-bed feeding, SLF-plastics were also fed into the bed by screw A, while for on-bed feeding SLF-plastics were thrown onto the bed by screw C.

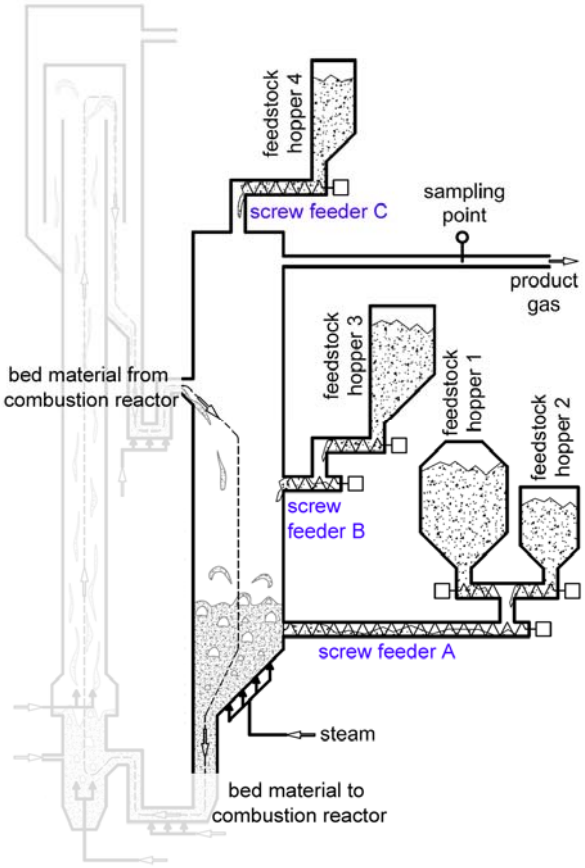

Figure 8.1: In- and on-bed feeding in the gasification reactor of the DFB pilot plant

8.1 Product gas composition

Figure 8.2 presents the product gas composition measured during series 1, 2, and 3. It shows similar trends for series 1 and 2, where wood pellets were used as feedstock. H_2 and CO_2 increased and CO, CH_4, and C_xH_y decreased when on-bed feeding was changed to in-bed feeding. The most significant changes in product gas composition were found in series 1. Minor changes occurred in series 2, because used olivine, which is the more reactive bed material, reduced the effect of the feeding position. Plastic residues, which were gasified in series 3, showed almost no differences in product gas composition when the feeding position was changed. It seemed that the constant stream of wood pellets into the bed in series 3 increased the turbulence in the bed and reduced the impact of the different feed points for SLF-plastics.

The measured gas composition was also compared to the water–gas shift equilibrium gas composition. In series 1 and 2, the product gas composition was closer to the water–gas shift equilibrium in case of in-bed feeding. When used olivine was employed as the bed material, the deviation from equilibrium of in-bed and on-bed was small due to its catalytic activity. During gasification of plastic residues, the deviation was large for both feeding positions. It seems that plastic residues reacted very fast, so that fewer fuel particles were gasified inside the fluidized bed while in contact with bed material. For both feed points the contact time of gas and bed material was too short to reach the water–gas shift equilibrium.

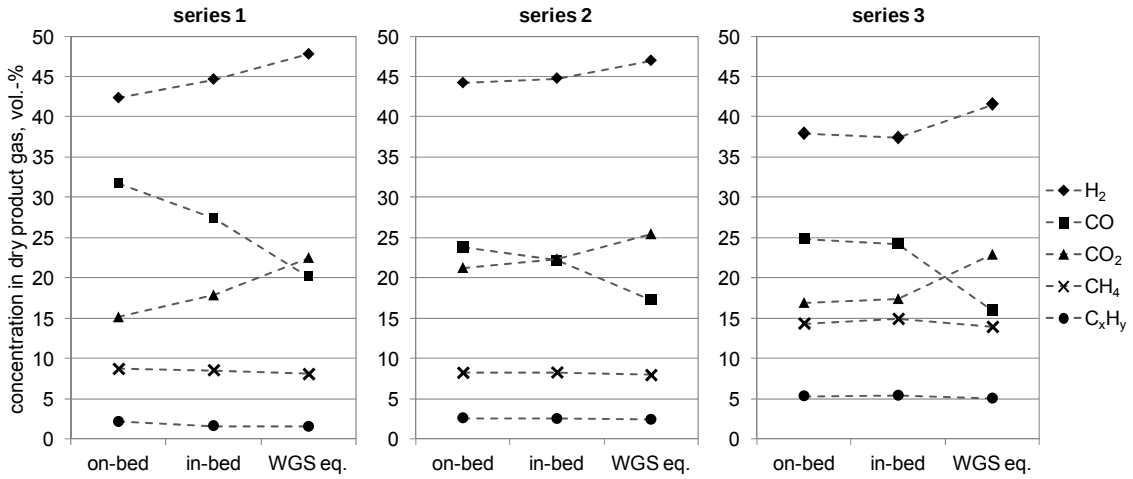

Figure 8.2: Measured product gas composition and water-gas shift equilibrium (WGS eq.) gas composition

8.2 Tar, dust and char

Figure 8.3 illustrates the tar, dust, and char in the product gas. In series 1, less GCMS tar was found when wood pellets are fed into the bed compared to on-bed feeding. The content of gravimetric tar and entrained char decreased slightly and the content of inorganic dust remained constant. In series 2, only minor changes in GCMS tar, gravimetric tar, and dust were observed due to the catalytic activity of used olivine. Series 3 differed considerably, as GCMS and gravimetric tar remained constant. The char content increased and dust decreased.

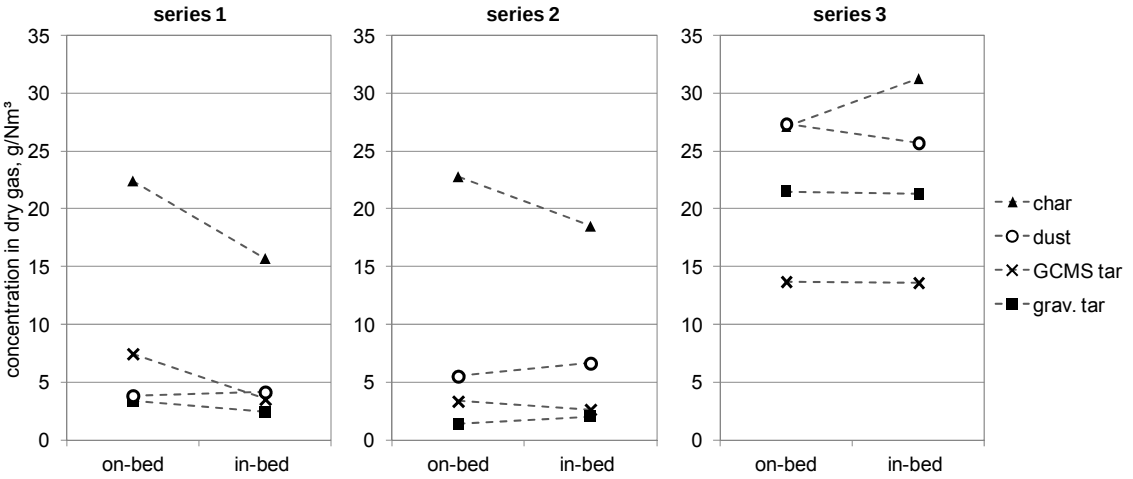

Figure 8.3: Tar, dust and char in dry product gas

Elutriated char decreased in series 1 and 2 but increased in series 3. A decrease in entrained char is an indicator that less char is present in the freeboard and that it is well mixed in the bed. This is coherent for series 1 and 2. There is no clear explanation why the char content increased in series 3. But the very fast devolatilization of plastic fuel particles in case of in-bed feeding influenced the bubbling fluidized bed. SLF-plastics decomposed into big and rapidly rising bubbles, which may lift up fine char particles inside the bed. Thus it was possible that fine

char particles from wood pellets were elutriated into the freeboard. The more active splash zone of the bubbling bed enhanced the release of fine char particles into the freeboard in case of series 3 and in-bed feeding of the SLF-plastics. With in-bed feeding of wood pellets in series 1 and 2 this phenomenon was not observed. This was probably due to the significantly slower devolatilization procedure of wood pellets compared to plastic materials. Tar measurement correlates with the considerations on the water–gas shift equilibrium. When the feed point was changed from on-bed to in-bed, tar concentration decreased and the deviation from the water–gas shift equilibrium was reduced.

8.3 Mass and energy balance

Table 8.2 lists several key parameters of the gasification process: specific power of combustion, gasification reactions and char transported to the combustion reactor, as well as gas formation, (Eqs. 7.1, 7.2 and 7.3). It was found that the specific power of gasification reactions was not affected when on-bed feeding was changed to in-bed feeding. Less char was transported to the combustion reactor during on-bed feeding, and therefore the specific power of combustion increased. This is an indication that there was less char in the lower parts of the bubbling bed in the gasification reactor and that the mixing quality decreased to some extent with on-bed feeding. Although volatile matter was released at different heights in the fluidized bed and mixing of fuel particles was influenced by the feed point, the product gas volume flow remained approximately constant when the feed point was changed.

Table 8.2: Key parameters of the gasification process

		Series 1		Series 2		Series 3	
		on-bed	in-bed	on-bed	in-bed	on-bed	in-bed
Specific power of combustion	kW/kW	0.22	0.17	0.12	0.10	0.20	0.18
Specific power of char	kW/kW	0.18	0.21	0.23	0.26	0.10	0.11
Specific power of gasification reactions	kW/kW	0.15	0.15	0.13	0.13	0.06	0.06
Product gas (operation conditions)	m³/h	160.3	160.2	163.1	162.2	137.1	134.9
Product gas (dry)	Nm³/h	22.7	23.5	22.0	21.9	19.1	18.5

8.4 Residence time of the gas phase in contact with the bed material

In order to benefit from the catalytic activity of the bed material, the contact time of bed material, fuel particles, and product gas is very important. The contact time is the residence time of the product gas in the bubbling fluidized bed and is mainly determined by the feeding position as well as by the formation and volume flow of the product gas.

Pressure measurements along the reactor are an indicator of the bed material distribution and the fluidization conditions in the gasification system. Changes in bed pressure were monitored, when on-bed feeding was changed to in-bed feeding. For these considerations a mean value of two pressure measurements within the bubbling fluidized bed was calculated, which amounted to approximately 70 mbar (relative to atmosphere) for on-bed feeding. In series 1 and 2, the mean bed pressure increased with in-bed feeding by about 5 mbar. When the fuel was fed directly into the bubbling fluidized bed of the gasification reactor, the intermixing of fuel particles into the fluidized bed was favored. Volatiles were released from the fuel particles in the bed and also acted as additional fluidization agent. Therefore, the particle hold-up increased and the pressures increased as well. In contrast, pressures were lower during on-bed feeding. Then, the overwhelming majority of volatiles were produced in the upper region above the bubbling fluidized bed. The location of devolatilization and product gas generation influences the conditions inside the bubbling bed. In series 3 (wood pellets + SLF plastics) no change was detected. It is very likely that the continuous stream of wood pellets into the bed stabilizes the bed pressure drop. As SLF-plastics devolatilize rapidly, fewer fuel particles remained in the bed to be gasified there. The gas phase reactions mostly took place in the freeboard section with limited contact with bed material. Thus, they were not affected by the change in the feeding position of the SLF-plastics. The unchanged bed pressure is in line with tar measurements and product gas properties, where no significant changes could be observed.

Figure 8.4 illustrates the gas production in the gasification reactor. The gas volume flow per height and its gradient were plotted schematically for in- and on-bed feeding and for the continuous stirred-tank reactor model (CSTR). In Figure 8.4 isothermal conditions are assumed, as all ingoing streams are heated immediately to the bed temperature. Thus, only changes in volume due to gas production are considered. In a continuous stirred-tank reactor the gas volume flow increases linearly along the height of the fluidized bed as the fuel particles are assumed to be evenly distributed over the whole bed volume. During in-bed feeding, volatiles are released mainly in the middle part of the fluidized bed. In-bed feeding favors a longer contact time of product gas and bed material, as the volatiles are in contact with the bed material when they flow through the bubbling bed. The gas-phase reactions are catalyzed by the bed material. Also, char, which remains after devolatilization, is mixed within the bed. Additionally, gases are generated from reactions with steam. They are also in contact with the bed material when they flow through the bubbling bed. During on-bed feeding gas production mainly occurs in the upper regions of the fluidized bed and the splash zone. Thus, the contact with the bed material is significantly shorter and consequently the catalytic effects of the bed material are lower. It is also possible that a defined amount of volatiles are produced in the freeboard if on-bed feeding is used, especially in case of very fast devolatilizing fuels.

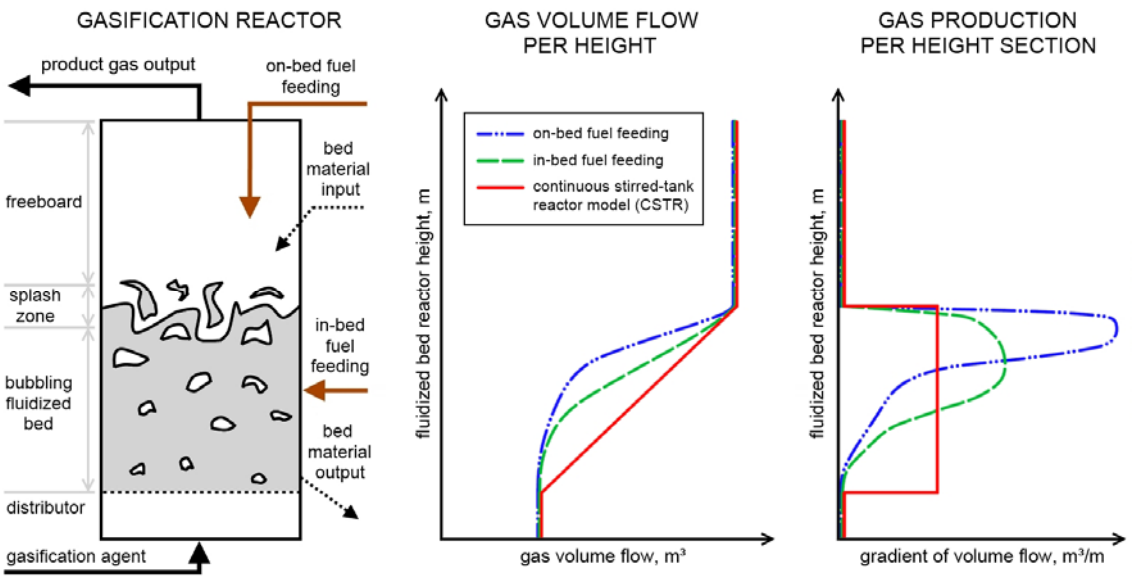

Figure 8.4: Illustration of product gas generation during in- and on-bed feeding

The benefit of catalytic activity can be described by the extent of tar formation and by deviation from water–gas shift equilibrium. When fresh olivine was used as bed material in series 1, the deviations in tar concentrations and water-gas shift equilibrium were considerably higher than in series 2. The less active the bed material is, the more important the contact time is for sufficient conversion. With on-bed feeding, the fuel was not mixed to the same extent within the bubbling bed. Therefore, the position of the fuel feeding had a greater effect on the gasification process if a less active bed material was used.

A recent publication by Saw and Pang [122] supports the presented experimental results. They varied the amount of bed material in a DFB gasifier. Thus, the position of the fuel input was varied relative to the surface of the bubbling bed, and the residence time of the gas phase in the bed was also varied. They showed similar influences on the gas–solid interaction: with an increase in residence time for the gas phase in the fluidized bed, the tar concentration decreases.

8.5 Conclusions

The comparison of in-bed and on-bed feeding showed that in-bed feeding was more favorable, because lower tar concentrations were achieved and the gas composition was closer to the water–gas shift equilibrium. Several parameters indicated better mixing of bed material and fuel particles during in-bed feeding, such as the amount of char transported to the combustion reactor and the higher bed pressure drop. However, extensive fuel accumulation was not observed on the surface on the bubbling bed, because intermixture was enhanced by the circulating bed material, which was constantly fed onto the surface of the bubbling fluidized bed in the gasification reactor. Variation in fuel devolatilization behavior influenced the gasification process. When SLF-plastics were gasified, changes in the feed point of SLF-plastics did not influence the process and the tar concentration also remained constant. As devolatilization of plastics occurred rapidly, the gas phase reactions mainly took place in the freeboard region with limited contact with the bed material. The use of fresh and used olivine showed the influence of catalytic bed materials. When a less active bed material such as fresh olivine is used, sufficient residence time of the fuel in the bubbling bed is important. With in-bed feeding, considerably better performance of the gasifier was achieved. More active bed material such as used olivine was capable of compensating for the shorter residence time of the gas phase in contact with the bed material during on-bed feeding. This underlines the importance of catalytically active bed materials for the gasification process. It also shows the relevance of fluidization conditions in the fluidized bed, because they have a major impact on the gas–solid contact.

9 Conclusion and outlook

The DFB gasifier presented in this thesis is proven technology for gasification of woody biomass and yields high quality product gas. This thesis aims to extend the range of feedstock for the DFB gasification process towards residues and waste.

Different kinds of waste wood, sawdust, SLF-plastics and plastics from municipal solid waste, as well as polymer production residues and PE regrind were tested in a 100 kW DFB gasification pilot plant at Vienna University of Technology. Extensive measurements were carried out during pilot plant experiments and mass and energy balances were evaluated. The process conditions in the pilot plant are in good agreement with industrial DFB gasifiers, therefore, the results are suitable for making statements on larger scale applications. Operation of the pilot plant showed that the selected residues and waste can be gasified without problems. A failure-free and stationary operation of the pilot plant was achieved and thus, DFB gasification of these materials is technologically feasible.

Residues and waste are mostly inhomogeneous, have varying quality and are most commonly challenging fuels for gasification plants. Therefore, the influence of specific waste fuel properties is discussed thoroughly within this thesis:

- fuels with high concentrations of nitrogen, sulfur and chlorine
- fuels with increased concentrations of fine particles
- fuels with extremely high concentrations of volatiles.

The product gas is found to be clearly influenced by the specific fuel properties. Nitrogen, sulfur and chlorine from the fuel were predominantly found in the product gas, either in the form of gases (nitrogen as NH_3, sulfur as H_2S) or bound to ash (chlorine, sulfur). Fuels with an increased concentration of fine particles or volatiles yielded higher tar loads in the product gas.

Figure 9.1 and Figure 9.2 illustrate the influence of the specific fuel properties on several parameters of the gasification process. In these diagrams, all effects are presented by changes relative to the gasification of wood pellets. For example, an increase of 100% means that the parameter has doubled compared to wood pellets. In the diagrams, arrows indicate general trends for specific fuel properties.

In Figure 9.1, the concentration of CH_4 in the product gas is referred to the amount of char from fuel transported to the combustion reactor. Together, these two parameters illustrate the part of the gasification reactor, in which fuel conversion mainly takes places. If fuel is mixed thoroughly within the bubbling bed, more char for combustion is available by tendency, because more fuel particles are present in the lower part of the bubbling bed. Fuels that are mainly gasified in the bubbling bed are more completely converted to gas. Thus, the CH_4 content, which is an indicator of tar formation, tends to be lower. Almost all data points in Figure 9.1 are found in the quadrant, in which less char is available and more CH_4 is formed than during the gasification of wood pellets.

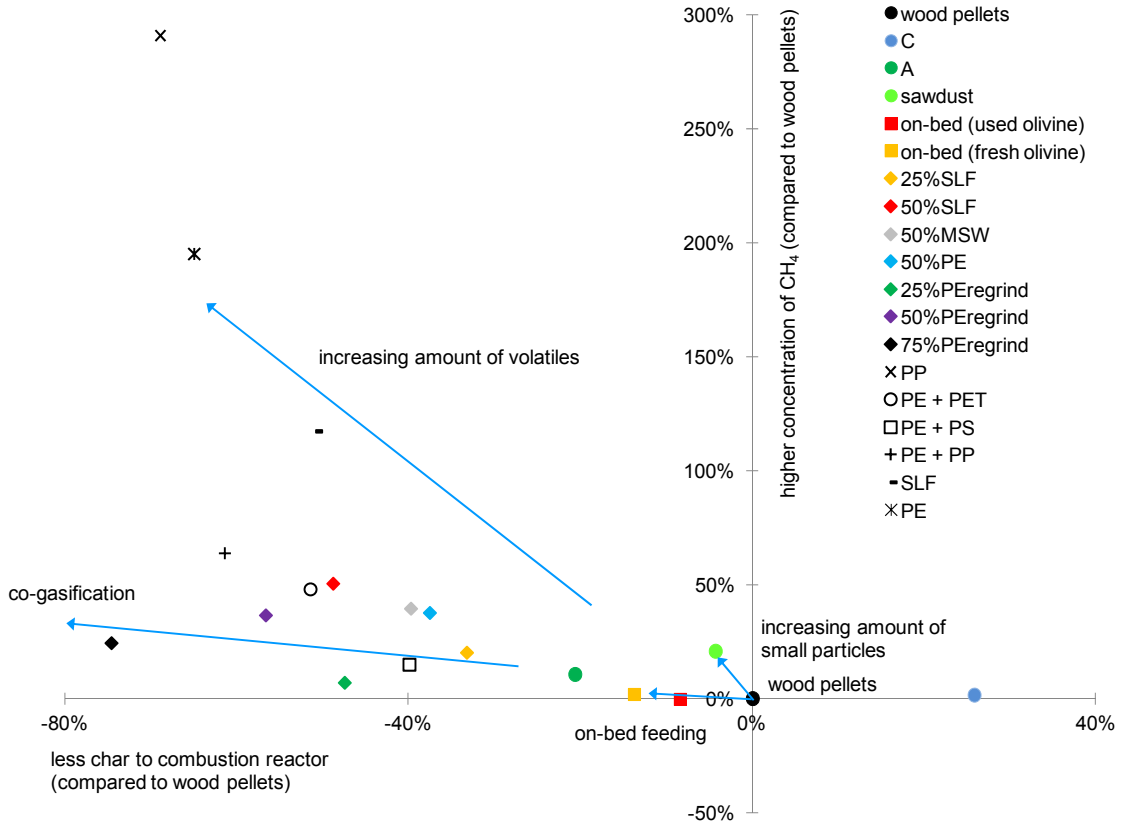

Figure 9.1: Correlation of CH_4 in product gas and char for combustion for all tested fuel properties

Sawdust and pellets show the influence of increasing amounts of small particles. More small fuel particles lead to slightly less char for combustion and more CH_4. The main reason is that small particles are carried out of the bubbling bed after feeding and react predominantly in the freeboard. Thus, fewer fuel particles are present in the lower part of the bubbling bed that could be transported to the combustion reactor by the bed material circulation. When the feed point is changed from in-bed to on-bed feeding, less char and more CH_4 was found. In this case, the reactions of the fuel also mainly take place in the upper part of the bubbling bed and in the freeboard. With increasing amount of volatiles in the fuel, a strong increase in methane production occurs, and the amount of char for combustion decreases markedly. This is mainly due to the volatile nature of the polymers. Consisting of almost 100% of volatile matter, polymers decompose by radical chain scission, whereas CH_4 and C_2H_4 are key decomposition products. Still, some char is formed. It is suggested that char is present in the form of a carbonaceous layer on the bed material, which is combusted in the combustion reactor. Co-gasification of biomass and plastics clearly shows that mixtures behave differently from the pure substances. The increase in CH_4 is not as pronounced as in mono-gasification of polymers and the amount of char decreases with an increasing share of plastics. Wood and plastics influence each other during gasification.

Figure 9.2 shows a correlation between the gravimetric tar in the product gas and water conversion. The water conversion sums up the effect of the reactions that consume steam and generate combustible product gas compounds. Tar formation is an indicator of the quality of fuel

conversion with high tar loads related to low conversions. Tar has to be removed from the product gas prior to almost all applications and is disposed of. Therefore both parameters illustrate the quality of conversion, in one case for the steam and in the other for the fuel. High process efficiency can be attained if water conversion is maximized and tar formation minimized. Because residues and waste are challenging fuels, most data points are found in the quadrant for increased tar formation and higher water conversion compared to gasification of wood pellets in Figure 9.2.

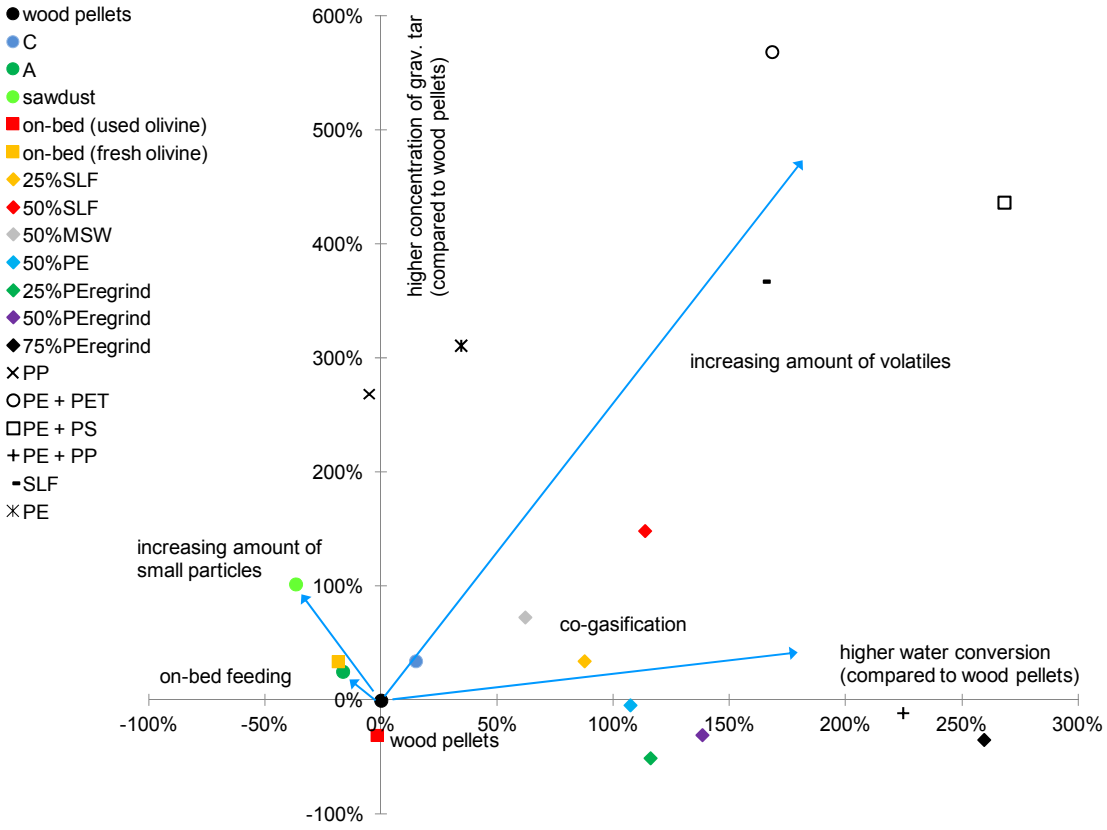

Figure 9.2: Correlation of gravimetric tar and water conversion for all tested fuel properties

With an increase in small particles in the fuel, the water conversion decreases and the tar formation increases. Steam reforming of tar would increase the water conversion and lower the tar concentration, which does not apply to small particles. It is also an indicator of a short residence time of fuel and product gas in contact with the bed material. Changing the fuel feed point from in-bed to on-bed feeding results in a similar behavior, but the effects are slightly weaker. When used olivine was used, the tar content decreases on a very small scale, which should rather be considered as constant. Higher concentrations of volatiles in the fuel do not result per se in higher water conversion rates. If pure polymers, such as PE or PP, are gasified separately, the water conversion is comparable to gasification of wood pellets. Mixtures of different kinds of polymers result in higher water conversion rates. In this case, more radicals of different types are available in the mixture, which interact more intensely. The tar formation increases considerably during mono-gasification of plastics. Co-gasification with biomass leads to significantly lower tar formation, most likely because of the presence of wood char that reduces tar.

The results compiled here and in the previous chapters emphasize that devolatilization is a crucial step in the gasification process. During devolatilization, volatile matter is released, but also nitrogen, sulfur and chlorine. Volatile matter contains higher hydrocarbons, the primary tar. In subsequent reactions with steam, char and catalytic bed material, volatile matter is converted into product gas. For these reactions, the residence time in contact with the bed material and, therefore, the location of volatile release is of great importance. In case of small fuel particles or on-bed feeding, the volatiles are more likely to be released in the splash zone or the freeboard with limited contact with the bed material. Thus, the product gas contains more tar and the gas composition deviates more from the water-gas shift equilibrium. It was also demonstrated, that interactions and synergistic effects occur within plastic mixtures and co-gasification of biomass and plastics. An important synergistic effect is that the presence of wood char lowered the tar formation from plastic materials considerably. The product gas composition and other process parameters cannot be predicted correctly from gasification of single substances. This also highlights the relevance of pilot plant experiments.

When residues and waste are used as feedstock, product gas cleaning is a crucial part of the DFB gasification process. For nitrogen and sulfur rich fuels, product gas scrubbers or other suitable cleaning devices are required according to emission legislation. If residues and waste are to be used in a combustion process, flue gas cleaning would also be mandatory. However, the volume of product gas from the DFB gasifier is considerably smaller than flue gas from a combustion process, which decreases the costs of the cleaning devices. Two groups of fuels were studied with an increased tendency for tar formation because of their particle size distribution or volatile matter content. For those materials, several measures are conceivable. In order to increase gas-solid contact, not only the location of the feed point should be considered, but also the design of the gasification reactor itself. A new design of the DFB gasifier has been recently suggested by Hofbauer and co-workers. It is expected to enhance the gas-solid interaction in the gasification reactor [123, 124]. For product gas with a high tar load, the downstream equipment of the gasifier also has to be adapted. Careful considerations are required in the design of the heat exchanger and the tar scrubber.

In its final analysis, this thesis demonstrates that DFB gasification is suitable for residues and waste and that it is a promising process for the chemical recycling of these materials.

10 Symbols, subscripts and abbreviations

Symbols

C_d	drag coefficient	-
δ_{WGS}	logarithmic deviation from the water–gas shift equilibrium	-
D	reactor diameter	m
d_n	diameter of a sphere with the same projection area	m
d_{p10}	particle diameter for more than 10% of the mass	m
d_{p90}	particle diameter for less than 90% of the mass	m
d_{sv}	equivalent diameter	m
d_v	diameter of a sphere with the same volume	m
K	equilibrium constant	-
K_1	Stokes' shape factor	-
K_2	Newton's shape factor	-
$\dot{m}$	mass flow	kg/h
p	(partial) pressure	Pa
p	specific power	W/W
p_{comb}	specific power of combustion	W/W
p_{react}	specific power of gasification reactions	W/W
p_{char}	specific power of char	W/W
P	power	W
Φ	sphericity	-
R^2	coefficient of determination	
Re	Reynolds number	-
S	surface area	m^3
S/C	steam-to-carbon ratio	kg/kg
U	superficial gas velocity	m/s
U_{mf}	minimum fluidization velocity	m/s
U_t	terminal velocity	m/s
$\dot{V}$	volume flow	m^3/h
V	volume	m^3
$X_{N\ to\ NH3}$	conversion of fuel nitrogen to ammonia	kg/kg
X_{H2O}	water conversion	kg/kg

Subscripts

bed, in	bed material going into gasification reactor
bed, out	bed material leaving gasification reactor
carbon, feedstock	carbon in feedstock
char	char for combustion
comb	combustion
eq.	equilibrium
feedstock	feedstock fed into gasification reactor
fluidization	fluidization
fuel, combustion	fuel fed into combustion reactor
gasif.	gasification
heat, steam	energy to superheat fluidization steam
H_2O, consumed	water consumed in gasification reactions
H_2O, fluidization	fluidization steam
H_2O, feedstock	fuel-bound water
losses	thermal losses
losses, gasif.	thermal losses of gasification reactor
mf	minimum fluidization
n	projection area
N in NH3	nitrogen in ammonia
N in feedstock	nitrogen in feedstock
particle	particle
react	gasification reactions
real	real conditions
sv	surface to volume ratio
t	terminal

Abbreviations

abs	absolute
comb.	combustion
CSTR	continuous stirred-tank reactor
DFB	dual fluidized bed

DT	deformation temperature	
DTG	differential thermogravimetry	
ER	equivalence ratio	
EU27	27 member states of the European Union	
FT	flow temperature	
G8	The Group of Eight	
GCMS	gas chromatograph with mass spectrometer	
IEA	International Energy Agency	
LCV	lower calorific value	MJ/Nm³ or MJ/kg
MSW	municipal solid waste	
Mtoe	Million tons of oil equivalent	41.868 GJ
Nm³	volume at 273.15 K and 101325 Pa	
OECD	Organization for Economic Co-operation and Development	
ORC	organic Rankine cycle	
PAH	polyaromatic hydrocarbons	
PE	polyethylene	
PET	polyethylene terephthalate	
PP	polypropylene	
PS	polystyrene	
REAP	Resource efficiency action plan	
SLF	shredder light fraction	
TGA	thermogravimetric analysis	
TGMS	thermogravimetry with mass spectrometer	
UNEP	United Nations Environment Programme	
vol.-%	concentration based on volume	m³/m³ *100%
WEEE	waste electrical and electronic equipment	
WGS	water-gas shift reaction	
WPC	wood polymer composites	
waf	water and ash free	
wt.-%	concentration based on weight	kg/kg *100%

11 References

[1] OECD. Resource productivity and waste. http://www.oecd.org/env/waste/resourceproductivityintheg8andtheoecd.htm (2013). Accessed 03/06/2013, 17:46.

[2] F. Krausmann, S. Gingrich, N. Eisenmenger, K.-H. Erb, H. Haberl, M. Fischer-Kowalski. Growth in global materials use, GDP and population during the 20th century. Ecological Economics 68(10):2696 – 2705 (2009).

[3] United Nations Environment Programme. Sustainable, resource efficient cities – making it happen! Technical report, UNEP (2012).

[4] International Energy Agency. World Energy Outlook 2012. OECD Publishing (2012).

[5] M. Wackernagel, N. B. Schulz, D. Deumling, A. C. Linares, M. Jenkins, V. Kapos, C. Monfreda, J. Loh, N. Myers, R. Norgaard, J. Randers. Tracking the ecological overshoot of the human economy. Proceedings of the National Academy of Sciences 99(14):9266–9271 (2002).

[6] D. H. Meadows, Club of Rome. The limits to growth; a report for the Club of Rome's project on the predicament of mankind. Universe Books New York (1972).

[7] World Commission on Environment and Development. Our common future. Oxford University Press (1987).

[8] United Nations Environment Programme. Global initiative for resource efficient cities. http://www.unep.org/pdf/GI-REC_4pager.pdf (2012). Accessed 03/11/2013, 18:01.

[9] OECD. Sustainable materials management. http://www.oecd.org/env/waste/smm.htm (2013). Accessed 03/06/2013, 17:00.

[10] Ministry of the Environment Japan. The 3r initiative. http://www.env.go.jp/recycle/3r/en/outline.html (2013). Accessed 03/15/13, 22:25.

[11] J. Fiksel. A framework for sustainable materials management. The Journal of The Minerals, Metals & Materials Society 58:15–22 (2006).

[12] Directive 2008/98/EC of the European Parliament and of the Council of 19 November 2008 on waste (2008).

[13] Eurostat. Generation of waste by economic activity – all NACE activities plus households (code: ten00106) (March 2013).

[14] D. Hoornweg, P. Bhada-Tata. What a waste: a global review of solid waste management. Urban Development & Local Government Unit, World Bank (2012).

[15] European Commission. Communication from the commission to the Council and the European Parliament on the Interpretative Communication on waste and by-products. Brussels (February 2007).

[16] N. Pajunen, G. Watkins, M. Wierink, K. Heiskanen. Drivers and barriers of effective industrial material use. Minerals Engineering 29:39 – 46 (2012).

[17] European Commission. Communication from the Commission to the European Parliament, the Council, the European Economic and Social Committee and the Committee of the Regions: a resource-efficient Europe – flagship initiative under the Europe 2020 Strategy (2011).

[18] S. Gordon, B. McBride. Computer program for calculation of complex chemical equilibrium composition, rocket performance, incident and reflected shocks and chapman-jouguet detonations. Technical Report SP-273, NASA (1971).

[19] M. Kaltschmitt, H. Hartmann, H. Hofbauer (Eds.). Energie aus Biomasse. Grundlagen, Techniken und Verfahren. Springer (2009).

[20] A. Zschetzsche, H. Hofbauer, A. Schmidt. Biomass gasification in an internal circulating fluidized bed. In: P. Chartier, A. A. Beenackers, G. Grassi (Eds.), Proceedings of the 8th European Conference on Biomass for Agriculture and Industry, pages 1771–1776. Elsevier, Oxford, UK (1994).

[21] H. Hofbauer, H. Stoiber, G. Veronik. Gasification of organic material in a novel fluidisation bed system. In: The Society of Chemical Engineers Japan (Ed.), Proceedings of 1st SCEJ Symposium on Fluidisation, pages 291–299. Tokyo (1995).

[22] H. Hofbauer, R. Rauch, K. Bosch, R. Koch, C. Aichernig. Biomass CHP plant Güssing – a success story, pages 527–536. CPL Press (2003).

[23] F. Kirnbauer, H. Hofbauer. Investigations on bed material changes in a dual fluidized bed steam gasification plant in Güssing, Austria. Energy & Fuels 25(8):3793–3798 (2011).

[24] J. Kotik. Über den Einsatz von Kraft-Wärme-Kopplungsanlagen auf Basis der Wirbelschicht-Dampfvergasung fester Biomasse am Beispiel des Biomassekraftwerks Oberwart. Ph.D. thesis, Vienna University of Technology (2010).

[25] T. Klotz. A regional energy-supply-showcase - the 15 MW fuel-power biomass gasification plant Villach. In: International Seminar on Gasification, Gothenburg (2010).

[26] Information on the gasification plant Senden (Germany). http://www.fnr-server.de/cms35/fileadmin/allgemein/pdf/veranstaltungen/Projekttag/7_Vitek_HGA_Senden_091125_Projekttag.pdf. Accessed 29/11/2011, 16:00.

[27] G. Falk, G. Weber, R. Rauch, H. Hofbauer, C. Weiß. Mixed alcohols from biomass steam gasification. In: H. Hofbauer, M. Fuchs (Eds.), Proceedings of the International Conference on Polygeneration Strategies (ICPS11), Vienna, pages 281–288. Society for the

Supportance of Sustainable Energy Technique Based on Polygeneration Strategies of Biomass (2011).

[28] B. Rehling, H. Hofbauer, R. Rauch, C. Aichernig. BioSNG process simulation and comparison with first results from a 1-MW demonstration plant. Biomass Conversion and Biorefinery 1:111–119 (2011).

[29] A. Sauciuc, A. Potetz, G. Weber, R. Rauch, H. Hofbauer, L. Dumitrescu. Synthetic diesel from biomass by Fischer-Tropsch synthesis. In: European Association for the Development of Renewable Energies, (Eds.), Proceedings of the International Conference of Renewable Energies and Power Quality (ICREPQ '11), April 14-15 2011, Las Palmas de Gran Canaria, Spain, page 328. European Association for the Development of Renewable Energies, Environment and Power Quality (EA4EPQ) (2011).

[30] Information on the GoBiGas project, Accessed 02/05/2013, 21:30.

[31] I. Gunnarson. The GoBiGas project. In: International Seminar on Gasification. Malmo (2011).

[32] R. Rauch, C. Pfeifer, K. Bosch, H. Hofbauer, D. Swierczynski, C. Courson, A. Kiennemann. Comparison of different olivines for biomass steam gasification. In: A. Bridgwater, D. Boocock (Eds.), Proceedings of the Conference for Science in Thermal and Chemical Biomass Conversion, pages 799–809. CPL Press, Newbury, Berks (2004).

[33] S. Koppatz, C. Pfeifer, H. Hofbauer. Comparison of the performance behaviour of silica sand and olivine in a dual fluidised bed reactor system for steam gasification of biomass at pilot plant scale. Chemical Engineering Journal 175:468–483 (2011).

[34] U. Wolfesberger, I. Aigner, H. Hofbauer. Tar content and composition in producer gas of fluidized bed gasification of wood - influence of temperature and pressure. Environmental Progress & Sustainable Energy 28(3):372–379 (2009).

[35] T. Pröll, H. Hofbauer. Development and application of a simulation tool for biomass gasification based processes. International Journal of Chemical Reactor Engineering 6:A89 (2008).

[36] T. Pröll, R. Rauch, C. Aichernig, H. Hofbauer. Fluidized bed steam gasification of solid biomass - performance characteristics of an 8 MWth combined heat and power plant. International Journal of Chemical Reactor Engineering 5:A54 (2007).

[37] Eurostat. Database on environment, generation of waste, data [env_wasgen] (March 2013).

[38] Bundesministerium für Land- und Forstwirtschaft, Umwelt und Wasserwirtschaft. Bundes-Abfallwirtschaftsplan 2011, Band 1. http://www.bundesabfallwirtschaftsplan.at/ (2011).

[39] Bundesministerium für Land- und Forstwirtschaft, Umwelt und Wasserwirtschaft. Resource efficiency action plan (REAP).

http://www.lebensministerium.at/publikationen/umwelt/umweltpolitik_nachhaltigkeit/REAP.html (January 2012).

[40] M. Bolhàr-Nordenkampf, I. Tschanun, S. Kaiser. Two new biomass fired FBC-plants with a high fuel flexibility. In: Proceedings of Power Generation Industry Conference and Exhibition, Spain (2007).

[41] Biocom-a fluidized bed combustion system for high efficiency and low emissions. http://www.hsenergie.eu/pdf/Prospekt%20BioCOM_080411_%20englisch_k.pdf (2010). Accessed 07/10/2010, 16:40.

[42] T. Brunner, I. Obernberger, M. Wellacher. Altholzaufbereitung zur Verbesserung der Brennstoffqualität - Möglichkeiten und Auswirkungen, volume 1891, pages 9–64. VDI-Bericht, Düsseldorf (2005).

[43] D. Granatstein. Case study on Lahden Lampovoima gasification project Kymijarvi power station, Lahti, Finland. Technical report. IEA Bioenergy Agreement Task 36 (2002).

[44] M. Spanjers, W. Willeboer. Biomass gasification for power generation – Essent's own developments. In: Proceedings of International Conference on Polygeneration Strategies (2010).

[45] PlasticsEurope. Plastics – the facts 2012, an analysis of European plastics production, demand and waste data for 2011. http://www.plasticseurope.org/Document/plastics-the-facts-2012.aspx?FolID=2 (2012).

[46] Eurostat. Environmental statistics and accounts in Europe. Eurostat Statistical Book. Publications Office of the European Union, Luxembourg (2010).

[47] H. Dominghaus. Kunststoffe: Eigenschaften und Anwendungen. 7th edition VDI-Buch. Springer, (2008).

[48] T. Bürgler. Kunststoffe im Hochofenprozess - Vorbereitung, Umsetzung und Ergebnisse. In: DepoTech 2008, pages 297–302 (2008).

[49] R. Wirthwein, K.-F. Scharf, P. Scur, S. Drebbelhoff. Betriebserfahrungen mit einem Wirbelschichtvergaser beim Einsatz von Sekundärstoffen für die Schwachgaserzeugung. ZKG International 55(1):61–69 (2002).

[50] J. Isaksson. Kymijärvi II waste gasification plant. In: Seminar on Advanced WtE Technologies (2012).

[51] T. Malkow. Novel and innovative pyrolysis and gasification technologies for energy efficient and environmentally sound MSW disposal. Waste Management 24(1):53–79 (2004).

[52] Feste Biobrennstoffe – Brennstoffspezifikationen und -klassen – Teil 2: Holzpellets für nichtindustrielle Verwendung. Deutsches Institut für Normung. Beuth Verlag (February 2011).

[53] F. Kirnbauer, V. Wilk, H. Kitzler, S. Kern, H. Hofbauer. The positive effects of bed material coating on tar reduction in a dual fluidized bed gasifier. Fuel 95:553–562 (2012).

[54] W. Caseri, K. Beutner. Polyethylene. In: Thieme Römpp Online. Georg Thieme Verlag (2012).

[55] I. Obernberger, G. Thek. Physical characterisation and chemical composition of densified biomass fuels with regard to their combustion behaviour. Biomass and Bioenergy 27(6):653 – 669 (2004).

[56] J. Leppälahti, T. Koljonen. Nitrogen evolution from coal, peat and wood during gasification: Literature review. Fuel Processing Technology 43(1):1–45 (1995).

[57] H. H. Nimz, U. Schmitt, E. Schwab, O. Wittmann, F. Wolf. Wood. In: Ullmann's Encyclopedia of Industrial Chemistry. VCH-Wiley (2000).

[58] F.-J. Tian, J.-I. Yu, L. J. McKenzie, J.-I. Hayashi, T. Chiba, C.-Z. Li. Formation of NOx precursors during the pyrolysis of coal and biomass. Part VII. Pyrolysis and gasification of cane trash with steam. Fuel 84(4):371–376 (2005).

[59] M. Fiorentino, A. Marzocchella, P. Salatino. Segregation of fuel particles and volatile matter during devolatilization in a fluidized bed reactor II. Experimental. Chemical Engineering Science 52(12):1909–1922 (1997).

[60] J. Zhou, S. M. Masutani, D. M. Ishimura, S. Q. Turn, C. M. Kinoshita. Release of fuel-bound nitrogen during biomass gasification. Industrial & Engineering Chemistry Research 39(3):626–634 (2000).

[61] C. van der Meijden, W. Sierhuis, A. van der Drift, B. Vreugdenhil. Waste wood gasification in an allothermal gasifier. In: Proceedings of the 19th European Biomass Conference and Exhibition, Berlin, pages 841–845 (2011).

[62] S. Q. Turn, C. M. Kinoshita, D. M. Ishimura, J. Zhou. The fate of inorganic constituents of biomass in fluidized bed gasification. Fuel 77(3):135–146 (1998).

[63] A. van der Drift, J. van Doorn, J. Vermeulen. Ten residual biomass fuels for circulating fluidized-bed gasification. Biomass and Bioenergy 20(1):45–56 (2001).

[64] B. Goldschmidt, N. Padban, M. Cannon, G. Kelsall, M. Neergaard, K. Stähl, I. Odenbrand. Ammonia formation and NOx emissions with various biomass and waste fuels at the Värnamo 18 MWth IGCC plant, pages 524–535. In: A.V. Bridgwater (Ed.), Progress in Thermochemical Biomass Conversion, Blackwell Science (2008).

[65] C. van der Meijden, H. J. Veringa, B. J. Vreugdenhil, B. van der Drift. Bioenergy II: Scale-Up of the Milena biomass gasification process. International Journal of Chemical Reactor Engineering 7:A53 (2009).

[66] S. Senkan, M. Castaldi. Combustion. In: Ullmann's Encyclopedia of Industrial Chemistry. VCH-Wiley (2003).

[67] T. Pröll, I. Siefert, A. Friedl, H. Hofbauer. Removal of NH3 from biomass gasification producer gas by water condensing in an organic solvent scrubber. Industrial & Engineering Chemistry Research 44(5):1576–1584 (2005).

[68] C. van der Meijden, P. Bergman, A. van der Drift, B. Vreugdenhil. Preparations for a 10 MWth Bio-DHP demonstration based on the MILENA gasification technology. In: Proceedings of the 18th European Biomass Conference and Exhibition, Lyon, pages 608–613 (2010).

[69] W. Nutsch. Holztechnik - Fachkunde. 20th edition Europa-Lehrmittel, Haan-Gruiten, (2005).

[70] H. Chen, B. Li, B. Zhang. Effects of mineral matter on products and sulfur distributions in hydropyrolysis. Fuel 78(6):713–719 (1999).

[71] S. van Paasen, M. Cieplik, N. Phokawat. Gasification of non-woody biomass: Economic and technical perspectives of chlorine and sulphur removal from product gas. Technical Report ECN-C-06-032, ECN (2006). Http://www.ecn.nl/docs/library/report/2006/e06032.pdf.

[72] I. Gulyurtlu, F. Pinto, M. H. Lopes, R. N. André, M. Dias, I. Cabrita. Prediction of H_2S and HCl formation during RDF and co-gasification in fluidized bed. In: Proceedings of the 16th European Biomass Conference & Exhibition, Valencia, Spain (June 2008).

[73] F. Pinto, H. Lopes, R. N. André, I. Gulyurtlu, I. Cabrita. Effect of catalysts in the quality of syngas and by-products obtained by co-gasification of coal and wastes. 2: Heavy metals, sulphur and halogen compounds abatement. Fuel 87(7):1050 – 1062 (2008).

[74] O. Brüggemann, K. Beutner. Polyvinylchloride. In: Thieme Römpp Online, RD-16-03650. Georg Thieme Verlag (2009).

[75] E. Björkman, B. Strömberg. Release of chlorine from biomass at pyrolysis and gasification conditions 1. Energy & Fuels 11(5):1026–1032 (1997).

[76] H. Hofbauer, R. Rauch, G. Löffler, S. Kaiser, E. Fercher, H. Tremmel. Six years experience with the FICFB-gasification process. In: Proceedings of the 12th European Biomass Conference, pages 982 – 985 (2002).

[77] I. Siefert. Stickstoff-, Chlor- und Schwefelbilanzen über das Biomasse- Block-Heiz-Kraftwerk Güssing. Ph.D. thesis, Vienna University of Technology (2004).

[78] C. Di Blasi. Kinetic and heat transfer control in the slow and flash pyrolysis of solids. Industrial & Engineering Chemistry Research 35(1):37–46 (1996).

[79] K. M. Bryden, K. W. Ragland, C. J. Rutland. Modeling thermally thick pyrolysis of wood. Biomass and Bioenergy 22(1):41–53 (2002).

[80] A. Bridgwater, D. Meier, D. Radlein. An overview of fast pyrolysis of biomass. Organic Geochemistry 30(12):1479–1493 (1999).

[81] K. M. Bryden, M. J. Hagge. Modeling the combined impact of moisture and char shrinkage on the pyrolysis of a biomass particle. Fuel 82(13):1633–1644 (2003).

[82] A. Bharadwaj, L. L. Baxter, A. L. Robinson. Effects of intraparticle heat and mass transfer on biomass devolatilization: Experimental results and model predictions. Energy & Fuels 18(4):1021–1031 (2004).

[83] L. Wei, S. Xu, L. Zhang, H. Zhang, C. Liu, H. Zhu, S. Liu. Characteristics of fast pyrolysis of biomass in a free fall reactor. Fuel Processing Technology 87(10):863–871 (2006).

[84] N. Jand, P. U. Foscolo. Decomposition of wood particles in fluidized beds. Industrial & Engineering Chemistry Research 44(14):5079–5089 (2005).

[85] S. Rapagnà, G. M. di Celso. Devolatilization of wood particles in a hot fluidized bed: Product yields and conversion rates. Biomass and Bioenergy 32(12):1123–1129 (2008).

[86] P. Lv, Z. Xiong, J. Chang, C. Wu, Y. Chen, J. Zhu. An experimental study on biomass air-steam gasification in a fluidized bed. Bioresource Technology 95(1):95–101 (2004).

[87] S. Rapagnà, A. Latif. Steam gasification of almond shells in a fluidised bed reactor: the influence of temperature and particle size on product yield and distribution. Biomass and Bioenergy 12(4):281–288 (1997).

[88] P. Ammendola, R. Chirone, F. Miccio, G. Ruoppolo, F. Scala. Devolatilization and attrition behavior of fuel pellets during fluidized-bed gasification. Energy & Fuels 25(3):1260–1266 (2011).

[89] DIN 66165. Partikelgrößenanalyse - Siebanalyse: Grundlagen. Deutsches Institut für Normung. Beuth Verlag (1987).

[90] P. Basu, S. A. Fraser. Circulating fluidized bed boilers: design and operations. Butterworth-Heinemann (1991).

[91] G. H. Ganser. A rational approach to drag prediction of spherical and nonspherical particles. Powder Technology 77(2):143–152 (1993).

[92] H. Cui, J. R. Grace. Fluidization of biomass particles: A review of experimental multiphase flow aspects. Chemical Engineering Science 62(1-2):45–55 (2007).

[93] C. L. Beyler, M. M. Hirschler. SFPE Handbook of Fire Protection Engineering, Chapter Thermal Decomposition of Polymers, 3rd edition, pages 110–131. NFPA, (2001).

[94] H. Bockhorn, A. Hornung, U. Hornung. Gasification of polystyrene as initial step in incineration, fires, or smoldering of plastics. International Symposium on Combustion 27(1):1343–1349 (1998).

[95] H. Bockhorn, A. Hornung, U. Hornung, D. Schawaller. Kinetic study on the thermal degradation of polypropylene and polyethylene. Journal of Analytical and Applied Pyrolysis 48(2):93–109 (1999).

[96] F. Mastral, E. Esperanza, C. Berrueco, M. Juste, J. Ceamanos. Fluidized bed thermal degradation products of HDPE in an inert atmosphere and in air-nitrogen mixtures. Journal of Analytical and Applied Pyrolysis 70(1):1–17 (2003).

[97] U. Arena, L. Zaccariello, M. L. Mastellone. Tar removal during the fluidized bed gasification of plastic waste. Waste Management 29(2):783–791 (2009).

[98] M. L. Mastellone, U. Arena. Olivine as a tar removal catalyst during fluidized bed gasification of plastic waste. AIChE Journal 54(6):1656–1667 (2008).

[99] J. A. Sancho, M. P. Aznar, J. M. Toledo. Catalytic air gasification of plastic waste (polypropylene) in fluidized bed. Part I: Use of in-gasifier bed additives. Industrial & Engineering Chemistry Research 47(4):1005–1010 (2008).

[100] R. Xiao, B. Jin, H. Zhou, Z. Zhong, M. Zhang. Air gasification of polypropylene plastic waste in fluidized bed gasifier. Energy Conversion and Management 48(3):778–786 (2007).

[101] E. Jakab, M. Blazsó, O. Faix. Thermal decomposition of mixtures of vinyl polymers and lignocellulosic materials. Journal of Analytical and Applied Pyrolysis 58-59:49–62 (2001).

[102] E. Jakab, G. Várhegyi, O. Faix. Thermal decomposition of polypropylene in the presence of wood-derived materials. Journal of Analytical and Applied Pyrolysis 56(2):273–285 (2000).

[103] V. Sharypov, N. Marin, N. Beregovtsova, S. Baryshnikov, B. Kuznetsov, V. Cebolla, J. Weber. Co-pyrolysis of wood biomass and synthetic polymer mixtures. Part I: influence of experimental conditions on the evolution of solids, liquids and gases. Journal of Analytical and Applied Pyrolysis 64(1):15–28 (2002).

[104] C. Dong, Y. Yang, B. Jin, M. Horio. The pyrolysis of sawdust and polyethylene in TG and U-shape tube reactor. Waste Management 27(11):1557–1561 (2007).

[105] F. Paradela, F. Pinto, I. Gulyurtlu, I. Cabrita, N. Lapa. Study of the co-pyrolysis of biomass and plastic wastes. Clean Technologies and Environmental Policy 11:115–122 (2009).

[106] C. Berrueco, J. Ceamanos, E. Esperanza, F. J. Mastral. Experimental study of co-pyrolysis of polyethylene/sawdust mixtures. Thermal Science 8(2):65–80 (2004).

[107] I. I. Ahmed, N. Nipattummakul, A. K. Gupta. Characteristics of syngas from co-gasification of polyethylene and woodchips. Applied Energy 88(1):165–174 (2011).

[108] F. Pinto, C. Franco, R. N. Andre, M. Miranda, I. Gulyurtlu, I. Cabrita. Co-gasification study of biomass mixed with plastic wastes. Fuel 81(3):291–297 (2002).

[109] G. Ruoppolo, P. Ammendola, R. Chirone, F. Miccio. H2-rich syngas production by fluidized bed gasification of biomass and plastic fuel. Waste Management 32(4):724–732 (2012).

[110] M. L. Mastellone, L. Zaccariello, U. Arena. Co-gasification of coal, plastic waste and wood in a bubbling fluidized bed reactor. Fuel 89(10):2991–3000 (2010).

[111] F. Pinto, R. N. Andre, C. Franco, H. Lopes, I. Gulyurtlu, I. Cabrita. Co-gasification of coal and wastes in a pilot-scale installation 1: Effect of catalysts in syngas treatment to achieve tar abatement. Fuel 88(12):2392–2402 (2009).

[112] M. L. Boroson, J. B. Howard, J. P. Longwell, W. A. Peters. Heterogeneous cracking of wood pyrolysis tars over fresh wood char surfaces. Energy & Fuels 3(6):735–740 (1989).

[113] T. A. Milne, N. Abatzoglou, R. J. Evans. Biomass Gasifier 'Tars': Their Nature, Formation, and Conversion. NREL, Golden, Colorado (1998).

[114] D. Elliott. Relation of reaction time and temperature to chemical composition of pyrolysis oils. In: E. Soltes, T. Milne (Eds.), Pyrolysis oils from biomass: Proceedings of the ACS Symposium Series 376 (1988).

[115] L. Devi. Catalytic removal of biomass tars; Olivine as prospective in-bed catalyst for fluidized-bed biomass gasifiers. Ph.D. thesis, Technische Universiteit Eindhoven (2005).

[116] A. Marcilla, A. Gomez-Siurana, F. Valdos. Catalytic pyrolysis of LDPE over H-beta and HZSM-5 zeolites in dynamic conditions: Study of the evolution of the process. Journal of Analytical and Applied Pyrolysis 79:433–442 (2007).

[117] D. P. Serrano, J. Aguado, J. M. Rodriguez, A. Peral. Catalytic cracking of polyethylene over nanocrystalline HZSM-5: Catalyst deactivation and regeneration study. Journal of Analytical and Applied Pyrolysis 79:456–464 (2007).

[118] P. Basu. Combustion and gasification in fluidized beds. CRC/Taylor & Francis (2006).

[119] G. Bruni, R. Solimene, A. Marzocchella, P. Salatino, J. Yates, P. Lettieri, M. Fiorentino. Self-segregation of high-volatile fuel particles during devolatilization in a fluidized bed reactor. Powder Technology 128(1):11–21 (2002).

[120] D. Ross, R. Noda, M. Horio, A. Kosminski, P. Ashman, P. Mullinger. Axial gas profiles in a bubbling fluidised bed biomass gasifier. Fuel 86(10-11):1417–1429 (2007).

[121] J. Corella, J. Herguido, F. Alday. Pyrolysis and steam gasification of biomass in fluidized beds. Influence of the type and location of the biomass feeding point on the product distribution. In A.V. Bridgwater, J.I. Kuester, Research in Thermochemical Biomass Conversion, pages 384-398. Elsevier Applied Science (1988).

[122] W. Saw, S. Pang. Influence of mean gas residence time in the bubbling fluidised bed on the performance of a 100-kW dual fluidised bed steam gasifier. Biomass Conversion and Biorefinery 2(3):197-205 (2012).

[123] H. Hofbauer, J. C. Schmid, J. Fuchs. Cold flow model study of an advanced dual fluid bed system for fuel conversion. In: 3rd International Symposium on Gasification and its Applications (iSGA-3). October 14-17, Vancouver, Canada (2012).

[124] J. Schmid, T. Pröll, H. Kitzler, C. Pfeifer, H. Hofbauer. Cold flow model investigations of the countercurrent flow of a dual circulating fluidized bed gasifier. Biomass Conversion and Biorefinery 2(3): 229-244 (2012).

Paper I

V. Wilk, H. Hofbauer.

Conversion of fuel nitrogen in a dual fluidized bed steam gasifier.

Fuel 106: 793-801(2013).

http://www.sciencedirect.com/science/article/pii/S0016236112010800

Paper II

V. Wilk, C. Aichernig, H. Hofbauer.

Waste wood gasification: Distribution of nitrogen, sulphur and chlorine in a dual fluidised bed steam gasifier.

In Pugsley, T. et al, editors, Proceedings of the International Conference on Circulating Fluidized Bed Technology (CFB10), Sunriver, Oregon, USA, May 1-5, 2011, pp. 209-216.

Paper III

V. Wilk, H. Hofbauer.

Influence of fuel particle size on gasification in a dual fluidized bed steam gasifier.

Fuel Processing Technology 115: 139-151 (2013).

http://www.sciencedirect.com/science/article/pii/S0378382013001732

Paper IV

V. Wilk, H. Hofbauer.

Conversion of mixed plastic wastes in a dual fluidized bed steam gasifier.

Fuel 107: 787-799 (2013).

http://www.sciencedirect.com/science/article/pii/S001623611300077X

Paper V

V. Wilk, H. Hofbauer:

Co-gasification of biomass and plastics in a dual fluidized bed steam gasifier.

Energy & Fuels 27(6): 3261-3273 (2013).

http://pubs.acs.org/doi/abs/10.1021/ef400349k

Paper VI

V. Wilk, J.C. Schmid, H. Hofbauer.

Influence of fuel feeding positions on gasification in dual fluidized bed gasifiers.

Biomass and Bioenergy 54: 46-58 (2013).

http://www.sciencedirect.com/science/article/pii/S0961953413001505